AIR SYSTEMS MODELING AND CONTROL FOR TURBOCHARGED ENGINES

Philippe Moulin

ParisTech
INSTITUT DES SCIENCES ET TECHNOLOGIES
PARIS INSTITUTE OF TECHNOLOGY

MINES ParisTech

École doctorale n°432 : Sciences des Métiers de l'Ingénieur

Doctorat ParisTech

T H È S E

pour obtenir le grade de docteur délivré par

l'École nationale supérieure des mines de Paris

Spécialité « Mathématique et Automatique »

présentée et soutenue publiquement par

Philippe MOULIN

le 05 Mai 2010

Modélisation et Commande des Systèmes d'Air des Moteurs Suralimentés

Directeur de thèse : **Pierre ROUCHON**

Jury

M. Carlos CANUDAS DE WIT, Directeur de Recherche, CNRS Gipsa-Lab	Président
M. Lino GUZZELLA, Professeur, ETH Zurich	Rapporteur
M. Wilfrid PERRUQUETTI, Professeur, Ecole Centrale Lille	Rapporteur
M. Pierre ROUCHON, Professeur, Ecole des Mines de Paris	Examinateur
M. Gilles CORDE, Docteur, IFP	Examinateur

MINES ParisTech
Mathématiques et Systèmes
60, Boulevard Saint Michel 75006 Paris

T H È S E

Philippe Moulin

MODÉLISATION ET COMMANDE DES SYSTÈMES D'AIR DES MOTEURS SURALIMENTÉS

Philippe Moulin
IFP, 1-4 Avenue de Bois Préau, 92500 Rueil Malmaison.
E-mail : philippe.moulin@ifp.fr

Key words and phrases. — Engine Control, Turbocharger Control, Nonlinear Control, Motion Planning, Feedback Linearization.

Mots clefs. — Contrôle Moteur, Commande Turbocompresseur, Commande Non Linéaire, Planification de Trajectoire, Linéarisation par Retour d'Etat.

Ce document représente le résultat d'un travail collectif que je n'aurais pas pu réaliser tout seul. Je tiens en premier lieu à remercier Pierre Rouchon pour avoir eu la gentillesse de diriger ma thèse, avoir donné du temps et des conseils qui ont orienté directement l'ensemble des travaux décrits ici. Je dois remercier Gilles Corde pour ses encouragements sans lesquels je n'aurais pas eu le courage de me lancer dans cette aventure ni de la poursuivre. Merci à toutes les personnes qui ont contribué aux travaux, avant tout à Olivier et Jonathan dont l'apport a été le plus important, mais aussi à tous les coauteurs des articles sur lesquels ce document s'appuie.
Je souhaite également remercier mes proches, mes parents ma famille et mes amis, dont le soutien m'a toujours beaucoup aidé. Merci en particulier à Séverine pour sa compréhension et tout ce qu'elle m'apporte chaque jour.

MODÉLISATION ET COMMANDE DES SYSTÈMES D'AIR DES MOTEURS SURALIMENTÉS

Philippe Moulin

Résumé **(Modélisation et Commande des Systèmes d'Air des Moteurs Suralimentés)**

Les performances des moteurs à combustion interne sont limitées par la quantité de gaz que leur système d'air peut apporter dans le cylindre. Les turbocompresseurs permettent d'augmenter cette quantité et c'est donc pour cette raison qu'ils sont maintenant couramment utilisés, parfois en combinaison avec d'autres composants. Ces systèmes présentent l'inconvénient d'entraîner une dynamique lente sur le moteur. Les stratégies de commande associées doivent donc exploiter au maximum la dynamique d'un système complexe. Cette thèse examine les problèmes de commande des systèmes d'air suralimentés à travers trois études de cas : un turbocompresseur à géométrie fixe sur un moteur essence, une turbine à géométrie variable sur un moteur Diesel avec deux circuits de recirculation des gaz brûlés, et un turbocompresseur à deux étages sur un moteur Diesel.

La démarche proposée consiste à réduire un modèle physique du système et à synthétiser des stratégies de commande simples basées sur l'analyse de ce modèle. Grâce à la simplicité du modèle réduit et de la loi de commande, on peut prouver des propriétés du système en boucle fermée telles que la convergence, la stabilité et le respect des contraintes. Des résultats expérimentaux sont fournis dans chaque cas pour démontrer la pertinence de la démarche.

Le premier problème considéré est à simple entrée simple sortie (SISO) avec des contraintes sur l'actionneur. Le système est non linéaire du premier ordre. La stratégie de commande développée consiste en une linéarisation par retour d'état avec planification de trajectoire sous contrainte. Elle se base sur l'inversion dynamique d'une représentation physique du système. Des problèmes pratiques tels que les contraintes sur l'actionneur

et l'anti emballement de l'intégrateur sont pris en compte à la fois dans les parties de prépositionnement et de bouclage du contrôleur. La démarche et les développements sont ensuite étendus à des applications plus complexes.

Le second système d'air considéré contient plusieurs sous systèmes avec de nombreuses interactions : turbocompresseur et circuits de recirculation des gaz brûlés. Un niveau de modélisation similaire à celui du premier cas est utilisé pour l'analyse du système. On montre que les dynamiques des circuits de recirculation des gaz brûlés sont plus rapides que celles du turbocompresseur et peuvent donc être négligées. Cependant, les interactions statiques entre les deux systèmes imposent des contraintes sur la commande du turbocompresseur. La structure de commande développée pour le premier exemple est adaptée à ce nouveau problème de commande.

La dernière application est la plus complexe. Le problème de commande peut être réduit à un problème à simple entrée et simple sortie (SISO), mais le système est du second ordre et des contraintes doivent être respectées sur l'un des états. Un modèle physique mais réduit du second ordre permet d'étudier les trajectoires du système en boucle fermée dans le plan des phases. Des stratégies de commande sont ainsi synthétisées pour forcer le système sur les trajectoires désirées tout en satisfaisant les contraintes.

La thèse montre donc que différents problèmes de commande de sytèmes d'air peuvent être traités avec des solutions similaires et cohérentes. La démarche globale et le niveau de modélisation retenu sont génériques. Ils pourront ainsi être étendus à de futurs problèmes de commandes de systèmes d'air, mais également à des problèmes de diagnostic pour lesquels ils sont bien adaptés.

INTRODUCTION GÉNÉRALE

Dans l'industrie automobile, les développements de nouvelles technologies de moteurs sont principalement liés à la nécessité de diminuer la consommation de carburant et les émissions polluantes. Cela entraîne la conception de systèmes à l'architecture complexe, combinant plusieurs sous systèmes avec de multiples interactions. C'est le cas en particulier pour les systèmes d'air qui apportent les gaz (air et gaz brûlés) dans le cylindre et qui sont donc limitants pour la combustion. C'est pourquoi les systèmes d'air contiennent la plupart du temps un turbocompresseur de qui permet d'augmenter la densité des gaz à l'admission du moteur et d'améliorer ses performances. L'inconvénient majeur des turbocompresseurs vient de leur temps de réponse lent. Il peut être compensé par l'utilisation d'une turbine à géométrie variable, ou par l'ajout d'autres dispositifs : par exemple un autre turbocompresseur ou un compresseur mécanique. Dans certains cas, les circuits de recirculation des gaz brûlés haute ou basse pression peuvent encore complexifier le système.

Les logiciels de contrôle moteur doivent aussi s'adapter à ces changements pour plusieurs raisons. En premier lieu, la législation plus stricte nécessite de meilleures performances en termes de précision et de robustesse pour les stratégies de commande. D'autre part, les systèmes considérés sont plus complexes, ce qui implique un nombre plus élevé de variables d'état et de capteurs. Dans ce contexte un défi important consiste à concevoir des lois de commande simples, faciles à calibrer, et flexibles de façon à assurer qu'une modification de l'architecture ne nécessite pas une nouvelle conception ou une nouvelle calibration complète du logiciel.

Dans cette thèse nous proposons d'étudier la commande des turbocompresseurs à travers trois architectures différentes de systèmes d'air qui correspondent à différents niveaux de complexité et illustrent donc bien ces problématiques :

- Un moteur essence avec un turbocompresseur à géométrie fixe
- Un moteur Diesel avec une turbine à géométrie variable et deux circuits de recirculation des gaz brûlés

– Un moteur Diesel avec un turbocompresseur à deux étages

Comme le système d'air est limitant pour la combustion, l'objectif est de minimiser le temps de réponse des turbocompresseurs. Mais la complexité du problème dépend des interactions avec les autres parties de la chaîne d'air. La démarche adoptée consiste à construire des modèles réduits non linéaires reposant sur une physique simplifiée et ne prenant en compte que les phénomènes dominants, puis à utiliser ces modèles pour synthétiser des lois de commande basées sur la planification de trajectoire et la linéarisation par retour d'état. Comme ces modèles sont simples ils permettent d'analyser les propriétés des systèmes bouclés et de prouver la convergence, la stabilité et le respect des contraintes. Les lois de commande sont ensuite validées expérimentalement sur les systèmes réels. Cette démarche est bien adaptée aux problématiques considérées parce qu'elle aboutit à des solutions flexibles. En effet, les modèles sur lesquels reposent les lois de contrôle s'appuyant sur une physique simplifiée, ils font intervenir des paramètres physiques qu'il suffit de changer en fonction des différentes architectures et dimensions.

Les contributions de la thèse sont les suivantes :

– Pour chaque cas d'étude :
  – Une analyse du système d'air aboutissant à un *modèle réduit*
  – *Une stratégie de commande validée expérimentalement* pour laquelle *la convergence, la stabilité et le respect des contraintes* sont prouvés sur le modèle réduit.
– *La démarche globale* et la démonstration que différents problèmes de commande de systèmes d'air peuvent être traités par des *solutions cohérentes*.

Plan

Ce document contient deux parties, chacune étant composée de trois chapitres. La première partie présente le contexte, la problématique, et propose des modèles pour les systèmes qui sont étudiés dans la seconde partie. Chaque chapitre de la seconde partie se concentre sur l'étude détaillée d'un cas d'application différent.

Partie 1 - Systèmes d'Air Suralimentés : Modélisation et Problématiques. —

Chapitre 1 - Moteurs à Combustion Interne et Problématiques. — Ce chapitre décrit brièvement la physique des moteurs à combustion interne, et les problématiques de développements. On s'attache en particulier à présenter l'impact des systèmes d'air sur les sorties moteur (couple, émissions polluantes, consommation de carburant). Cette analyse aboutit à l'exposé des avantages apportés par les turbocompresseurs :

– Sur les moteurs Diesel, les turbocompressseurs facilitent la recirculation des gaz brûlés et ont donc un impact sur les émissions polluantes.

– Sur les moteurs essence, les turbocompresseurs permettent d'améliorer la consommation de carburant et les émissions de CO_2 grâce à la technique de downsizing.

Chapitre 2 - Description et Modélisation des Systèmes d'Air. — Les principaux composants des systèmes d'air sont décrits : turbocompresseurs, systèmes de recirculation des gaz brûlés, blocs moteurs, capteurs et actionneurs. On propose un modèle physique simplifié pour chaque composant. Les trois architectures étudiées dans la suite sont introduits et chaque système d'air est modélisé.

Chapitre 3 - Problèmes de Commande des Systèmes d'Air. — En se basant sur les deux premiers chapitres, on construit les problématiques de la commande des systèmes d'air en général et des turbocompresseurs en particulier. Ces problématiques sont détaillées pour chacune des trois applications de façon à souligner leurs similitudes et leurs différences.

Partie 2 - Études de Cas. —

Chapitre 4 - Moteur Essence avec Turbocompresseur à Géométrie fixe. — Ce chapitre se concentre sur une application simple. Le système considéré est non linéaire du premier ordre. Le problème de commande est à une entrée une sortie (SISO) avec des contraintes sur l'actionneur. Un modèle physique mais orienté commande est proposé pour ce système et analysé de façon à comprendre ses principales propriétés. On propose une stratégie de commande basée sur une linéarisation par retour d'état et une planification de trajectoire sous contrainte. Elle consiste en l'inversion dynamique d'une représentation physique du système. La convergence et la stabilité du système bouclé sont prouvées. Des problèmes pratiques tels que les contraintes sur l'actionneur et l'anti emballement de l'intégrateur sont pris en compte à la fois dans le prépositionnement et dans le terme de bouclage du contrôleur. Des résultats expérimentaux montrent la pertinence de l'approche. La démarche et les développements de ce chapitre sont ensuite étendus dans les chapitres suivants à des applications plus complexes.

Ces travaux ont été publiés dans **[11, 13, 12]**.

Chapitre 5 - Moteur Diesel avec deux circuits d'EGR et VGT. — Le système d'air considéré dans ce chapitre est plus complexe car il contient plusieurs sous systèmes avec de multiples interactions. On utilise un niveau de représentation similaire à celui du chapitre 4 pour analyser le système. On montre que les dynamiques des circuits de recirculation des gaz brûlés sont plus rapides que celles du turbocompresseur et peuvent donc être négligées. Cependant les interactions statiques entre les systèmes imposent des contraintes sur la commande du turbocompresseur. La structure développée au chapitre 4 est adaptée à ce nouveau problème de commande. Les propriétés du système bouclé sont conservées. Des résultats expérimentaux sont montrés pour valider cette stratégie.

Ces travaux ont été partiellement publiés dans [**9, 6**], l'analyse de l'impact de l'EGR sur les trajectoires du système a été soumise pour publication dans [**14**]. La stratégie de commande a été brevetée en partie dans [**17**].

Chapitre 6 - Turbocompresseur double étage sur un moteur Diesel. — Cette dernière application est la plus complexe. On montre que le problème de commande peut être réduit à un problème à une entrée et une sortie (SISO), mais le système est du second ordre et des contraintes doivent être respectées sur un des états. On utilise des techniques similaires à celles des chapitres précédents. Un modèle réduit du second ordre en boucle fermée permet d'étudier les trajectoires du système dans le plan des phases. Des stratégies de commande sont ainsi synthétisées pour amener le système sur la trajectoire désirée tout en satisfaisant les contraintes.

Ces travaux ont été partiellement publiés dans [**5, 15**]. L'analyse du système du second ordre dans le plan des phases n'a pas encore été soumise pour publication. Une version simplifiée de la stratégie de commande a été brevetée dans [**10**].

CONCLUSION GÉNÉRALE

Cette thèse décrit le développement de stratégies de commande de turbocompresseurs basées sur un modèle physique réduit du système. Elle étudie trois architectures différentes :

- Un moteur essence avec turbocompresseur à géométrie fixe
- Un moteur Diesel avec turbocompresseur à géométrie variable et deux circuits de recirculation des gaz brûlés.
- Un moteur Diesel avec une suralimentation à deux étages.

On propose des solutions similaires pour chaque cas d'étude, tout en prenant en compte leurs spécificités. Le premier cas est le plus simple, le système est du premier ordre est SISO mais des contraintes sur la commande douvent être prises en compte. La stratégie de commande est basée sur la linéarisation par retour d'état et planification de trajectoire sous contrainte. Pour le second cas, les dynamiques de l'EGR sont négligées mais la trajectoire du turbocompresseur est modifiée pour assurer que la consigne d'EGR peut être atteinte. Le troisième cas est du second ordre, l'analyse dans le plan des phases des trajectoires du système bouclé conduit à la proposition d'une loi de commande simple qui assure un suivi rapide de la consigne tout en satisfaisant une contrainte sur l'un des états du système.

Les stratégies de commande sont donc basées sur un modèle réduit des turbocompresseurs qui est adapté à chaque cas d'étude par des modifications simples. Ce modèle tient compte des interactions entre le système considéré et les composants environnants, découplant ainsi les dynamiques des différents sous systèmes. On synthétise des stratégies de commande non linéaires simples qui tirent avantage des parties statiques et dynamiques du modèle.

Cette démarche offre la possibilité de prouver avec le modèle réduit des propriétés du système en boucle fermé, telles que la convergence, la stabilité et le respect des contraintes. La pertinence des stratégies est démontrée expérimentalement sur les système réels, justifiant ainsi a posteriori les hypothèses utilisées pour la réduction du modèle.

L'application de modèles similaires à trois architectures différentes montre que la représentation choisie est générique, et que le niveau de détail est pertinent. Ainsi, les développements proposés dans ce document fournissent une base utilisable pour l'étude des prochains systèmes d'air plus complexes.

On répond donc aux éléments principaux du cahier des charges d'un contrôle du système d'air :

- Une solution générique qui peut être adaptée à différentes architectures
- Une calibration réduite
- De bonnes performances transitoires
- Le découplage des différentes dynamiques

Perspectives

Futures évolutions des systèmes d'air. — D'autres systèmes d'air sont envisagés dans l'industrie, consistant en des architectures complexes avec des turbocompresseurs parfois associés avec d'autres types de suralimentation (une revue de systèmes à deux étages est publiée dans [**62**]; des compresseurs à onde de pression sont étudiés dans [**84**]). D'autre part, l'EGR est maintenant utilisé à forte charge sur des moteurs essence. Le problème de commande considéré au chapitre 5 est alors modifié car dans ce cas la combustion est stoechiométrique et donc l'EGR impacte directement la production de couple. Pourtant les développements présentés dans cette thèse sont suffisamment flexibles pour être adaptés facilement à ces nouvelles architectures parce qu'ils sont basés sur une description des interactions entre les différents sous systèmes et leur découplage.

Electrification du groupe motopropulseur. — L'hybridation des groupes motopropulseurs peut conduire à l'introduction de composants électriques dans le système d'air. Des turbocompresseurs assistés électriquement ou des systèmes de turbines combinées électriques et thermiques sont étudiées respectivement dans [**56**] et [**22**]. Ces systèmes nécessiteront le développement de nouvelles stratégies de commande. Les stratégies développées dans cette thèse permettant de prendre en compte des interactions avec d'autres composants, elles pourront être adaptées facilement à ce nouveau contexte.

D'autre part, les problématiques de commande de la boucle d'air sont modifiées dans un contexte hybride car le respect de la demande de couple est moins important pour le moteur thermique si un moteur électrique peut fournir une puissance additionnelle. Dans ce cas, la trajectoire calculée dans les différents exemples traités dans cette thèse peuvent être utilisées pour la supervision des moteurs thermiques et électriques. En effet, la trajectoire calculée au chapitre 4 est représentative du couple maximal qui peut être produit par le moteur thermique. Celle du chapitre 5 est représentative d'une contrainte de pollution.

Dans les deux cas ces contraintes peuvent être traduites en une contrainte sur le couple thermique et donc en une demande supplémentaire de couple électrique.

Diagnostic. — Le diagnostic est également en train de devenir une problématique cruciale pour ces systèmes complexes à cause de nouvelles normes plus contraignantes. Le diagnostic basé sur modèle semble bien approprié, et les réductions de modèles réalisées pour synthétiser des stratégies de commande et pour calculer des trajectoires peuvent également être utilisées pour diagnostiquer les systèmes. De premiers résultats concernant l'estimation de fuite dans le circuit d'admission d'un moteur Diesel avec EGR HP ont été publiés dans [**24, 23**]. L'extension des travaux présentés dans cette thèse à l'estimation de l'efficacité du turbocompresseur pour du diagnostic sera publiée dans [**25**]. Dans cet article un observateur de l'efficacité turbine est basé sur un niveau de modélisation similaire à celui utilisé au chapitre 5. Une analyse de sensibilité de l'observateur permet de calculer l'impact des dispersions capteurs ou système sur cette estimation, et de synthétiser un seuil représentatif du domaine de fonctionnement du système dans des conditions normales. Une erreur est détectée lorsque l'efficacité estimée est inférieure à ce seuil.

Le reste de ce document, pour la plus grande partie issu de travaux déjà publiés, est rédigé en langue Anglaise.

CONTENTS

Introduction Générale v
Plan vi

Conclusion Générale ix
Perspectives x

Contents xi

General Introduction xix
Outline xx

Notations and acronyms xxiii

Part I. Turbocharged Air Systems : Modeling and Issues 1

1. Internal combustion engines and issues 3
1.1. Introduction 3
1.2. Internal combustion engines 3
1.3. Air systems 10
1.4. Aftertreatment systems 11
1.5. Issues and trends for new engines developments 12
1.6. Conclusion 14

2. Description and Modeling of air systems 15
2.1. Introduction 15
2.2. Turbochargers 16
2.3. Exhaust Gas Recirculation 21
2.4. Engine model 24

2.5. Heat transfers 27
2.6. Interfaces with controllers : sensors and actuators 27
2.7. Description of three examples of air path architectures 29
2.8. Conclusion 36

3. Air Systems Control Issues 37
3.1. Introduction 37
3.2. Engine Control basics 37
3.3. First analysis of air systems 39
3.4. Air systems control issues 43
3.5. Sate of the art 48
3.6. Claims of the proposed control strategies 50
3.7. Conclusion 52

Part II. Case Studies 53

4. Gasoline engines with fixed geometry turbines 55
4.1. Introduction 55
4.2. Air system model reduction 56
4.3. System analysis 64
4.4. Feed forward and Motion planning: design of a feasible trajectory 69
4.5. Control strategy 71
4.6. Experimental validation 75
4.7. Conclusion 82

5. Diesel engines with two EGR loops and VGT 85
5.1. Introduction 85
5.2. Comprehensive engine model 86
5.3. Dynamics separation and EGR control 89
5.4. Model reduction for turbocharger control 91
5.5. Reduced model analysis 95
5.6. Turbocharger control strategy 100
5.7. Complete air system control strategy 104
5.8. Experimental results 105
5.9. Limits of the approach and potential improvements 110
5.10. Conclusion 110

6. Two stage turbochargers on Diesel engines 113
6.1. Introduction 113
6.2. Reference single stage turbocharger control 114

6.3. Analysis of two stage turbocharger control issues . . . 117
6.4. Design of a two stage turbocharger control strategy . . . 127
6.5. Simulation and experimental results . . . 136
6.6. Conclusion . . . 141
Appendix . . . 142

General Conclusion . . . 143
Perspectives . . . 144

A. Gas exchanges modeling . . . 147
A.1. Receivers and manifolds . . . 147
A.2. Restrictions and Valves . . . 150

Personal publications and patents . . . 153

Bibliography . . . 155

AIR SYSTEMS MODELING AND CONTROL FOR TURBOCHARGED ENGINES

Abstract. — The performances of internal combustion engines are limited by the quantity of fresh air and burned gas that can be brought into the cylinder by their air system. Turbochagers enable to increase this quantity and this is the reason why they are now used commonly, often combined with other complex components. These systems generate a slow dynamics on the engine. The associated control strategies are therefore complex because they must utilize the full dynamics of a complex system. This thesis investigates the control problems of turbocharged air systems through three case studies : a fixed geometry turbocharger on a gasoline engine, a variable geometry turbine on a Diesel engine fitted with two exhaust gas recirculation circuits, and a two stage turbocharger on a Diesel engine.

The proposed approach consists in the reduction of a physical model of the system and in the design of simple control strategies based on the analysis this model. Thanks to the simplicity of both the reduced model and the control law, it is possible to prove properties of the closed loop system such as the convergence, the stability and the satisfaction of constraints. Experimental results are provided for each case study in order to demonstrate the relevance of the approach.

The first problem considered is single input single output (SISO) with constraints on the actuator. The system is non linear and first order. The control strategy is based on feedback linearization and constrained motion planning. It consists in a dynamic inversion of a physical representation of the system. Practical issues such as actuator constraints and integrator anti wind up are taken into account in both feedforward and feedback terms of the controller. The approach and the developments are then extended to more complex applications.

The second air system considered contains several subsystems with many interactions : turbocharger and exhaust gas recirculation circuits. A similar level of representation as for the first case is used for the system analysis. It is shown that the dynamics of the

exhaust gas recirculation circuits are faster than that of turbochargers and can therefore be neglected. However the static interactions between the two systems impose constraints on the turbocharger control. The control structure developed for the first example is adapted to this new control problem.

The last application is the most complex one. The control problem can be reduced to a single input single output (SISO) problem, but the system is second order and constraints must be respected on one of the states. A reduced physical second order model allows to study the trajectories of the closed loop system in the phase plane. Control strategies are thus designed to force the system to the desired trajectory while satisfying the constraints.

The thesis thus shows that different air systems control problems can be addressed with similar coherent solutions. The global approach and the chosen modeling level are generic. They can therefore be extended to future air systems control problems, but also to diagnostic problems for which they are well adapted.

GENERAL INTRODUCTION

In the automotive industry, the reduction of fuel consumption and pollutant emissions is the main driving force for the development of new engine technologies. It leads to the design of systems with complex architectures, combining several subsystems with many interactions. This is particularly the case for new engines air systems which bring the gas (air and burned gas) into the cylinder and therefore impose a limit on the combustion. This is why the air systems contain most of the times a turbocharger in order to increase the gas density at the intake of the engine and to improve its static performances. The drawback of turbochargers comes from their slow response time. It can be compensated for by the use of variable geometry turbine, or by the addition of other devices : for example another turbocharger or a mechanical compressor. In some cases, high or low pressure exhaust gas recirculation circuits make the system even more complex.

The engine control softwares must also be adapted to these changes for several reasons. First the more stringent legislation asks for better performances in terms of accuracy and robustness for the control strategies. At the same time the systems considered are more complex, implying an increased number of state variables and actuators. In this context an important challenge consists in the design of simple, easy to calibrate, and flexible control laws in order to ensure that a modification of the architecture does not require a new design or a new calibration of the complete software.

In this thesis we propose to study the control of turbochargers through three different air systems architectures corresponding to different levels of complexity which illustrate these issues :

- Gasoline engines with fixed geometry turbines
- Diesel engines with variable geometry turbocharger and two exhaust gas recirculation loops
- Diesel engines with two stage turbochargers

Since the air system is limiting for the combustion, the objective is to minimize the response time of turbochargers. However, the complexity of the control problem depends on the interactions with the other parts of the air systems. The approach consists of building reduced nonlinear models relying on a simplified physics and taking into account only the main phenomena, and then of using these models to design control strategies based on motion planning and feedback linearization. Because these models are simple they allow to analyze the properties of the closed loop systems and to prove the convergence, the stability and the constraints satisfaction. The control strategies are then validated experimentally on the real systems. This approach is well adapted to the issues considered because it results in flexible solutions. Since the models on which the control laws are based rely on a simplified physics, they embed physical parameters that can be changed easily for various architectures or dimensions.

The contributions of the thesis are the following :

- For each case study :
  - The analysis of the air system leading to a *reduced model*
  - *The control strategy* validated experimentally for which *the convergence, the stability and the constraints satisfaction* are proved with the reduced model.
- *The global approach* and the demonstration that different air systems control problems can be addressed with similar *coherent solutions*.

Outline

This document contains two parts, each consisting of three chapters. The first part presents the context, the issues and proposes a model of the systems studied in the second part. Each chapter of the second part focuses on the detailed study of a different application.

Part 1 - Turbocharged Air Systems : Modeling and Issues. —

Chapter 1 - Internal combustion engines and issues. — This chapter describes shortly the physics of internal combustion engines, and the issues faced in their developments. The impact of the air systems on the engine outputs (torque, pollutant emissions, fuel consumption) is highlighted. This analysis shows that the advantages brought by the turbochargers are :

- On Diesel engines, turbochargers help the recirculation of exhaust gas and have therefore an impact on pollutant emissions.
- On gasoline engines, turbochargers enable to improve the fuel consumption and CO_2 emissions thanks to the technique called downsizing.

Chapter 2 - Description and modeling of air systems. — The main components of the air systems are described : turbochargers, exhaust gas recirculation systems, engines, sensors and actuators. We propose a simplified physical model for each component. The three architectures studied in the following are introduced and each of their air systems are modeled completely.

Chapter 3 - Air systems control issues. — Based on the two first chapters, the control issues are deduced for air systems in general and for turbochargers in particular. These issues are detailed for each of the three applications, in order to underline their similarities and their differences.

Part 2 - Case Studies. —

Chapter 4 - Gasoline engines with fixed geometry turbines. — This chapter focuses on a simple application. The system considered is non linear and first order. The control problem is single input single output (SISO) with constraints on the actuator. A physical but control oriented model is proposed for this system and analyzed in order to understand its main properties. It presents a control strategy based on feedback linearization and constrained motion planning. It consists in a dynamic inversion of a physical representation of the system. The convergence and stability of the closed loop system are proved. Practical issues such as actuator constraints and integrator anti wind up are taken into account in both feedforward and feedback terms of the controller. Experimental results show the relevance of the approach. The approach and the developments of this chapter are then extended in the next chapters to more complex applications.

This work has been published in [**11, 13, 12**].

Chapter 5 - Diesel engines with two EGR loops and VGT. — The air system considered in this chapter is more complex because it contains several subsystems with many interactions. We use a similar level of representation as in chapter 4 in order to analyze the system. We show that the dynamics of the EGR circuits are faster than that of turbocharger and can therefore be neglected. However the static interactions between the two systems impose constraints on the turbocharger control strategy. The control structure developed in chapter 4 is adapted to this new control problem. The properties of the closed loop system are conserved. Experimental results are shown to validate this strategy.

This work has been partly published in [**9, 6**], the analysis of the impact of EGR on the system trajectories has been submitted for publication in [**14**]. The control strategy is partially patented in [**17**].

Chapter 6 - Two stage turbochargers on Diesel engines. — This last application is the most complex one. We show that the control problem can be reduced to a single input single output (SISO) problem, but the system is second order and constraints must be

respected on one of the states. We use similar techniques as in the previous chapters. A reduced second order model allows to study the trajectories of the closed loop system in the phase plane. Control strategies are thus designed to bring the system to the desired trajectory while satisfying the constraints.

This work has been partly published in [**5, 15**]. The analysis in the phase plane of the second order system has not been submitted for publication yet. Simplified versions of the control strategy have been patented in [**10**].

NOTATIONS AND ACRONYMS

Acronyms

EGR	Exhaust Gas Recirculation
VGT	Variable Geometry Turbine
WG	Wastegate
BGR	Burned Gas Ratio
NOx	Nitrogen Oxides
CO	Carbon monoxide
CO2	Carbon Doxides
HC	Unburned hydrocarbons
PM	Particulates Matters
MIMO	Multiple Inputs Multiple Outputs
SISO	Single Inputs Single Outputs
HP	high pressure
LP	low pressure
PI	Proportional Integral controller

Notations

The derivative of variable x with respect to time $\frac{dx}{dt}$ is noted $\dot{x}$.

Var.	Quantity	Unit
$\mathcal{W}$	Work	J
$\mathcal{P}$	Power	W
$\mathcal{T}$	Torque	N.m
P	Pressure	Pa
T	Temperature	K
M	Mass	kg
F	Burned gas mass fraction	-
Π	Pressure ratio	-
S	Cross-section	m^2
J	Inertia	$kg.m^2$
V	Volume	m^3
λ_s	Fuel air stoichiometry ratio	-
AF_s	Air fuel stoichiometry ratio	-
η	Efficiency	-
η_{vol}	Engine volumetric efficiency	-
γ	Ratio of specific heat	-
R	Mass gas constant	$J.kg^{-1}.K^{-1}$
C_p	Specific heat capacity	$J.kg^{-1}.K^{-1}$
D	Mass flow	kg/h
N_t	Turbocharger speed	$rad.s^{-1}$
N_e	Engine speed	rpm

Subscripts

t	turbine
c	compressor
u	upstream
d	downstream
wg	wastegate
vgt	variable geometry turbine
exh	exhaust manifold
man	intake manifold
int	intercooler
amb	ambiant
air	fresh air
asp	aspirated
f	fuel
pf	particulate filter
cyl	cylinder
ind	indicated
eff	effective
sp	set-point
eq	equilibrium
st	stroke

PART I

TURBOCHARGED AIR SYSTEMS : MODELING AND ISSUES

CHAPTER 1

INTERNAL COMBUSTION ENGINES AND ISSUES

1.1. Introduction

The purpose of this chapter is to introduce the problem considered in the document : air systems control for turbocharged engines. We first describe the functioning of the internal combustion engines, in order to show the role of their air systems. We then explain the main issues driving the developments of new engines technologies and of their control strategies. We do not intend to give an exhaustive description of these topics but to provide sufficient information for the understanding of the objectives targeted in the developments of the following chapters. More information can be found for example in [**47, 44**].

1.2. Internal combustion engines

The purpose of an internal combustion engine is to produce a mechanical torque. This torque is the result of the expansion of high temperature and pressure gases produced by the combustion of a mixture of fuel and air. In automotive engines the combustion is intermittent. It occurs in a closed cylinder and the released energy is transformed into mechanical energy via the motion of pistons connected to a crankshaft.

Figure 1.1 shows the diagram of a turbocharged gasoline engine. The gases enter and exit the cylinder through valves which are also connected to the crankshaft. The air system consists in the components located upstream the intake valve and downstream the exhaust valve. It has an impact on the thermodynamics properties (pressure, temperature and

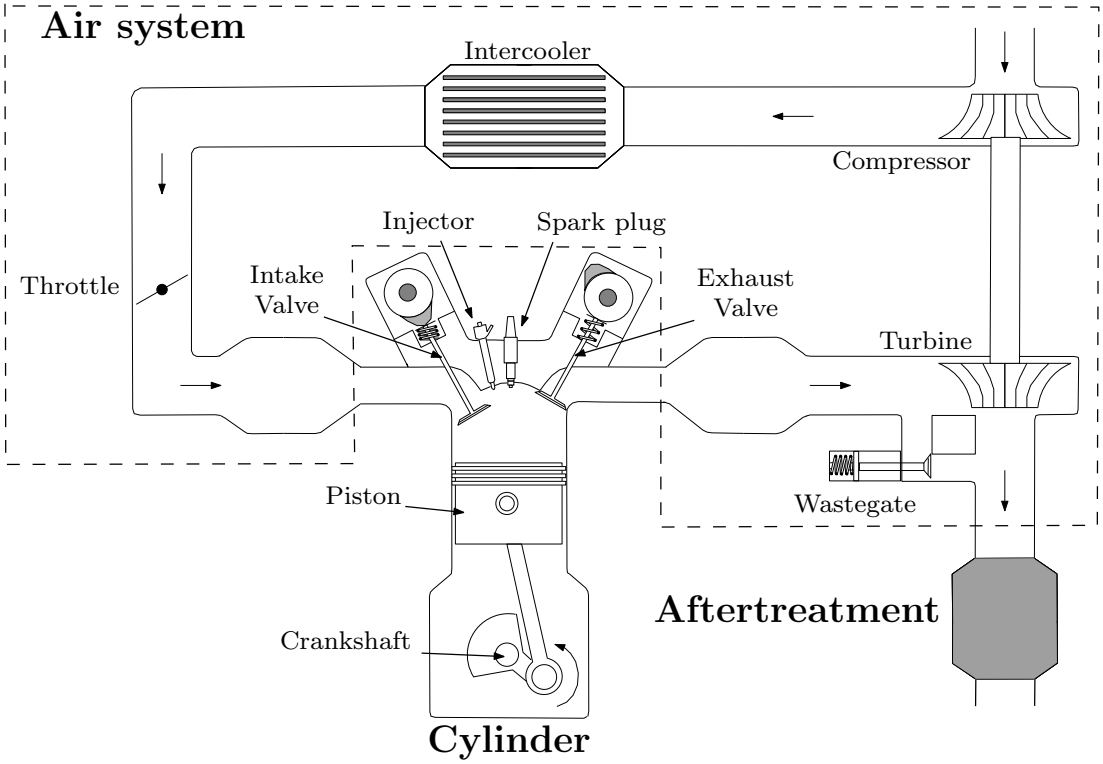

FIGURE 1.1. Gasoline Turbocharged Engine

composition) of the gas mixture which is trapped in the cylinder when the valves are closed. Therefore it influences the combustion and its results : the torque produced and the pollutant emissions. The following subsections describe this effect on the pollutant formation and on the thermodynamic cycle of a four stroke internal combustion engines.

1.2.1. Thermodynamic cycle. — The left hand side of figures 1.2 shows the cylinder pressure, the cylinder volume, and the lift of intake and exhaust valves during two revolutions corresponding to a full thermodynamic cycle of a four stroke combustion engines. The cycle can be split in four phases : intake, compression, expansion and exhaust. The combustion occurs at the beginning of the expansion phase.

Since the force of the gases on the piston is equal to the product between the cylinder pressure and the piston surface, the work $\mathcal{W}_{th}$ produced during the cycle is equal to the

integral

$$\mathcal{W}_{th} = \int_{4\pi} P_{cyl} dV$$

This work can be decomposed into four parts corresponding to each phase of the cycle :

$$\mathcal{W}_{th} = \mathcal{W}_{int} + \mathcal{W}_{comp} + \mathcal{W}_{exp} + \mathcal{W}_{exh}$$

On the diagram shown on the right hand side of figure 1.2, $\mathcal{W}_{th}$ corresponds to the area inside the pressure curve. The upper area (high pressure) is called $\mathcal{W}_{hp}$, and the lower area (low pressure) is called $\mathcal{W}_{lp}$. We have $\mathcal{W}_{hp} = \mathcal{W}_{comp} + \mathcal{W}_{exp}$ and $\mathcal{W}_{lp} = \mathcal{W}_{int} + \mathcal{W}_{exh}$.

The different phases are analyzed in the seuqel.

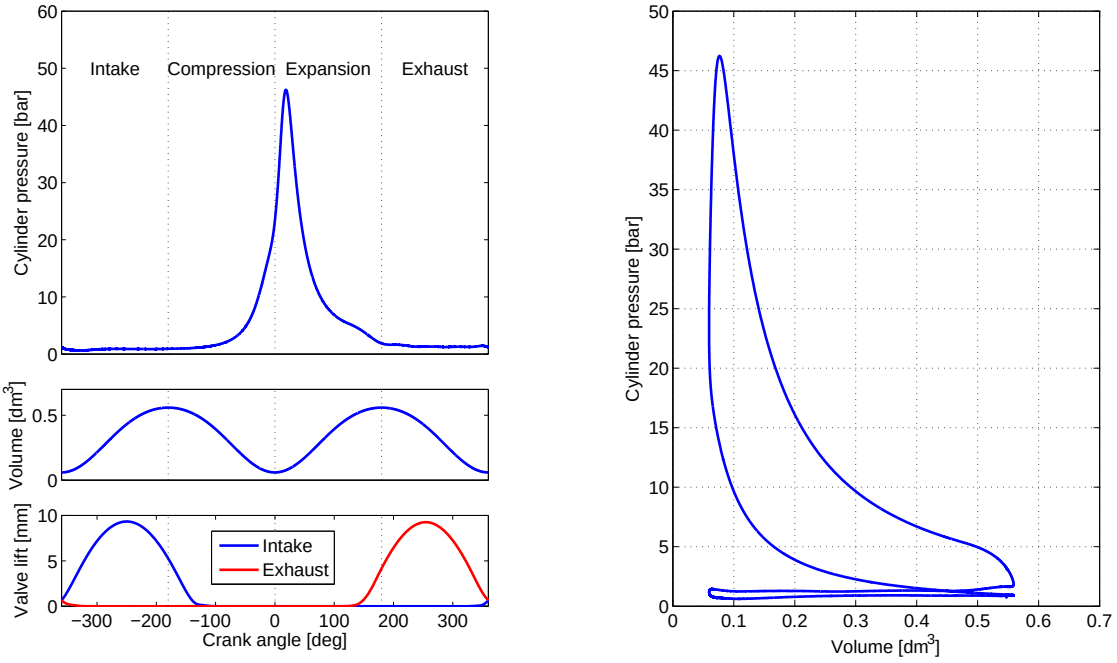

FIGURE 1.2. Thermodynamic cycle : cylinder pressure, cylinder volume and valves lifts (left hand side figure), and PV diagram (right hand side figure).

Intake. — The intake valve is opened and the cylinder volume increases. Gases enter in the cylinder through the intake valve. The gas mass M_{asp} aspirated in the cylinder can be

computed as :

$$M_{asp} = \eta_v \frac{P_{man} V_{cyl}}{R T_{man}} \tag{1.1}$$

where V_{cyl} is the cylinder volume and η_v is the volumetric efficiency.

The gas composition in the cylinder is the consequence of the mixture between residual burned gas in the cylinder after the exhaust phase and intake gas that have the same composition as in the intake manifold. The residual gas are often neglected because their proportion is very small. Therefore, the mass of air in the cylinder at the start of combustion is :

$$M_{air} = (1 - F_{man}) M_{asp} \tag{1.2}$$

So, from (1.1) :

$$M_{air} = (1 - F_{man}) \eta_v \frac{P_{man} V_{cyl}}{R T_{man}} \tag{1.3}$$

Also, we consider as a first approximation that the cylinder pressure is constant during this phase. It is equal to the pressure in the intake manifold : $P_{cyl} = P_{man}$. This assumption leads to :

$$\mathcal{W}_{int} = P_{man} V_{cyl,d} \tag{1.4}$$

where $V_{cyl,d}$ is the volume displaced by the cylinder, equal to the difference between maximum and minimum volume : $V_{cyl,d} = V_{cyl,max} - V_{cyl,min}$

Compression. — The intake valve is closed and the cylinder volume decreases. The gases in the cylinder are compressed. The gases mass and composition are not affected during this phase. Because the cylinder volume decreases, the work $\mathcal{W}_{comp}$ is negative.

Combustion and Expansion. — The combustion occurs at the end of the compression and before the expansion phase. During the combustion, fuel and air are transformed into burned gas. If the mixture is stoichiometric (gasoline engines), only burned gas remain in the cylinder at the end of the combustion and therefore in the exhaust line. For lean mixtures (Diesel engines), all the fuel is burned. The burned gas concentration in the cylinder at the end of the combustion and during the expansion phase is therefore :

$$F_{cyl} = \frac{M_{fuel}(AF_s + 1) + F_{man} M_{asp}}{M_{asp} + M_{fuel}} \tag{1.5}$$

where the constant AF_s is the stoichiometric equivalent air fuel ratio.

A high quantity of energy is released in the cylinder during the combustion and the cylinder pressure and temperature raise to high values. Then the cylinder volume increases and the gases are expanded. The work produced during this phase $\mathcal{W}_{exh}$ is positive.

The high pressure work $\mathcal{W}_{hp}$ is the sum of $\mathcal{W}_{comp}$ and $\mathcal{W}_{exp}$. It depends on the quantity of fuel and fresh air trapped in the cylinder. It can be approximated as :

$$\mathcal{W}_{hp} = \eta_{ind} \min\{M_{fuel}, \frac{M_{asp}(1 - F_{man})}{AF_s}\} Q_{lhv} \tag{1.6}$$

where η_{ind} is the indicated efficiency and the constant Q_{lhv} is the fuel lower heating value. For simplicity reasons we will consider that η_{ind} does not depend on the air system. This is an approximation that does not affect the conclusions made below.

Exhaust. — The exhaust valve is opened and the cylinder volume decreases. The cylinder gases exit the cylinder through the exhaust valve.

As for the intake phase, we can consider that the cylinder pressure is constant during the exhaust phase, equal to the pressure in the exhaust manifold : $P_{cyl} = P_{exh}$. So :

$$\mathcal{W}_{exh} = -P_{exh} V_{cyl,d} \tag{1.7}$$

From (1.4) and (1.7), we deduce that :

$$\mathcal{W}_{lp} = (P_{man} - P_{exh}) V_{cyl,d} \tag{1.8}$$

There is a simple proportional dependency between the low pressure work and the difference between intake and exhaust pressures. If the exhaust pressure is higher than the intake pressure, this work is negative.

1.2.2. Torque production and efficiency. —

Indicated torque. — The torque produced during the combustion is called the indicated torque. The work $\mathcal{W}_{th}$ produced during the cycle and the engine indicated torque $\mathcal{T}_{ind}$ are proportional : $\mathcal{W}_{th} = 4\pi \mathcal{T}_{ind}$.

Gathering (1.6) and (1.8), we have :

$$\mathcal{T}_{ind} = \frac{1}{4\pi}(\eta_{ind} \min\{M_{fuel}, \frac{P_{man}(1 - F_{man})}{RT_{man}} \frac{\eta_v V_{cyl}}{AF_s}\} Q_{lhv} + (P_{man} - P_{exh}) V_{cyl,d}) \tag{1.9}$$

Maximum torque. — The maximum indicated torque that can be produced by an engine can be deduced from (1.9). It is generally obtained with $F_{man} = 0$. It is limited by the maximum intake manifold pressure, and is equal to :

$$\mathcal{T}_{ind,max} = \frac{1}{4\pi}(\eta_{ind} \frac{P_{man,max}}{RT_{man}} \frac{\eta_v V_{cyl}}{AF_s} Q_{lhv} + (P_{man,max} - P_{exh}) V_{cyl,d}) \tag{1.10}$$

Equations (1.9) and (1.10) highlight the main influence of the air system on the torque

production : the torque is limited by the quantity of air trapped in the cylinder, and the losses depend on the engine size and on the difference between exhaust and intake pressure.

Effective torque. — The brake torque or effective torque $\mathcal{T}_{eff}$ is the torque transmitted by the engine crankshaft to the transmission. It is lower than the indicated torque because of mechanical friction losses $\mathcal{T}_{fric}$. We have :

$$\mathcal{T}_{eff} = \mathcal{T}_{ind} - \mathcal{T}_{fric} \tag{1.11}$$

These losses are increasing with respect to engine speed. It is also generally considered that they depend on the mass of the moving elements, and therefore on the engine size. This increases the dependence on the cylinder volume that can be found in equation (1.9).

Efficiency. — The system efficiency can be defined as the ratio between the effective work and the total energy brought in the system : $\eta_{eff} = \dfrac{4\pi\mathcal{T}_{eff}}{M_{fuel}Q_{lhv}}$

From (1.9) and (1.11) :

$$\eta_{eff} = \eta_{ind}\min\{1, \frac{P_{man}(1-F_{man})}{RT_{man}}\frac{\eta_v V_{cyl}}{M_{fuel}AF_s}\} + \frac{(P_{man}-P_{exh})V_{cyl,d} - 4\pi\mathcal{T}_{fric}}{M_{fuel}Q_{lhv}} \tag{1.12}$$

Specific fuel consumption. — The brake specific fuel consumption ($BSFC$) is the ratio between the fuel mass injected in the engine during a cycle and the output power $\mathcal{P}_{eng} = \mathcal{T}_{eff}N_e 2\pi$. So :

$$BSFC = \frac{4\pi}{\eta_{eff}Q_{lhv}} \tag{1.13}$$

1.2.3. Pollutant emissions. — The main by-products of the combustion are carbon dioxide and water, but other chemical species can be found at the exhaust of the engine. Some of these products are considered as pollutant emissions and are limited by the legislation. It is the case for unburned hydrocarbons (HC), nitrogen oxides (NO_x), carbon monoxide (CO) and particulate matters (PM). The production of these pollutant emissions during the combustion is the result of a complex process. It depends on local thermodynamic conditions in the cylinder chamber during the combustion. Since this document focuses on air systems control, we do not describe in detail these dependencies.

However, we are interested in the impact of the air system on the thermodynamic conditions of the gas trapped in the cylinder at the end of the intake phase, and therefore on the engine pollutant emissions. For example, figure 1.3 shows the effect of a variation of the concentration in burned gas in the intake manifold F_{man} on the four main pollutant emissions for various engine operating points of a Diesel engine. First we can notice that it is

not possible to find a concentration that minimizes the four pollutant emissions. Whereas NO_x emissions decrease with respect to F_{man}, CO and PM tend to increase and HC have a parabolic shape with a minimum at medium F_{man}. These trends can be generalized to other operating points.

This short analysis shows the complex link between the different pollutant emissions and the influence of the air system. The effect of a variation of intake gas composition on the pollutant emissions must be underlined. It implies that if the air system allows a high level of burned in the cylinder, then it offers a potential for pollutant emissions.

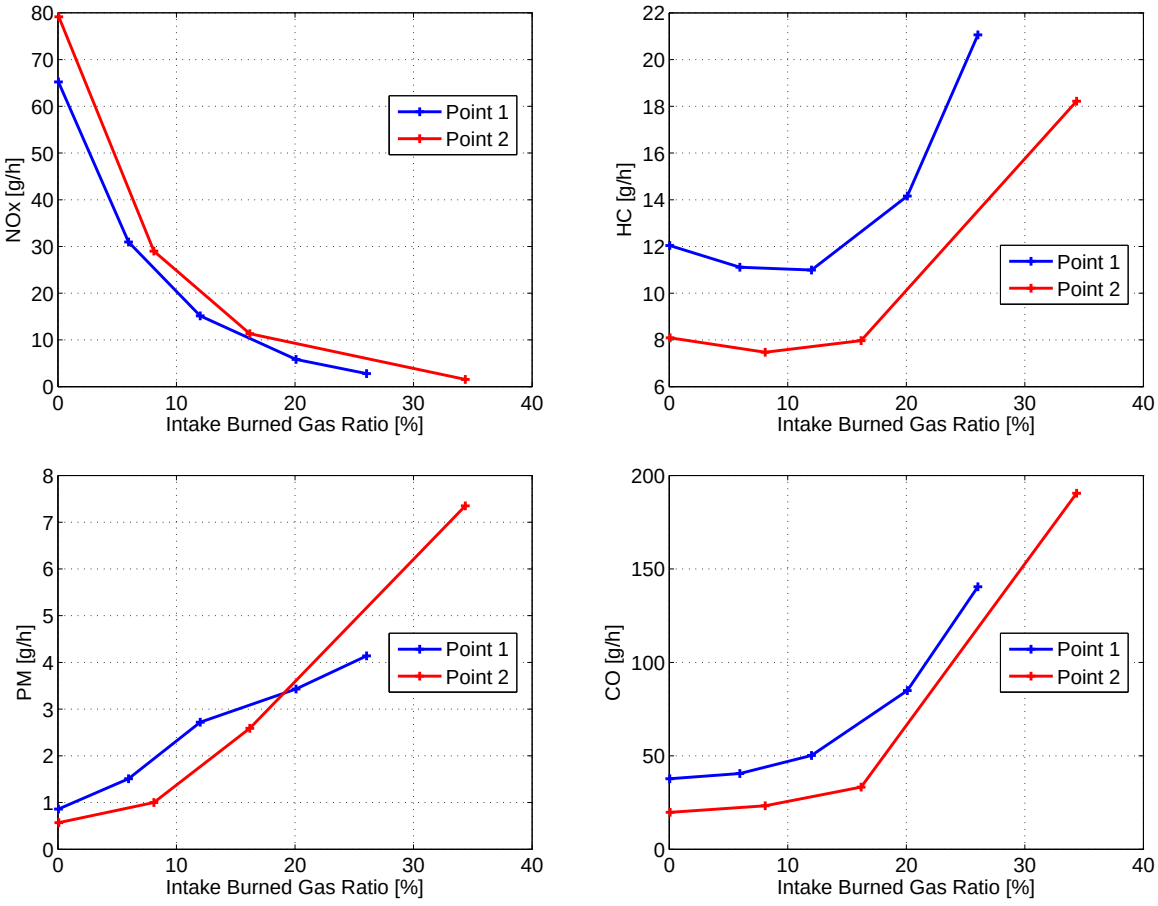

FIGURE 1.3. Pollutant emissions of a Diesel engine for two different operating points. Point 1 : Ne=2000rpm, Mfuel=13mg/st. Point 2 : Ne=1500rpm, Mfuel=16.5mg/st

1.3. Air systems

1.3.1. Definition and short description. — The detailed description of the different components of air systems is given in chapter 2. We call air system the part of the engine in charge of bringing fresh air at the intake of the cylinder and of bringing the exhaust gases through the aftertreatment system and down to the atmosphere. They are made of various components, some of which generate connections between the intake and the exhaust part. The main components that will be considered in this document are the following :

- *Throttles, valves* : these actuators are used to generate pressure drops in the system and therefore to control the gas flow between two components.
- *Manifolds* : these volumes are used to distribute gas to the cylinders or to collect it at the exhaust.
- *Compressors* : This component transforms mechanical (or electrical) energy into enthalpy. The gas density downstream from this component is increased, and as a consequence the gas density (and mass) in the cylinder can be increased (equation (1.3)).
- *Turbines* : These components are symmetric to compressors. The purpose of turbines is to convert the energy contained in the exhaust gases into mechanical energy. Therefore they enable to increase the system global efficiency.
- *Heat exchangers* : Heat is transfered to an exterior medium, often a coolant circuit or the atmosphere.

We often consider subsystems which are composed by several of these components. The main ones are :

- *Turbochargers* : composed by a compressor and a turbine connected by a common shaft, this system is widely used to transfer exhaust energy to the intake. It will be studied in detail in this document.
- *Exhaust Gas Recirculation circuits (EGR)* : exhaust gases are transfered to the intake system via a specific circuit. This system enables to modify the composition of the intake gas and therefore offers a means of action on the combustion and on the pollutant emission.

1.3.2. Impact of the air systems on the combustion. — The air systems determine the mass and composition of the gas in the cylinder before the combustion. Following equations (1.9), (1.10) and (1.12) and the analyses exposed above, we can deduce the main influences of the air systems on the combustion outputs : torque production, engine efficiency and pollutant emissions.

Effect of intake gas composition. — There is no effect on the efficiency as long as the mixture is lean. The effect is important on pollutant emissions. However, the cylinder air mass and hence the available energy is decreasing with respect to F_{man} for a constant intake gas density. For a constant fuel mass and intake manifold density, the burned gas concentration F_{man} (and hence the level of action on the pollutant emissions) is therefore limited in order to ensure that the mixture is lean. The limit value is

$$F_{lim} = 1 - M_{fuel}\frac{RT_{man}}{P_{man}}\frac{AF_s}{\eta_v V_{cyl}}$$

This limit also affects the potential impact on the pollutant emissions. This value is decreasing with respect to fuel mass and increasing with respect to intake manifold density.

Effect of intake gas density. — When the air density $\frac{P_{man}}{RT_{man}}$ is increased, it is possible to increase the mass of gas in the cylinder before the combustion. It follows that the maximum engine torque and therefore the engine power capacity are increased. Also, there is an indirect effect on the pollutant emissions because the limit F_{lim} on the intake burned gas concentration is increased. The efficiency is increased because the low pressure work is increasing with respect to P_{man}. The maximum torque is increased.

Effect of engine exhaust pressure. — The efficiency is decreasing with respect to exhaust pressure.

1.4. Aftertreatment systems

Aftertreatment systems are located in the exhaust system downstream from the engine. They are in charge of decreasing the level of pollutant emissions of the engine in the atmosphere. Different types of systems can be found in the industry. The main ones are :

- *Three Way Catalysts (TWC).* These chemical converters are in charge of three different reactions : reduction of nitrogen oxides into nitrogen and oxygen, oxidation of carbon monoxide to carbon dioxide, and oxidation of unburned hydrocarbons into carbon dioxide and water. The gas mixture must be in stoichiometric conditions in order to ensure a correct functioning of the converters. In this case and in hot conditions their efficiency is close to 100%. Therefore these systems are widely used on gasoline engines but cannot be applied to Diesel engines.
- *Diesel Oxidation Catalysts (DOC).* These systems are similar to TWC except that they only deal with the oxidation reactions. They are used on Diesel engines to decrease CO and HC emissions.

- *NO_x traps.* For lean gas mixtures, these systems trap NO_x molecules thanks to a special washcoat containing zeolites. Once the trap is full it must be regenerated, requiring specific thermodynamic conditions and therefore specific actions from the engine management system. The regenerations also induce additional fuel consumption. The frequency of these regenerations depend on the size of the trap and on the raw NO_x emissions of the engine. In order to avoid frequent regenerations, the engine raw emissions must be diminished.
- *Diesel Particulate filters (DPF).* Similarly to the NO_x trap, these systems capture the particulate matters present in the exhaust gases, and must be regenerated when full.
- *Selective Catalytic Reduction (SCR).* These catalysts convert nitrogen oxides with the help of reductants, usually ammonia or urea.

The study of these systems is out of the scope of air systems control. They have a light impact on the system functioning, only because they generate pressure drops that can be considered as disturbances. However they are very important on the pollutant emissions and therefore on the constraints imposed on the operating conditions of the engines. As a consequence they affect the control issues that must be addressed by the engine control.

1.5. Issues and trends for new engines developments

The developments of new technologies in the automotive industries are driven by two major requirements imposed by the legislation and the market needs : the decrease of CO_2 emissions (and hence the fuel consumption), and the constraints on pollutant emissions.

These two requirements have similar effects on the new technologies of engines : they imply an increase in complexity of the system and require at the same time a more complex and a more accurate control for the system.

1.5.1. Pollutant emissions. — The legislation tends to increase the restrictions imposed on the pollutant emissions of vehicles. The required levels force to combine internal combustion engines with efficient aftertreatment systems. However these requirements have a different impact on gasoline and Diesel engines.

Concerning gasoline engines, three way catalysts can be used. They are very efficient after the warm up phase, but they impose to operate with a stoichiometric mixture in the exhaust system. In this case the raw engine emissions are not an issue, and there is no requirement for the air system : an exhaust gas recirculation system is not necessary.

On the contrary, Diesel engines operate with a lean mixture. Their aftertreatment systems are generally composed by a combination of DOC and DPF. The addition of

NO_x traps is not necessary for Euro V standards but will probably be necessary for the next legislation (Euro VI). Even with NO_x traps the engine raw NO_x emissions are an issue because the frequency of the regenerations must be decreased. Therefore the use of complex air systems is necessary including exhaust gas recirculation and supercharging.

1.5.2. Fuel consumption and CO_2 emissions. — Fuel consumption has been an important concern for the automotive industry because it adds value for the clients. It is now becoming even more important because of the future legislation on CO_2 emissions.

In fact, CO_2 emissions depend directly on fuel consumption and therefore on the system efficiency. Equation (1.12) highlights the main level of actions to improve the efficiency : the indicated efficiency η_{ind}, the low pressure work $(P_{man} - P_{exh})V_{cyl,d}$ and the friction torque $\mathcal{T}_{fric}$.

The indicated efficiency is linked with the type of combustion : it is higher for Diesel engines than for gasoline engines. It is not impacted by air systems.

The use of supercharging or turbocharging with an air cooler enables to increase P_{man} and therefore has a positive impact on the efficiency and on the maximum torque. For a given maximum toque, an increase of intake manifold pressure enables to decrease the cylinder volume, which has also a positive impact on the efficiency (if $P_{exh} > P_{man}$). This has also an effect on the friction torque : a lower cylinder volume implies a lower engine size and therefore less friction losses.

The technique consisting of decreasing the size of the engine and using turbocharging to compensate for the loss of power is called downsizing. It has been detailed in various publications (see for example [**45, 61, 72, 58, 40**]). It is used mostly for gasoline engines. It can also be applied to Diesel engines but to a lesser extent because a lower cylinder volume would limit the quantity of exhaust gas recirculated.

1.5.3. Resulting engines air systems architectures. — Engine air systems are adapted to help address the main issues for the development of modern engines. In particular supercharging or turbocharging techniques are of interest and they become more and more necessary.

Gasoline engines. — Modern gasoline engines are more and more often associated with turbochargers. These systems enable to improve the fuel consumption and CO_2 emissions thanks to the technique called downsizing. They are fitted with efficient aftertreatment systems and thus have low pollutant emissions.

Diesel engines. — On Diesel engines, exhaust gas recirculation circuits are necessary for pollution reasons. Turbochargers increase the maximal fraction of burned gas that can be brought to the cylinder. Downsizing the engine requires a very high level of supercharging. Current Diesel engines are therefore generally fitted with a turbocharger and a high pressure EGR circuit. Newer technologies use two stage turbochargers.

Future technologies. — Other types of air systems architectures are under investigation for gasoline and Diesel engines. They always involve the use of supercharging techniques : mechanical superchargers, turbochargers power assist systems (electrical superchargers in [**56**], turbo compound in [**22**]), combination of different types of supercharging (see a survey of dual stage boosting systems in [**62**]). For these various technologies the objectives are similar : reduction of CO_2 and pollutant emissions by increasing the quantity of gas in the combustion chamber.

1.6. Conclusion

This chapter introduces the document by a description of the context : internal combustion engines and the issues that drive the new developments in the automotive industry. The role of the air systems of the engines with respect to the torque production and the pollutant emissions is highlighted, showing the interest in the use of supercharging.

The main conclusions are the following :

– On Diesel engines, turbochargers help the recirculation of exhaust gas and have therefore an impact on pollutant emissions.
– On gasoline engines, turbochargers enable to improve the fuel consumption and CO_2 emissions thanks to the technique called downsizing.

However, the effect of turbochargers on the combustion is not instantaneous : their dynamics imply a time response and therefore a limit on the engine. Next chapter describes in detail the various components of the air systems, emphasizing the dynamics induced by these components and the interactions between them. Models are proposed for each component and for complete air systems. The objectives and issues of the turbocharger control strategies described in chapter 3 will naturally result from the analysis made in these two first chapters.

CHAPTER 2

DESCRIPTION AND MODELING OF AIR SYSTEMS

2.1. Introduction

The approach adopted for the development of the control strategies consists in an iterative process containing three steps where the models of the systems play a crucial role :

- Understanding of the system based on a complete physical representation of the system
- Proposition of a control strategy based on a reduced model with simplified physics
- Validation of the strategy on the simulator relying on a much more detailed physics
- Experimental validation

This approach and the detail of the complete simulators have been published for the applications described further in [**59**] (gasoline engine), [**4**], [**1**] and [**2**] (Diesel engine), [**3**], [**8**] and [**7**] (two stage turbocharged Diesel engine). This process can also be found in the structure of the applications chapters 4, 5 and 6 where we first model the system, then propose a reduced model, analyze it and design a control strategy. Simulation validation tests are followed by experimental results.

We give in this chapter a description of the main components of the air system of internal combustion engines, and propose models. We focus in this chapter on turbochargers and exhaust gas recirculation systems whereas the fundamentals of gas exchange models are given in appendix A. The models presented here are very similar to that used in simulation to validate the control strategies, but they are still too complex to be used in the structure of the control strategies. The following chapters will describe, for each application, how they can be reduced for this purpose while keeping the specificities of each system.

The level of details chosen is zero dimension, meaning that we consider that the thermodynamics conditions in each component are homogeneous. This assumption is often referred to as mean value. The equations listed below can be found with more details in various publications. We only give in this document what is strictly necessary for the applications described in chapters 4, 5 and 6. The most interesting references are for example in [**47**], [**36**] and [**44**] .

2.2. Turbochargers

Turbochargers are composed by a turbine driven by the exhaust gas and connected via a common shaft to the compressor, which compresses the air in the intake. Two main types of turbines are used in the industry : fixed and variable geometry turbines. The actuation and the performances of each system are different, however the main physical characteristics are the same, and the representation is similar. We describe in this document centrifugal turbochargers, fitted with fixed or variable geometry turbines. These systems are shown in figures 2.1 and 2.2.

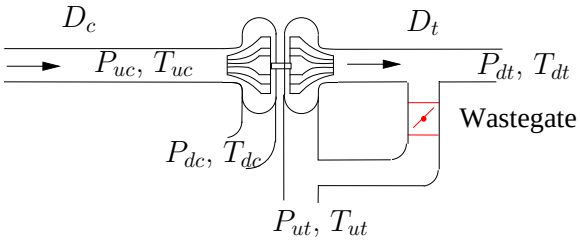

FIGURE 2.1. Turbocharger with fixed geometry turbine

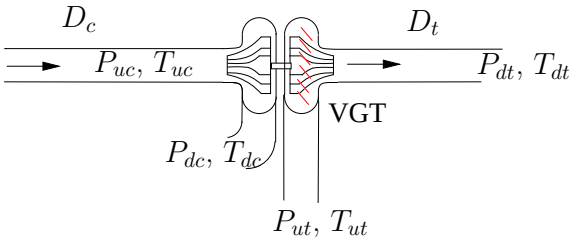

FIGURE 2.2. Turbocharger with variable geometry turbine

2.2.1. State equation. — The rotational speed of the turbocharger shaft N_t can be derived from a power balance between the turbine $\mathcal{P}_t$ and the compressor side $\mathcal{P}_c$

$$\frac{d}{dt}(\frac{1}{2}J_t N_t^2) = \mathcal{P}_t - \mathcal{P}_c \tag{2.14}$$

where J_t is the inertia of the turbocharger.

2.2.2. Compressor. — The compressor power results from the first law of thermodynamics. Neglecting heat losses, the compressor power is related to the enthalpy flow variation in the component :

$$\mathcal{P}_c = D_c c_p (T_{dc} - T_{uc})$$

The compressor efficiency is introduced as the ratio between isentropic and actual compression powers.

$$\eta_c = T_{uc} \frac{\Pi_c^{\frac{\gamma-1}{\gamma}} - 1}{T_{dc} - T_{uc}} \tag{2.15}$$

where $\Pi_c \triangleq \frac{P_{dc}}{P_{uc}}$ the compressor pressure ratio, and γ the specific heat ratio of the gas. The compressor power can be written as :

$$\mathcal{P}_c = D_c c_p T_{amb} \frac{1}{\eta_c} \left(\Pi_c^{\frac{\gamma-1}{\gamma}} - 1 \right) \tag{2.16}$$

The compressor speed, flow, pressure ratio and efficiency are linked, depending on the geometry of the component. Different representations can be found in the literature, among which a commonly used one consists in mapping the pressure ratio and efficiency against flow and speed. These maps are extrapolated from data measured during characterization tests. Several extrapolation methods have been proposed (for example a very commonly used is [**49**], later improved in [**83**], see also [**51**]). In order to take account of the variations in the compressor upstream conditions, these variables are corrected as follow

$$D_{c,cor} = D_c \frac{\sqrt{T_{uc}}}{P_{uc}} \quad \text{and} \quad N_{c,cor} = \frac{N_t}{\sqrt{T_{uc}}}$$

and

$$\left\{ \begin{array}{rcl} \Pi_c & = & \phi_{\Pi_c}(D_{c,cor}, N_{c,cor}) \\ \eta_c & = & \phi_{\eta_c}(D_{c,cor}, N_{c,cor}) \end{array} \right. \tag{2.17}$$

Compressors cannot operate at any conditions. Three operating zones can be identified, as illustrated in figure 2.3 :

1. Normal operating zone
2. Choke : the gas flow through the compressor is too high. The pressure ratio across the compressor is less than one. The compressor functions as a restriction.
3. Surge : the gas flow through the compressor is too low. The compressor can be damaged. This area must be avoided.

The map extrapolation methods have been designed for the normal operating conditions. They are not valid in choke or surge areas for which it is difficult to obtain experimental data. However, specific methods have been proposed in various publications, particularly in [**37**]. In this document we aim at describing air components for control purposes, for which these aspects do not need to be accounted for, except in chapter 6 where it is specifically discussed. We therefore only consider normal operating conditions. Various works have been published on surge control, for example [**66**].

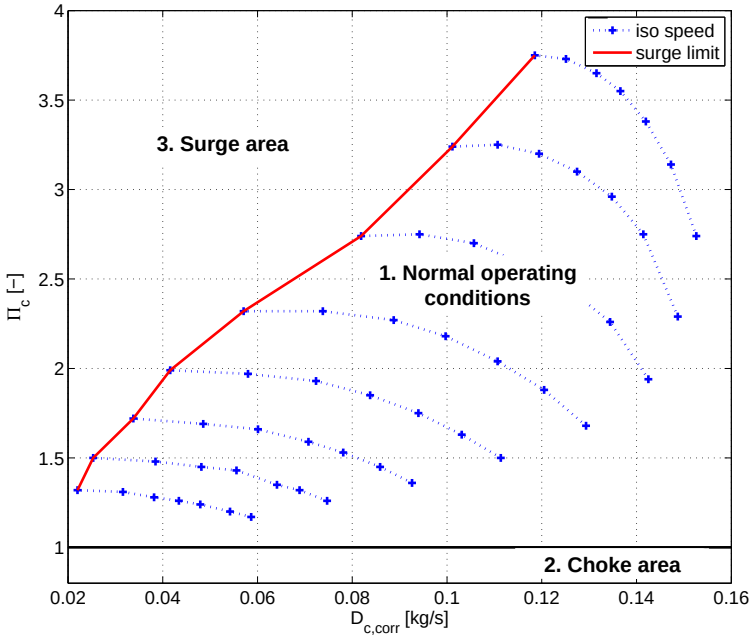

FIGURE 2.3. Compression ratio as a function of corrected flow through the compressor for various turbocharger speed. The blue dots show the characterization measurements.

Typical compressor pressure ratio and efficiency maps after extrapolation are represented in figures 2.4.

2.2.3. Turbine. —

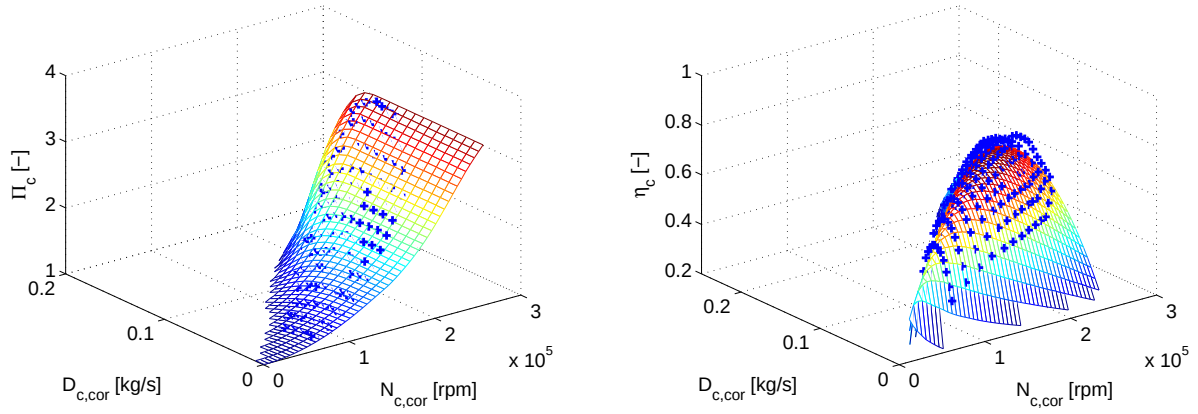

FIGURE 2.4. Compressor maps : compression ratio Π_c (left) and compressor efficiency η_c (right) as a function of corrected flow through the compressor $D_{c,cor}$ and corrected compressor crankshaft speed $N_{c,cor}$. The blue dots show the characterization measurements.

2.2.3.1. Fixed geometry turbines. — As for the compressor, the turbine mechanical power is related to the enthalpy flow variation in the component. The turbine efficiency is computed as :

$$\eta_t = \frac{T_{ut} - T_{dt}}{T_{ut}(1 - \Pi_t^{\frac{1-\gamma}{\gamma}})} \tag{2.18}$$

where $\Pi_t \triangleq \frac{P_{ut}}{P_{dt}}$ is the turbine expansion ratio, γ the specific heat ratio. The turbine power is :

$$\mathcal{P}_t = D_t c_p T_{ut} \eta_t \left(1 - \Pi_t^{\frac{1-\gamma}{\gamma}}\right) \tag{2.19}$$

In this case, the corrected turbine flow $D_{t,cor}$ and isentropic efficiency η_t are mapped versus the pressure ratio across the turbine and the corrected turbocharger shaft speed $N_{t,cor}$ (Figure 2.5). As for compressor maps, different methods have been proposed to obtain these maps from test data (see [**67**]). The corrected variables are defined as :

$$D_{t,cor} = D_t \frac{\sqrt{T_{ut}}}{P_{ut}} \quad \text{and} \quad N_{t,cor} = \frac{N_t}{\sqrt{T_{ut}}}$$

and

$$\left\{ \begin{array}{rcl} D_{t,cor} & = & \phi_{D_t}(\Pi_t, N_{t,cor}) \\ \eta_t & = & \phi_{\eta_t}(D_{t,cor}, N_{t,cor}) \end{array} \right. \tag{2.20}$$

This can be rearranged in the following form, for more commodity :

$$D_t = \phi_{D_t}(\Pi_t, N_{t,cor})\Pi_t \frac{P_{dt}}{\sqrt{T_{ut}}} \tag{2.21}$$

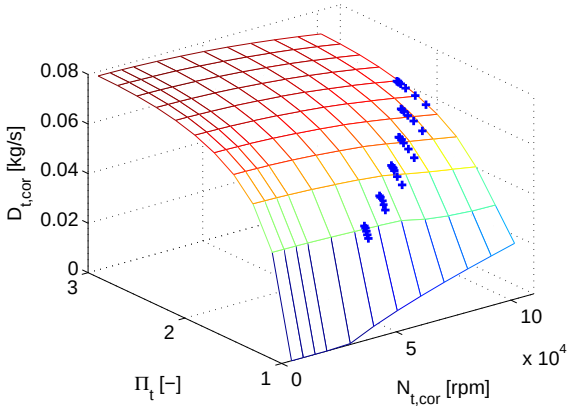

FIGURE 2.5. Corrected flow through the turbine as a function of expansion ratio and corrected speed. The blue crosses show the characterization measurements.

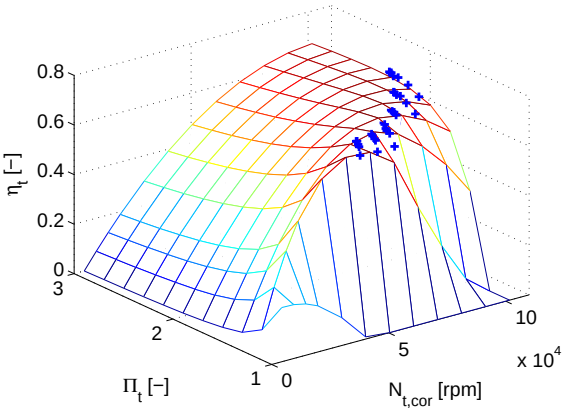

FIGURE 2.6. Turbine efficiency as a function of expansion ratio and corrected speed. The blue crosses show the characterization measurements.

The discharge valve, named waste gate, is used to control the flow through the turbine, and thus the turbocharger. It can be modelled with the standard equations of compressible gas flow through an orifice.

$$D_{wg} = S_{wg}\phi_{wg}(\Pi_t)\frac{P_{dt}}{\sqrt{T_{ut}}}$$

where

$$\phi_{wg}(\Pi_t) \triangleq S_{wg}\frac{\Pi_t}{\sqrt{R}}\sqrt{\frac{2\gamma}{\gamma-1}\left(\Pi_t^{\frac{-2}{\gamma}} - \Pi_t^{\frac{-\gamma-1}{\gamma}}\right)}$$

2.2.3.2. Variable geometry turbines. — In this case the turbine is equipped with guide vanes whose angles are adjusted via an actuator that is noted u_{vgt}. The actuator affects both the angle of the gas flow on the turbine blades, and therefore its efficiency, and the turbine effective flow area. By these means, it is possible to maintain a high boost even at low engine speed, and to improve the system dynamics perfomance.

The flow and efficiency maps depend also on the actuator. Figures 2.7 and 2.8 show characterisation measurements plotted against pressure ratio. The dependency on VGT position is obvious, particularly for the mass flow. We have :

$$\begin{cases} D_{t,cor} &= \phi_{D_t}(\Pi_t, N_{t,cor}, u_{VGT}) \\ \eta_t &= \phi_{\eta_t}(D_{t,cor}, N_{t,cor}, u_{VGT}) \end{cases} \tag{2.22}$$

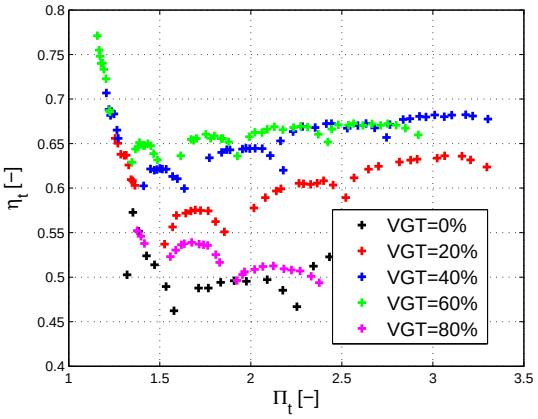

FIGURE 2.7. Turbine efficiency against pressure ratio, for different actuator position

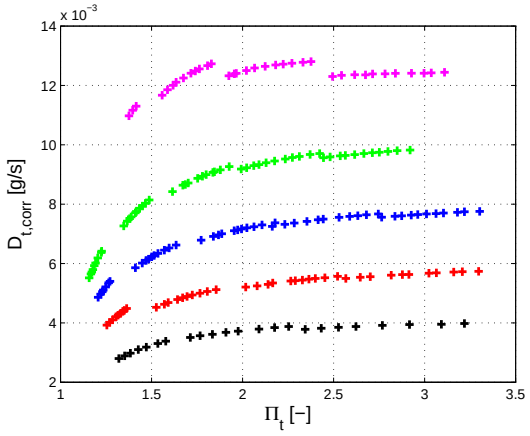

FIGURE 2.8. Turbine corrected flow against pressure ratio, for different actuator position

2.2.4. System limits. — Due to plastic deformation, the compressor needs to be maintained below a maximum speed. A maximum compressor outlet temperature and maximum turbine inlet temperature must be respected.

2.3. Exhaust Gas Recirculation

We propose here models for the EGR systems that will be studied in the other chapters of this document. These models are based on the equations for gas exchanges given in A.

Exhaust Gas Recirculation (EGR) systems connect exhaust and intake systems. Exhaust gas flows to the intake if the exhaust manifold pressure is superior to the intake manifold pressure. These systems can be used sometimes on gasoline engines and are now necessary on Diesel engines in order to maintain low NOx emissions. Two main types of EGR systems are distinguished, whether it is located on the high or low pressure side of the turbocharger.

They are therefore called HP or LP. Their functioning and composition are basically the same, but their effects on the air system differ.

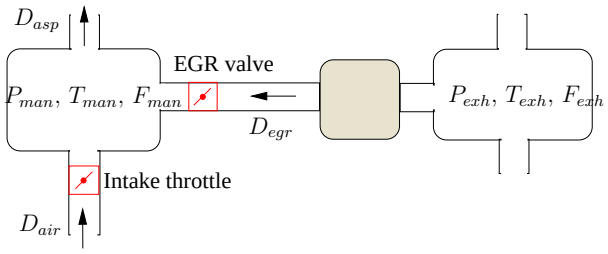

FIGURE 2.9. HP EGR circuit scheme

2.3.1. HP EGR. — Figure 2.9 shows the schematics of an HP EGR circuit. It connects exhaust and intake manifolds. It consists usually in a heat exchanger and a valve. The valve is located downstream from the exchanger in order to be protected from high exhaust temperature. Usually a compressor and a heat exchanger are located upstream the intake circuit. A throttle, located between this cooler and the intake manifold, can be used to slow down the fresh air flow and accelerate the EGR flow. However, the pressure difference between exhaust and intake manifold is generally sufficient to provide the desired EGR flow in steady state. Since the intake throttle generates losses in the system and penalizes the consumption, it is used only when necessary, for example during special operations for aftertreatment regeneration.

It can be noticed that the pressure difference between intake and exhaust manifolds also depends on the turbocharger actuation which modifies the restriction on the flow downstream from the EGR circuit on the exhaust of the engine. There is an interaction between the two systems, and in steady state the VGT or wastegate can be used to increase the EGR capacities. This was briefly discussed in 1 and will be described in detail in 5.

For engine control purposes, it is relevant to model the dynamics in the intake manifold from the equations given by (A.1). In the case of cooled HP EGR, we usually consider that the exchange in the intake manifold is isothermal. This assumption is justified when the temperatures of the incoming flows do not vary too much. This is the case when the heat exchangers are efficient enough. With the sign convention given in 2.9 for the flows, the equations governing its behavior are :

$$\begin{cases} \dfrac{dP_{man}}{dt} &= \dfrac{RT_{man}}{V_{man}}\left(D_{air} + D_{egr} - D_{asp}\right) \\ \dfrac{dF_{man}}{dt} &= \dfrac{RT_{man}}{P_{man}V_{man}}\left(D_{egr}\left(F_{exh} - F_{man}\right) + D_c\left(F_1 - F_{man}\right)\right) \end{cases} \tag{2.23}$$

Similarly, on the exhaust manifold we can consider the following representation :

$$\begin{cases} \dfrac{dP_{exh}}{dt} &= \dfrac{RT_{exh}}{V_{exh}}\left(D_{asp} + D_{inj} - D_{egr} - D_{turb}\right) \\ \dfrac{dF_{exh}}{dt} &= \dfrac{RT_{exh}}{P_{exh}V_{exh}}\left(D_{asp}\left(F_{man} - F_{exh}\right) + D_f\left(AF_s + 1 - F_{exh}\right)\right) \end{cases} \tag{2.24}$$

The exhaust gas concentration is often considered as an input because it can be measured by a sensor. In this case the second equation of (2.24) is not taken into account. However, it is important because it provides the relationship between intake and exhaust burned gas fractions.

The gas flow across the circuit is determined by the succession of the pressure drop across the exchanger and the pressure ratio across the EGR valve. Since the pressure ratio across each component is close to unity, corresponding to the right hand side of figure A.2, it is difficult to characterize the circuit globally from measurements in the manifolds. This issue will prove to be important when considering the EGR observation.

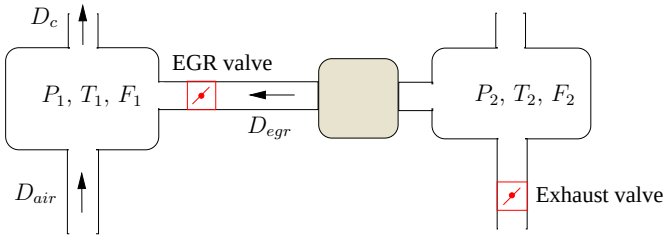

FIGURE 2.10. LP EGR circuit scheme

2.3.2. LP EGR. — The low-pressure loop delivers exhaust gas from downstream the turbocharger and aftertreatment system to upstream the compressor (figure 2.10). The LP circuit includes an EGR valve and an EGR cooler. Since volume 1 is located at the outlet of the air filter, and volume 2 is at the inlet of the exhaust line, pressure P_1 and P_2 are very close to atmospheric pressure. So the pressure difference across the EGR circuit is insufficient to provide enough EGR flow. Therefore, an exhaust valve is often used to

create a sufficient pressure difference. As for HP EGR, the gas flow across the circuit is determined by the succession of the pressure drop across the exchanger and the pressure ratio across the EGR valve. However, the pressure ratios are very close to one, which corresponds to very high dynamics, and a low accuracy in equation A.6.

The isothermal assumption can be used, and the evolution of system 1 can be described by :

$$\begin{cases} \dfrac{dP_1}{dt} &= \dfrac{RT_1}{V_1}\left(D_{air} + D_{egr} - D_c\right) \\ \dfrac{dF_1}{dt} &= \dfrac{RT_1}{P_1 V_1}\left(D_{egr}\left(F_2 - F_1\right) - D_{air}F_1\right) \end{cases} \tag{2.25}$$

Then, the gas are transfered on the intake line down to the engine. This transfer can be modeled from the equations given in the basic example (A.5).

2.4. Engine model

A detailed combustion modeling is out of the scope of this document. Instead, we describe in this section mean value models intended to represent the interactions between engine and air systems. The engine can be considered as a volumetric pump, where additional energy is brought by the injected fuel. It is a resistive component on the air system, that determines the flows (mass and enthalpy) from the conditions at its intake and exhaust. We therefore focus on the model of gas flow through the engine and exhaust gas enthalpy flow. The impact of variable distribution is discussed very briefly.

2.4.1. Engine gas flow and composition. —

2.4.1.1. Conventional case. — The engine flow is deduced from (1.1) :

$$D_{asp} = \eta_v \frac{P_{man} V_{cyl}}{RT_{man}} \frac{N_e}{120} \tag{2.26}$$

The volumetric efficiency is usually mapped as a function of engine speed and intake manifold pressure or density : $\eta_v = f(P_{man}, N_e)$ or $\eta_v = f(\rho_{man}, N_e)$.

Further in this document we will use a formulation with the compressor pressure ratio. If a compressor is located upstream from the intake manifold, then the intake manifold pressure is the product of the compression ratio times the upstream pressure and the engine flow can be expressed as :

$$D_{asp} = \eta_v \Pi_c \Psi \tag{2.27}$$

with $\Psi \triangleq \frac{V_{cyl} P_{uc} N_e}{120 R T_{man}}$.

A correction depending on exhaust pressure may be included to account for the residual gas present in the cylinder at the closing of the exhaust valve. This effect is neglected in this document but could be interesting when studying the air fuel ratio control for turbocharged gasoline engines.

The exhaust mass flow is the addition of aspirated gas flow and fuel injected mass D_f :

$$D_{exh} = D_{asp} + D_f \tag{2.28}$$

On a gasoline engine operating at stoichiometry, the fuel mass flow is proportional to the aspirated flow, leading to : $D_{exh} = (1 + \lambda_s) D_{asp}$.

2.4.1.2. Variable valve actuation. — Variable valve actuation is outside of the scope of this document. For details on variable valve timing control, interesting references are **[64]** for the control and estimation on a gasoline engine, and **[65]** for the Diesel case. In this document we will only verify that the air system control (EGR, turbochargers) is compatible with this technology. We are therefore only interested in the impact of variable valve on the engine gas flow.

The variation of camshaft timing change the exhaust manifold pressure and the residual gas mass trapped inside the cylinder at intake valve closing. This makes the mapping of η more complex. However, in **[64]**, an expression with two dimension look up tables is proposed for gasoline engines with variable valve timing :

$$D_{asp} = \alpha_1 \frac{P_{man} V_{ivc}(\theta_{int})}{R T_{man}} - \alpha_2 \frac{OF(\theta_{int}, \theta_{exh})}{N_e} - \alpha_3 V_{evc}(\theta_{exh}) \tag{2.29}$$

where α_i are mapped as a function of intake manifold pressure and engine speed. The dependencies on valve timings θ_{int} and θ_{exh} is only in the overlap factor OF and the cylinder volume at intake and exhaust valve closure V_{ivc} and V_{evc}.

Thanks to this expression, the model of engine gas flow remains simple enough for our purposes. A simple estimation of the cylinder gas composition is also proposed in this paper. This allows to base on (2.26) the design of the air system control strategies in the following chapters without losing generality when considering variable valve actuation.

2.4.1.3. Gas composition in the cylinder. — We are interested in the composition of the gases at the exhaust of the engine, because these gases then flow through the exhaust line and the EGR circuits. From (1.5) the burned gas concentration in the cylinder at the exhaust is therefore :

$$F_{cyl} = \frac{D_f(AF_s + 1) + F_{man}D_{asp}}{D_{asp} + D_f} \tag{2.30}$$

As for the engine flow model (equation (2.26)), this expression neglects the influence of the residual gas at the exhaust valve closure.

2.4.2. Engine exhaust enthalpy flow. — The engine exhaust temperature determines the enthalpy flow in the exhaust system of engines, thus influencing turbine power. It is the consequence of the combustion efficiency and the expansion stroke before exhaust valve opening. In this document we will keep a very simple representation, considering that the exhaust temperature is a function of the injected fuel mass and the engine speed :

$$T_{exh} = f(D_f, N_e) \tag{2.31}$$

This assumption is illustrated in figures 2.11 and 2.12 which show exhaust temperature on the whole operating range of an engine for gasoline and Diesel. The introduction of burned gas in the cylinder can affect the exhaust temperature. This is not taken into account in this document.

The exhaust enthalpy flow derives from this temperature and the engine mass flow. It is therefore determined essentially by the engine speed and the fuel flow.

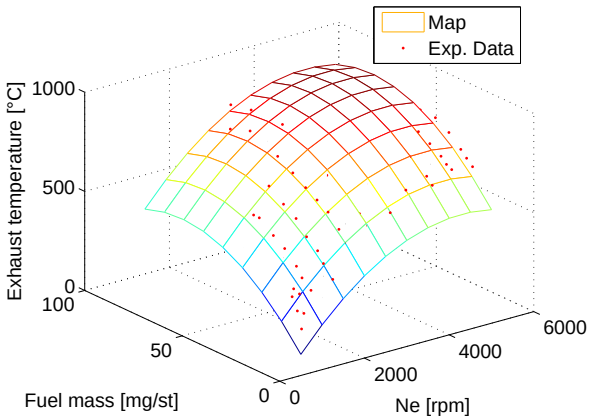

FIGURE 2.11. Engine exhaust manifold temperature as a function of injected fuel mass and engine speed for a gasoline engine.

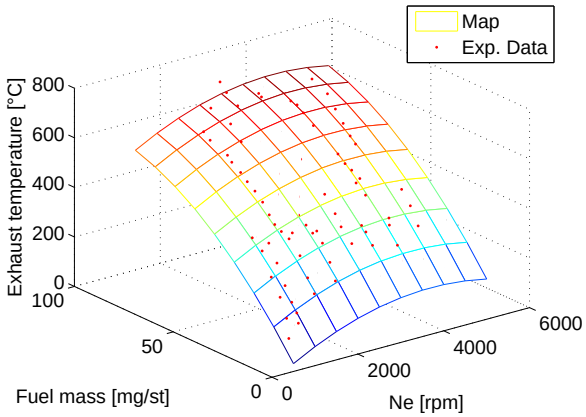

FIGURE 2.12. Engine exhaust manifold temperature as a function of injected fuel mass and engine speed for a Diesel engine.

2.5. Heat transfers

We neglect in this document thermal losses through the air circuit walls and the temperature dynamics due to the components thermal inertia. These effects are slower than the gas exchanges dynamics. They are considered as perturbations. A general review of exhaust thermal models is given in **[35]**.

2.6. Interfaces with controllers : sensors and actuators

Since we want eventually to control the systems, we have to consider the actuators which are used to act on the system and sensors which are used to measure internal variables. These components introduce dynamic and steady state effects that can not always be neglected. They must at least be considered when studying the robustness of the strategies.

2.6.1. Actuators. —

2.6.1.1. General case. — Actuators are important when considering control issues because they are the means of action on the system. Various types can be found on the air systems, for example :

– Throttles with position sensors
– Valves without position sensor
– Valves with position sensor
– Pneumatic actuator

In the case of actuators with position sensors, a decentralized control strategy is usually in charge of the position tracking. The system therefore can be represented with a dynamic transfer function that is often approximated as a first order filter. A typical time constant for throttles or valves is 100ms.

On the air system, valves and throttles are modeled as orifices with variable sections. The gas flow through these components are given by (A.6).

2.6.1.2. Pneumatic actuators. — This technology is of particular interest because VGT and wastegates are often controled via a pneumatic system, as schematized in figure 2.13 in the case of wastegate. The following model was proposed in similar forms in **[68, 70, 41]**. The pressure dynamics P_{act} in the actuator chamber is given by the mass conservation controlled by the command u_{pwm} and the difference between atmospheric pressure P_{atm}

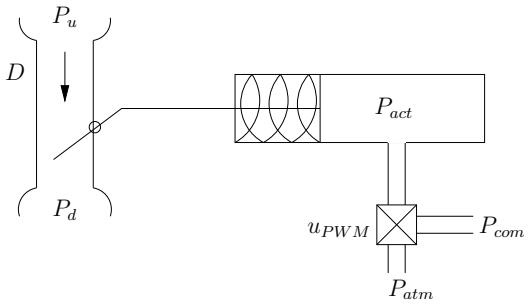

FIGURE 2.13. Typical pneumatic actuator

and a command pressure P_{com}.

$$\frac{dP_{act}}{dt} = \frac{RT_{act}}{V_{act}}(u_{pwm}(P_{com} - P_{act}) - (1 - u_{pwm})(P_{act} - P_{atm})) \tag{2.32}$$

Various configurations can be found : P_{com} can be connected to a void circuit or to the intake manifold. The pressure difference across the diaphragm creates a force that changes the wastegate position. The spring closes the wastegate when there is no pressure difference. The dynamics of the wastegate position x_{WG} are given by the forces balance :

$$m\frac{d^2x_{wg}}{dt^2} + C\frac{dx_{wg}}{dt} = S(P_{act} - P_{atm}) - k(x_{wg} - x_0) - F_{gas} \tag{2.33}$$

where S is the diaphragm section, k is the spring stiffness, m is the moving system mass, C is the damping and F_{gas} is the force applied by the flow D on the wastegate plate. Since the flow is not laminar, this force cannot be computed simply, but it can be assumed that it depends only on the pressure difference $P_u - P_d$ and the plate angle and thus the wastegate position x_{wg}. A similar representation was proposed in [**70**].

The steady state of the system composed by (2.32) and (2.33) is given by :

$$\begin{cases} P_{act} = u_{pwm}P_{com} + (1 - u_{pwm})P_{atm} \\ S(P_{act} - P_{atm}) - k(x_{wg} - x_0) - F_{gas} = 0 \end{cases} \tag{2.34}$$

In a control strategy, this algebraic model can be inverted to transform the position x_{wg} into a command u_{pwm}.

In the case of VGT this representation is also correct, except the force F_{gas} is different and probably much smaller (in [**68**] it is neglected). No assumption will be given here since there is a lack of experimental measurements.

However, in reality, some friction forces on the diaphragm affect the behavior of the system, both in terms of dynamics and steady state, generating hysteresis effects. The

global system is very difficult to predict without a position measurement. Therefore, we do not propose here a more detailed description of these aspects. We will have to check the robustness of the designed strategies with respect to unmodeled dynamics and actuator modeling errors.

2.6.2. Sensors. — When designing a control strategy for a given system, the number of available sensors, their location on the system and their accuracy are crucial information. The most common ones are the following :

- Intake manifold pressure
- Intake manifold temperature
- Inlet air mass flow
- Exhaust manifold temperature
- Exhaust manifold pressure
- Particulate filter pressure drop
- Exhaust air fuel ratio
- Atmospheric pressure
- Ambient temperature

With conventional series sensors it is not possible to measure accurately the intake manifold gas composition nor the EGR mass flow, which will justify the need for estimating these variables. Also, in the application studied the need to use the minimum number of sensors will be discussed specifically.

The dynamics of the pressure and mass flow sensors are neglected. The dynamics of temperature sensors and air fuel ratio sensors are slower and may not be neglected in the control strategies.

2.7. Description of three examples of air path architectures

In this section we introduce the systems that will be studied in the following chapters, and propose a model for each of them based on the equations given in the previous sections.

2.7.1. Turbocharged Gasoline engine. —

2.7.1.1. System description. — The first engine considered is a four cylinder turbocharged gasoline engine shown in Figure 2.14. Fresh air enters in the engine through the compressor which increases the air density. The air is burnt in the cylinder where the combustion results in the production of mechanical torque. At the exhaust of the system, the turbine

converts part of the gas enthalpy into mechanical power on the turbocharger shaft, whose dynamics are the consequence of the balance between the compressor and turbine powers.

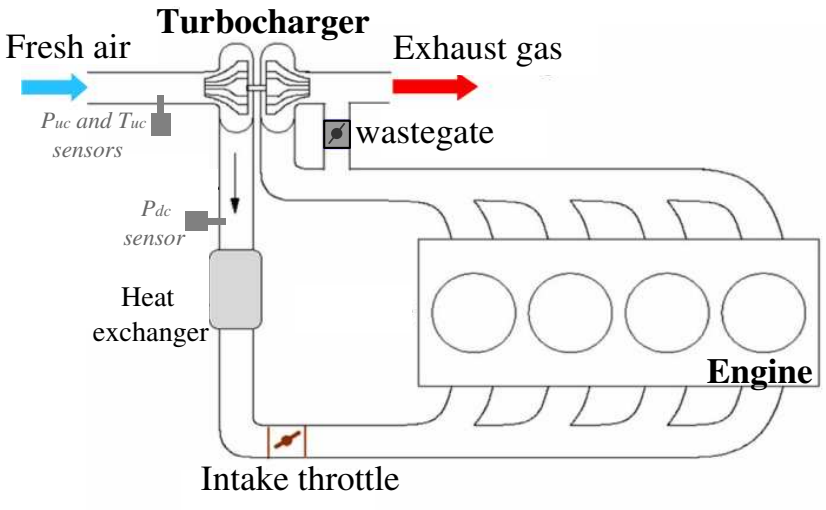

FIGURE 2.14. Engine diagram. The actuator is the wastegate, the measurements are the compressor upstream temperature and pressure and the downstream pressure.

Two actuators are available on the air system. The wastegate diverts part of the exhaust gas from the turbine, resulting in a change of the energy provided to the turbocharger shaft. The intake throttle acts on the intake manifold pressure by creating a pressure drop downstream from the compressor and heat exchanger.

The turbocharger has a direct influence on compression and expansion ratios, and on temperatures downstream from the compressor and the turbine. Its behavior, however, depends on variables related to other components, including : engine speed, atmospheric pressure, ambient temperature, exhaust manifold temperature and pressure downstream turbine. In this paper these variables are referred to as environmental variables or conditions. They can be measured or estimated easily (see appendix for further details).

The following measurements are available on the system :

– Engine speed N_e.
– Compressor downstream pressure P_{dc}.
– Compressor upstream pressure and temperature P_{uc} and T_{uc}.

2.7.1.2. Complete model. — The model is based on the equations given above. Since there is no EGR circuit, and since the gasoline engine operates at stoichiometry, we consider only one gas species in each volume : fresh air at the intake and burned gas at the exhaust.

The following equations represent the dynamics of the system

$$\left\{\begin{array}{rcl} \dfrac{d}{dt}(\dfrac{1}{2}J_t N_t^2) & = & \phi_{Dt}(\Pi_t, N_{t,cor}) c_p P_{dt}\sqrt{T_{ut}}\eta_t\phi_t(\Pi_t) - D_c c_p T_{uc}\dfrac{1}{\eta_c}\phi_c(\Pi_c) \\ \dfrac{dP_{ut}}{dt} & = & \dfrac{RT_{ut}}{V_{ut}}\Big((1+\lambda_s)\eta_v\Pi_c\Psi - (\phi_{Dt}(\Pi_t, N_t)\Pi_t + S_{wg}\phi_{wg}(\Pi_t))\,\dfrac{P_{dt}}{\sqrt{T_{ut}}}\Big) \\ \dfrac{dP_{dc}}{dt} & = & \dfrac{RT_{dc}}{V_{dc}}(D_c - \eta_v\Pi_c\Psi) \end{array}\right. \tag{2.35}$$

where $\phi_t(\Pi) \triangleq \Pi(1-\Pi^{\frac{1-\gamma}{\gamma}})$ and $\phi_c(\Pi) \triangleq \Pi^{\frac{\gamma-1}{\gamma}} - 1$.

In order to take into account the interactions with the other components of the air system, it is necessary to express these dependencies explicitly. This is the reason why the formulations used in this model take into account parameters external to the turbocharger itself : temperatures upstream the compressor and turbine, pressure downstream the turbine.

2.7.2. Diesel engine with LP and HP EGR and variable geometry turbocharger. —

2.7.2.1. System description. — The system under consideration (figure 2.15) is a four cylinder engine working in conventional Diesel mode or in LTC mode. The exhaust-treatment system consists in a Diesel oxidation catalyst (DOC) and a particulate filter (PF). The air path system contains three different parts : the high-pressure EGR system, the low-pressure EGR system and the air system. The low-pressure loop delivers exhaust gas from downstream the turbocharger to upstream the compressor. The LP route includes an EGR valve, an EGR cooler and an exhaust throttle is necessary to create sufficient pressure drop in the EGR system to ensure the EGR flow. The high-pressure loop uses a valve located downstream of the EGR cooler to deliver exhaust gas from the exhaust manifold to the intake manifold. The HP loop is also fitted with an EGR cooler. An intake throttle, located downstream of the air cooler, can be used in transient operations to slow down the air flow (in HP EGR operation only). A turbocharger with a variable geometry turbine (VGT) controls the boost pressure. The turbine converts the gas enthalpy into mechanical power that drives the compressor. The pressure ratio across the compressor, and thus the intake manifold pressure, depends on the VGT position.

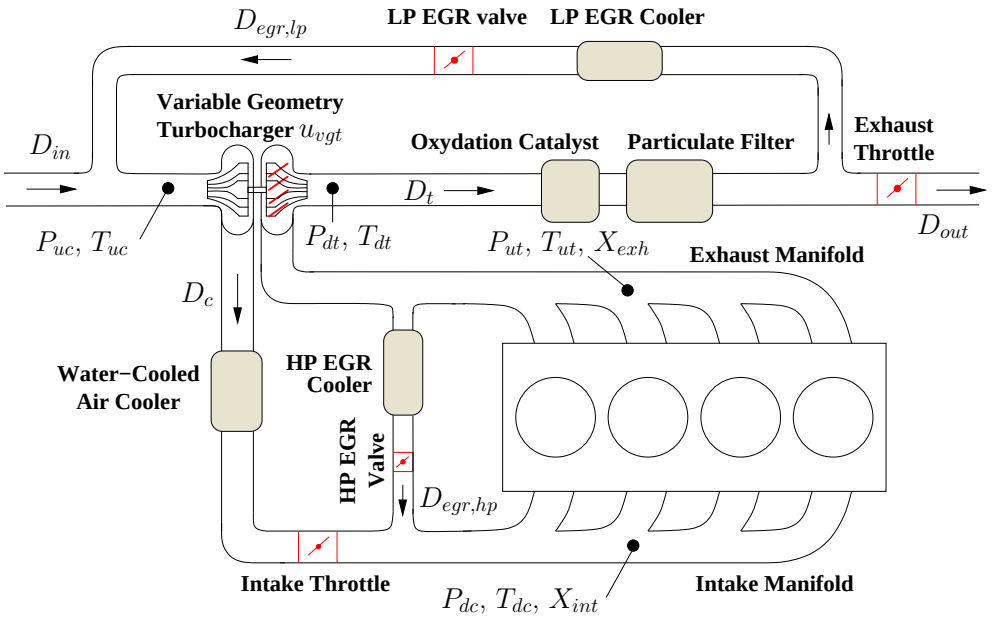

FIGURE 2.15. Dual mode Diesel-LTC engine architecture including a variable geometry turbocharger, a cooled high-pressure EGR loop and a cooled low-pressure EGR loop.

The air path architecture has five actuators to control the air, HP EGR and LP EGR flows :

- The VGT position u_{vgt} that drives the turbocharger.
- The HP EGR valve position $u_{egr_{hp}}$ that drives the HP EGR flow.
- The intake throttle position u_{ith}. The intake throttle is considered as an additional actuator and it can be used to decrease the air flow in some specific cases. This actuator is not considered in this paper.
- The LP EGR valve position $u_{egr_{lp}}$ controls the flow through the low pressure route.
- The exhaust throttle position u_{eth} is required to control the pressure drop across the LP system.

The sensors used in the proposed control structure measure :

- the air mass flow D_{air},
- the compressor upstream pressure P_{uc} and temperature T_{uc},
- the intake manifold pressure P_{dc} and temperature T_{dc},
- the exhaust equivalence ratio F_{exh},
- the positions of the air and EGR actuators cited before.

2.7.2.2. Model. — We can describe this system from a combination of the equations presented in the previous sections, which leads to :

$$\begin{cases} \frac{d}{dt}(\frac{1}{2}J_t N_t^2) &= \phi_{D_t}(\Pi_t, \frac{N_t}{\sqrt{T_{ut}}}, u_{vgt}) P_{dt} c_p T_{ut} \eta_t \sqrt{T_{ut}} \phi_t(\Pi_t) - D_c c_p T_{uc} \frac{1}{\eta_c} \phi_c(\Pi_c) \\ \frac{dP_{ut}}{dt} &= \frac{RT_{ut}}{V_{ut}} \big(\eta_v \Pi_c \Psi + D_f - D_{egr,hp} - \phi_{D_t}(\Pi_t, \frac{N_t}{\sqrt{T_{ut}}}, u_{vgt}) \Pi_t \frac{P_{dt}}{\sqrt{T_{ut}}}\big) \\ \frac{dP_{dt}}{dt} &= \frac{RT_{dt}}{V_{dt}} \big(\phi_{D_t}(\Pi_t, \frac{N_t}{\sqrt{T_{ut}}}, u_{vgt}) \Pi_t \frac{P_{dt}}{\sqrt{T_{ut}}} - D_{out} - D_{egr,lp}\big) \\ \frac{dP_{uc}}{dt} &= \frac{RT_{uc}}{V_{uc}} (D_{air} + D_{egr,lp} - D_c) \\ \frac{dP_{dc}}{dt} &= \frac{RT_{dc}}{V_{dc}} (D_c + D_{egr,hp} - \eta_v \Pi_c \Psi) \\ \frac{dF_{uc}}{dt} &= \frac{RT_{uc}}{P_{uc} V_{uc}} \left(D_{egr,lp} \left(F_{exh} - F_{uc}\right) - D_{air} F_{uc}\right) \\ \frac{dF_{dc}}{dt} &= \frac{RT_{dc}}{P_{dc} V_{dc}} \left(D_{egr,hp} \left(F_{exh} - F_{dc}\right) - D_c \left(F_{uc} - F_{dc}\right)\right) \\ \frac{dF_{exh}}{dt} &= \frac{RT_{exh}}{P_{exh} V_{exh}} \left(\eta_v \Pi_c \Psi \left(F_{dc} - F_{exh}\right) + D_f \left(AF_s + 1 - F_{exh}\right)\right) \end{cases} \tag{2.36}$$

where $\phi_t(\Pi) \triangleq \Pi(1 - \Pi^{\frac{1-\gamma}{\gamma}})$ and $\phi_c(\Pi) \triangleq \Pi^{\frac{\gamma-1}{\gamma}} - 1$.

This model is comprehensive for turbocharger and EGR systems description. The last three equations concern only gas fractions in the receivers, they do not affect the turbocharger. On the contrary, the first equations describe the turbocharger behavior. They account for parameters external to the turbocharger itself (temperatures upstream the compressor and turbine, pressure downstream the turbine) and represent the interactions with the EGR circuits.

2.7.3. Diesel engine with two stage turbocharger. —

2.7.3.1. Engine description. — The engine considered is a 2,0 L diesel engine fitted with high pressure exhaust gas recirculation (EGR) and a particulate filter (see figure 2.16). The specificity of this engine is the two sequential turbochargers : the air entering the system is first compressed by a low pressure (LP) turbocharger, and then by a high pressure (HP) turbocharger. The pressure at the output of the HP compressor is called boost pressure. Both turbochargers have a fixed geometry and a waste gate valve. A by-pass

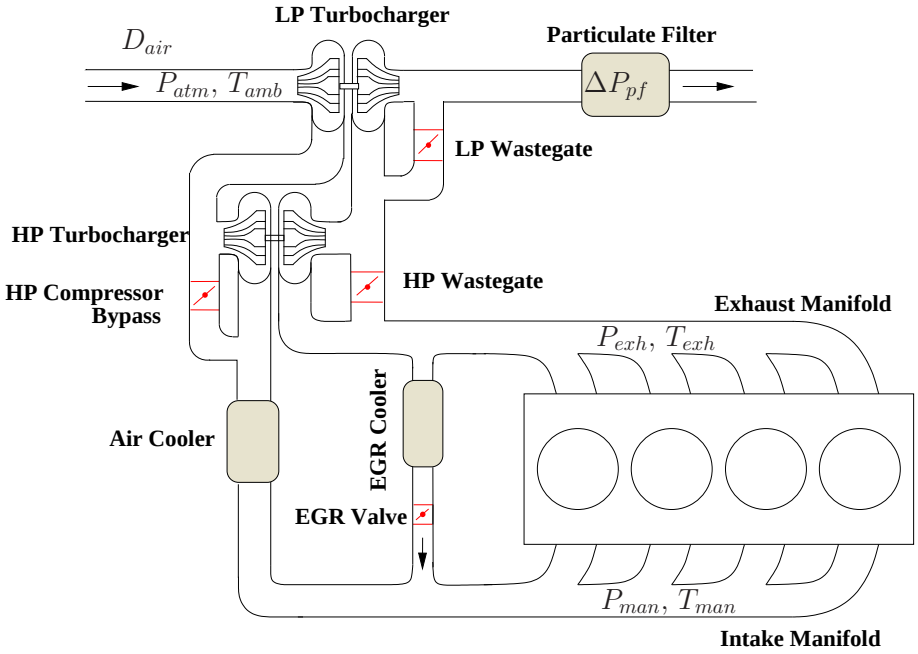

FIGURE 2.16. Diesel engine with two stage turbochargers

valve is mounted on the HP compressor in order to avoid pressure drop through the HP compressor when operating only with the LP compressor. A description of a two stage turbocharging system can be found in [**31**]. For more details on the engine, refer to [**8**] which describes the development of the simulator designed to analyze the system.

When mounted on an engine, the size of the turbine and compressor wheels have to be adapted in order to match the engine air flow characteristics. Compared to single stage systems, it is possible in two stage sequential systems to use different sizes for both turbochargers. The LP turbocharger is matched in order to operate at high air flow, providing compression for high engine speed and increasing the engine power, whereas the HP turbocharger is used at low air flow in order to increase the engine torque at low speed. The HP turbocharger dynamics are also useful to compensate for the slow dynamics of the LP turbocharger. However, an increased complexity is the cost for these advantages, particularly in terms of control strategies.

The sensors available on the system are : air mass flow, atmospheric pressure, external temperature, intake manifold pressure and temperature, exhaust manifold pressure

and temperature and particulate filter differential pressure. The system is relatively well instrumented, except that no measurement is available between the two turbochargers.

2.7.3.2. Model. — The system consists in twice a single stage turbocharger. We will consider in the sequel that $D_{EGR} = 0$ for several reasons. First, the specific control issues of this case study concern mainly high loads (hence without EGR) because at low loads the system could be used as a single stage turbocharger. Also, the calibration of this type of engine usually results in closing both turbochargers wastegates in the EGR operating zone in order to minimize the pollutant emissions. It was the case on the engine studied. However, we assumed that the interactions between EGR and turbochargers could be dealt with similar solutions as proposed in chapter 5 for the previous case study.

The following equalities follow from this assumption : $D_{asp} = D_{c,lp} = D_{air}$, and when the HP compressor bypass is closed $D_{c,hp} = D_{air}$. We use subscripts 1 and 2 respectively for LP and HP turbochargers. The following model represents the system :

$$
\left\{
\begin{array}{rcl}
\frac{d}{dt}(\frac{1}{2}J_{t,1}N_{t,1}^2) &=& \phi_{D_t}(\Pi_{t,1}, N_{t,1,cor})c_pP_{dt,1}\sqrt{T_{ut,1}}\eta_t\phi_t(\Pi_{t,1}) - D_{c,1}c_pT_{uc,1}\frac{1}{\eta_{c,1}}\phi_c(\Pi_{c,1}) \\
\frac{d}{dt}(\frac{1}{2}J_{t,2}N_{t,2}^2) &=& \phi_{D_t}(\Pi_{t,2}, N_{t,2,cor})c_pP_{dt,2}\sqrt{T_{ut,2}}\eta_t\phi_t(\Pi_{t,2}) - D_{c,2}c_pT_{uc,2}\frac{1}{\eta_{c,2}}\phi_c(\Pi_{c,2}) \\
\frac{dP_{ut,2}}{dt} &=& \frac{RT_{ut,2}}{V_{ut,2}}\Big(\eta_v\Pi_{c,1}\Pi_{c,2}\Psi + D_{fuel} \\
& & - \left(\phi_{D_{t,2}}(\Pi_{t,2}, N_{t,2})\Pi_{t,2} + S_{wg,2}\phi_{wg,2}(\Pi_{t,2})\right)\frac{P_{dt,2}}{\sqrt{T_{ut,2}}}\Big) \\
\frac{dP_{ut,1}}{dt} &=& \frac{RT_{ut,1}}{V_{ut,1}}\Big(\left(\phi_{D_{t,2}}(\Pi_{t,2}, N_{t,2})\Pi_{t,2} + S_{wg,2}\phi_{wg,2}(\Pi_{t,2})\right)\frac{P_{dt,2}}{\sqrt{T_{ut,2}}} \\
& & - \left(\phi_{D_{t,1}}(\Pi_{t,1}, N_{t,1})\Pi_{t,1} + S_{wg,1}\phi_{wg,1}(\Pi_{t,1})\right)\frac{P_{dt,1}}{\sqrt{T_{ut,1}}}\Big) \\
\frac{dP_{dc,2}}{dt} &=& \frac{RT_{dc,2}}{V_{dc,2}}(D_{bp} + D_{c,2} - \eta_v\Pi_{c,1}\Pi_{c,2}\Psi) \\
\frac{dP_{dc,1}}{dt} &=& \frac{RT_{dc,1}}{V_{dc,1}}(D_{c,1} - D_{c,2} - D_{bp})
\end{array}
\right. \tag{2.37}
$$

where $\phi_t(\Pi) \triangleq \Pi(1 - \Pi^{\frac{1-\gamma}{\gamma}})$ and $\phi_c(\Pi) \triangleq \Pi^{\frac{\gamma-1}{\gamma}} - 1$.

2.8. Conclusion

We give in this chapter the bases for the representation of the systems that will be considered in the sequel. We try to keep them as generic as possible with respect to the combustion and to the engine technology. Short considerations on the properties of global air systems are made in order to understand the issues linked to physical properties of the components that can arise when controlling these systems. In chapters 4, 5 and 6 the reference models proposed in this chapter will be reduced in order to build control oriented models adapted for the specific examples studied.

CHAPTER 3

AIR SYSTEMS CONTROL ISSUES

3.1. Introduction

In chapter 2 we have proposed three different air systems architectures corresponding to applications that will be studied in the following chapters. The present chapter aims at describing global air systems control issues and the specificities of each application.

After a short introduction of engine control and an analysis of the systems presented in section 3.3, we describe in this chapter the air systems control objectives and issues in section 3.4. This is followed by an analysis of the conventionnal strategies and the presentation of various publications found on the topic. Since the developments described in the following chapters concern turbocharger control, we focus on this topic. Concerning the control and estimation of EGR systems, we will use results already published (mostly in [**26**]). However the turbochargers and EGR systems have many interactions, therefore it is important to integrate both controls in a global air systems control structure. This is discussed in this chapter and detailed in the sequel for each application studied.

3.2. Engine Control basics

3.2.1. Definition and Objectives. — Modern engines are fitted with an Electronic Control Unit (ECU) which determines the command of the actuators based on the measurements of the sensors. The software in charge of this task is called engine control.

Since the purpose of a combustion engine is to produce a mechanical torque, the purpose of the engine control system in a vehicle is to ensure that this torque satisfies the requirements coming from the other systems : driver, transmission, air conditioning system, alternator, electronic stability control (ESC), anti brake system (ABS) ... As explained in chapter 1 the system must also respect constraints on the pollutant emissions and on the system safety.

3.2.2. Engine control architecture. — The diagram of figure 1.1 shows the main actuators of a turbocharged gasoline engine : throttle, wastegate, injector and spark plug. The associated commands are respectively : throttle position, wastegate position, injected mass, injection timing, spark timing.

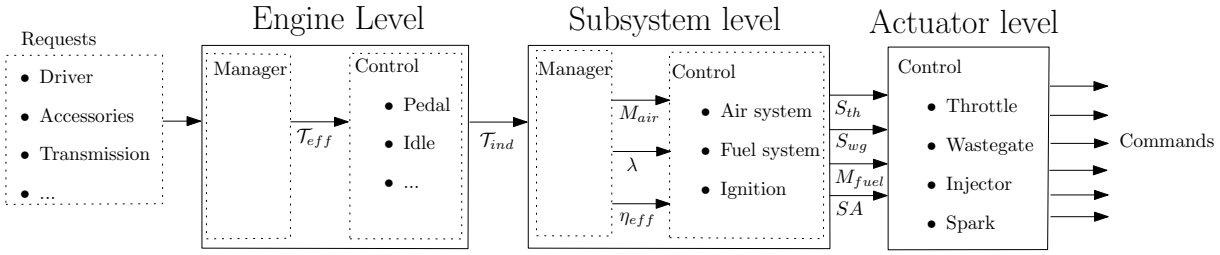

FIGURE 3.1. Schematized engine control structure

These commands cannot be computed straightforwardly from an engine torque request. The engine control software is therefore organized in a *torque based* structure with different levels in a hierarchical manner. Each layer is in charge of transforming requests from the upper level layer to setpoints for the lower level layer. This structure is illustrated in figure 3.1, showing three main levels :

- *Engine* : The vehicle requests are transformed into an indicated torque request $\mathcal{T}_{ind}$. This level is in charge of the management of the engine : start up, idle speed control, ...
- *Subsystem* : The indicated torque request is transformed into requests for the different subsystems of the engine : M_{air} for the air system, air fuel ratio λ for the fuel system, efficiency η_{eff} for the ignition system. This level contains the control strategies for the different subsystems. Concerning the air systems : intake manifold pressure control, turbocharger control, ... The outputs of this level are setpoints for the actuator.
- *Actuator* : The actuators are controlled to their setpoints. This is the level where are located the throttle position control, the wastegate position control, the injection

timing determination, ... The characteristics of the electronic signals sent to the actuators are computed.

This structure enables to take into account the physical interactions of the different parts of the engine. The addition of a new subsystem or the increase of complexity of the air system has an impact limited to one level. It does not require a complete redesign of the software.

This document describes the development of turbochargers control strategies. They concern the level corresponding to the air subsystem.

3.2.3. Control development concerns and issues. — The introduction of new control strategies in the automotive industry and their implementation in production is a complex process because it is difficult to prove that the advantages brought by a new strategy justifies to change a software that is already in production. The main motivations are the following :

- *Introduction of new technologies* : This is the most obvious motivation. When the system is more complex it is necessary to design new strategies.
- *Reduction of the number of sensors or actuators* for cost reasons.
- *Improvement of pollutant emissions or fuel consumption* : This is very attractive, but generally it is linked with the system and the control strategy in itself has no impact.

When developing control strategies, other constraints have to be taken into account. The main concerns are :

- *Performance and robustness*
- *Calibration complexity*
- *Software consistency* : the software developed by an automotive manufacturer is applied to many engines, with different characteristics. A small change in the architecture must imply limited modification of the strategies. All the different control strategies must be generic enough to be adaptable to different setups.

These criteria will be used to justify the claims and the choices made further in the document.

3.3. First analysis of air systems

First, we can apply elementary tests on the air systems introduced in chapter 2 in order to highlight the main properties of the systems that have to be taken into account when designing adequate control strategies.

3.3.1. Turbocharger and engine interactions : turbocharger lag. —
We first consider the turbocharged gasoline engine described in figure 2.14 and modeled by (2.35). The turbocharger dynamics depend on the operating point of the engine, and particularly on engine speed, for two reasons : the state equation (2.14) and the compressor and turbine powers depend on the gas mass flow which is proportional to engine speed, and the system is driven by the turbine power which is closely linked to the exhaust enthalpy flow and thus engine speed (2.4). At low engine speed, not enough energy is available at the exhaust and the system cannot provide any boost even if the actuator is fully closed. On the contrary, more boost is available when the engine speed increases, and at the same time the system dynamics are accelerated. This combination of steady state and transient effects leads to the phenomenon called turbocharger lag.

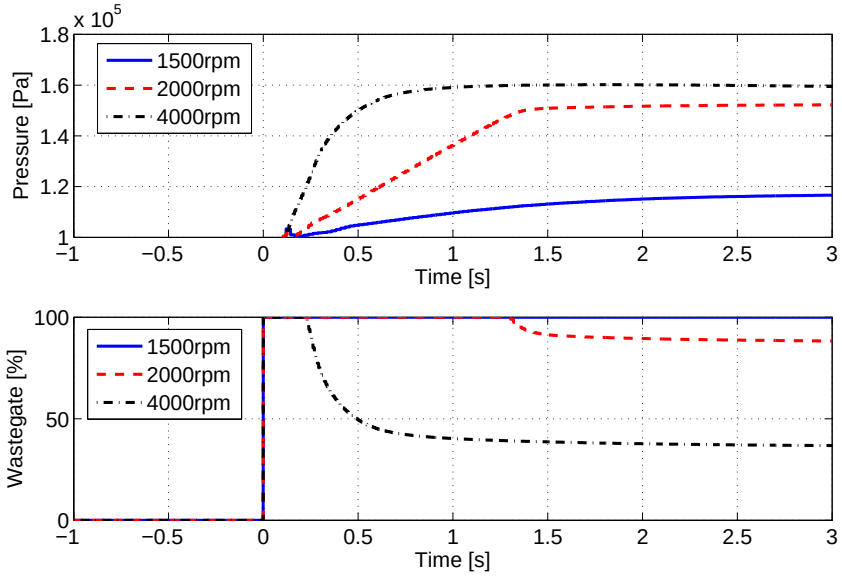

FIGURE 3.2. Influence of engine speed on turbocharger dynamics : intake manifold pressure (top) and wastegate command (bottom).

The lag is amplified by the fact that in a vehicle the engine acceleration depends on the vehicle inertia and on the torque produced by the engine. The global system dynamics (vehicle and engine) has therefore a positive loop. A small increase or decrease of torque at any time of a trajectory has strong repercussions on the following of the trajectory.

Figure 3.2 illustrates the turbocharger lag by showing load transients made at various engine speeds in simulation. At the start of each test the wastegate is fully closed to ensure

that the intake manifold dynamics are representative of the turbocharger dynamics. The dependence on engine speed is obvious during the transient. In steady state at 1250rpm the maximum value reached by the system remains low even if the wastegate is fully closed.

A typical transient test on a vehicle consists in a load transient starting at low engine speed. At the start of the test no boost is available, but when enough speed is reached the actuator must be actuated sufficiently to prevent overboost. This explains one of the main issue of downsized turbocharged engines for which there is a lack of torque at low engine speed.

3.3.2. EGR and turbocharger interactions. —

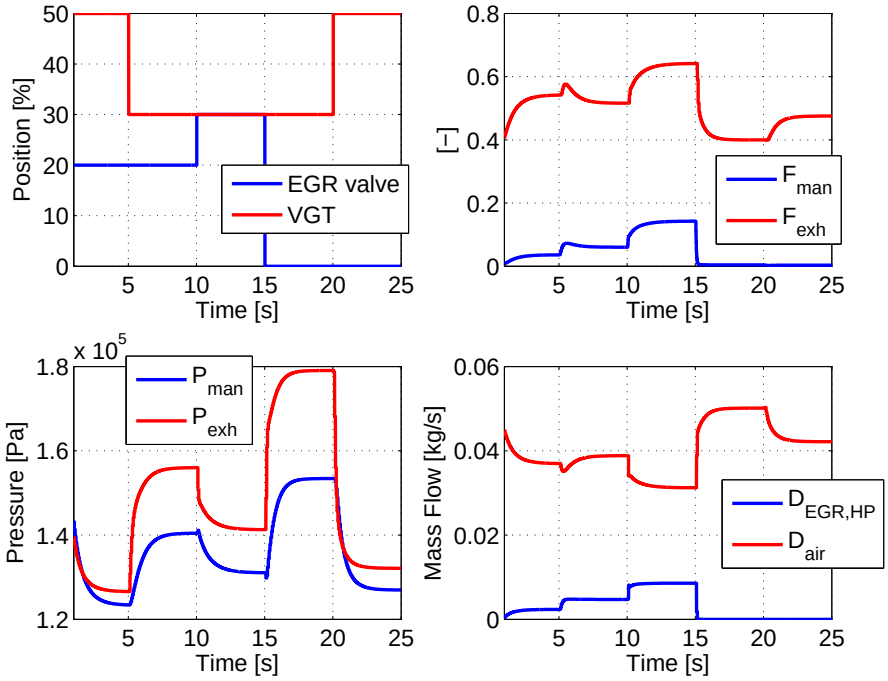

FIGURE 3.3. Impact of VGT and HP EGR actuator variations on the system. Engine operating point : 2000rpm, 20mg/st

We now consider the Diesel engine with two EGR loops described by (2.36). In the case of HP EGR, the compressor and turbine mass flows do not depend only on engine speed, but also on the gas mass flow through the EGR circuit. For the same reasons

which explain the turbocharger lag above, the dynamics and steady state of the system are affected. Since the EGR flow depends on the pressure difference between exhaust and intake manifolds, the turbocharger state also influences the EGR circuit functioning. These cross interactions increase the complexity of the dimensioning and the control of the systems. They are highlighted in figure 3.3 where VGT and EGR valve are actuated at different positions. The effect of EGR on the turbocharger and VGT on EGR flow are obvious. This was pointed out in various publications, for example in [**48**], [**50**], [**85**] and [**57**] but also in [**27**] and [**28**] which will be used as a starting point for the control and estimation of EGR systems in the following chapters.

In the case of LP EGR, turbocharger and EGR circuit are less dependent (figure 3.4) because the EGR circuit is located at the boundaries of the turbocharger. However, some interactions remain, that can be explained mostly by the effect of inlet temperature variations on the compressor.

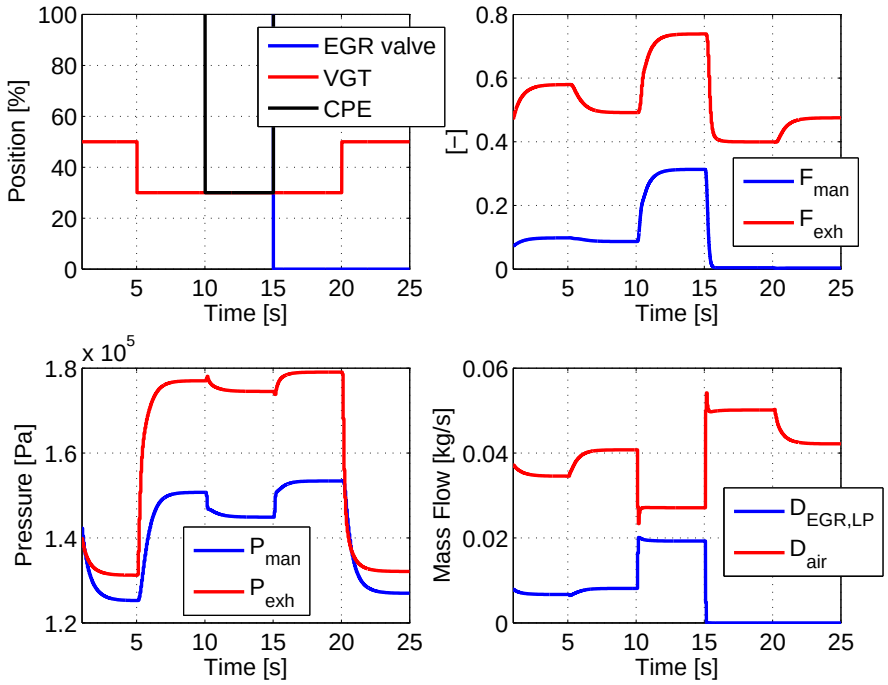

FIGURE 3.4. Impact of VGT and LP EGR actuator variations on the system. Engine operating point : 2000rpm, 20mg/st

3.3.3. Interactions between series two stage turbochargers. —
In the case of single stage turbocharger, the turbocharger behavior does not depend only on engine speed. Also, the compressor upstream pressure and temperature depend on atmospheric pressure and ambient temperature. The impact of the variation of environment conditions changes on the systems is taken into account in equations (2.16) and (2.17). Similarly, on the exhaust side the pressure downstream from turbine depends on aftertreatment back pressure and atmospheric pressure.

In the case of two stage series turbocharger (as described by (2.37)), the conditions upstream the HP compressor and downstream the HP turbine depend on the LP turbocharger. The interactions between the two systems are therefore complex. The impact of environment conditions variations on the global system is also much more complex. A variation of atmospheric pressure first affects the LP turbocharger and then the HP turbocharger. The effect on the intake manifold pressure results from the two compression stages.

Figure 3.5 shows elementary tests consisting of actuator steps applied to each turbocharger of a two stage systems. The effect on the manifold pressures as well as on the compression and expansion ratios of each stage are represented. The effect of the command on compression ratio for each stage is similar to those obtained for a single stage turbocharger, but the intake manifold pressure evolution is more complex because it is the consequence of the two consecutive compressions.

3.4. Air systems control issues

As highlighted in the previous section, the air systems of turbocharged engines are complex, with many nonlinearities and interactions between the different subsystems. We discuss in this section the objectives of the air systems control strategies in order to deduce global issues.

3.4.1. Objectives with respect to engine control. — The main objective of the engine control strategies is to produce a required mechanical torque on the engine shaft. It must also ensure that the pollutant emissions remain below the legislated limits. When these two objectives are met, the engine fuel consumption must be the lowest possible. The relationships between these engine outputs and the air systems have been underlined in chapter 1.

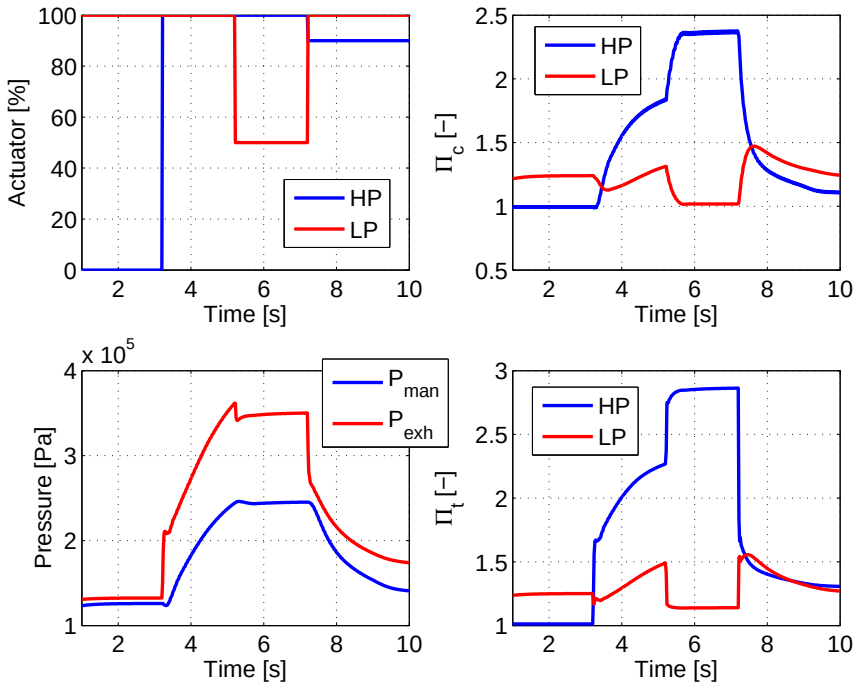

FIGURE 3.5. Impact of HP and LP actuators variations on the two stage turbocharged engine.

Within this scope, the objective of the air system management structure is to control the quantity and the composition of the gas masses entering the engine. As explained in 2.4 the engine mass flow and the composition of the gas entering the cylinder depend on the intake manifold pressure and composition for a fixed distribution engine. Thus, the objectives of the air system control can be focused on the intake manifold control. A fast control of the intake manifold is required.

The pollutant emissions and combustion noise are linked with the thermodynamics conditions (pressure, temperature, composition) in the cylinder at the start of combustion. An accurate control of these variables is therefore necessary.

The consumption consideration leads to minimize the energy losses on the air system in order to maximize the global efficiency. Two examples can be given. This leads to minimize the pressure difference across the engine (see chapter 6), or to avoid generating

unnecessary pressure drop across closed throttles when they are located downstream a compressor (see chapters 4, 5).

3.4.2. Constraints. — The system safety must be ensured. This implies respecting the following constraints :

– Maximum exhaust manifold pressure, for safety reasons
– Maximum turbocharger speed (see 2.2)
– Maximum compressor outlet temperature (see 2.2)

These constraints correspond to high solicitation of the turbocharger, so they are active mostly in turbocharging conditions. They require a specific action of the controllers. We will take these constraints into account mostly for two stage turbochargers in chapter 6 because the system must be operated close to its limits. On the contrary, for Diesel engines with two EGR loop in chapter 5 we focus more on the pollutant emissions and the multivariable control problem, with no consideration on these constraints.

The actuators positions are also limited by constraints on their position : fully closed and fully open. The action on the system is then limited by the physical dimensions of the systems. These constraints induce limitations for the controllers.

3.4.3. Robustness. — The controller has to be robust with respect to other subsystems behavior. This includes environmental conditions changes : the thermodynamic conditions at the boundaries of the system will affect its behavior. This requirement also means that a change in the calibration of the engine or the EGR system must not imply the recalibration of the turbocharger control strategy. This is very important for complex systems such as two EGR circuits or two stage turbochargers.

The strategies must also be robust with respect to production dispersions. The components of two engines, including actuators and sensors, are not identical. This requirement is generally taken into account in the calibration of the strategies rather than in the control structure. However, the impact of these dispersions on the closed loop system must be studied for each case study.

3.4.4. Performance requirements. — The performance and accuracy required for the intake manifold conditions control depend on the technology used.

Diesel engines specificities. — In Diesel engines the combustion is lean, so the torque production depends primarily on the injected fuel quantity. The quantity of fresh air in the cylinder is of second order, as long as it is in excess. The effect on pollutant emissions however is important : the smoke emissions increase dramatically with high

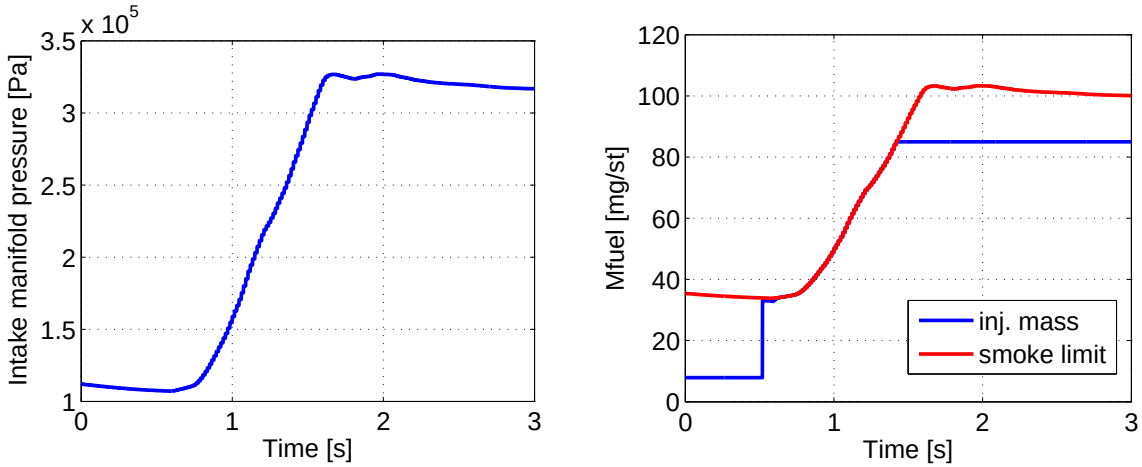

FIGURE 3.6. Limitation of fuel mass injected during intake manifold pressure transient.

fuel air equivalent ratios. Therefore the fresh air mass induces a constraint on the fuel that can be injected. The strategy in charge of the fuel mass limitation is called smoke limiter, which is included in the fuel control strategy. Concerning the air system, the intake manifold pressure control must be as fast as possible when the smoke limitation is active. Undershoots must be avoided, but overshoots and oscillations can be accepted up to a reasonable amount. Figure 3.6 illustrates the smoke limitation during a load transient. Because of the slow dynamics of the intake manifold pressure, the mass injected is limited in transient in order to maintain the cylinder fuel air equivalent ratio below a limit. The smoke limit is deactivated when there is enough air in the cylinder and the effect of oscillations or even steady state errors in the intake manifold pressure control does not affect the torque produced.

Gasoline engines specificities. — Once they are warmed up, gasoline engines operate at stoichiometry in order to ensure a correct functioning of the exhaust catalytic filter. In this case the torque is directly linked with the air mass aspirated by the cylinder which in turn depends on the intake manifold air density. The pressure overshoots, undershoots or oscillations must be suppressed because they would be felt by the driver.

3.4.5. Specific cases. —

3.4.5.1. Supercharging mode. — We consider here only the mode when the EGR circuit is closed. Generally (Diesel and gasoline engines), two actuators remain : the intake throttle and the turbocharger actuator. However, the system can be considered as single input

single output. Indeed in this case the goal of air path management is to control the intake manifold pressure P_{man}^{sp}. The intake throttle allows fast direct action on this variable, but is constrained by its upstream pressure at the compressor outlet. Since energy losses are minimized when the throttle is open, the aim of the turbocharger control strategy is to respect a compressor downstream pressure setpoint $P_{dc}^{\text{sp}} = P_{man}^{\text{sp}}$ via the turbocharger actuator. Throttle and turbocharger controls can be active simultaneously. However, good tracking of the compressor downstream pressure setpoint will ensure that the throttle is fully open in the turbocharging operating zone. On the contrary, a throttle closure will compensate for overshoots on compressor downstream pressure when they are to be avoided absolutely, i.e. in the case of gasoline engines.

In this document, the throttle and turbocharger control are considered independently and only the turbocharger control will be discussed. However, when analyzing the experimental results it is important to verify that the overshoots of the turbocharger control strategy do not generate any action on the throttle on gasoline engines. A description of the throttle control strategy can be found for example in [**63**].

Because of turbocharger lag, the whole bandwidth of the actuator must be used. As explained before, a decrease of torque at the start of a vehicle transient could result in significantly lower performances.

3.4.5.2. Control with EGR. — In this case the system is multivariable. The EGR operating zone corresponds to low load and speed. In this region the smoke limit is generally not active in transient because there is always an excess of air. Therefore the performance of the air control does not affect the torque production. However, it has a strong impact on the pollutant emissions. Since there is no gas composition sensor in the intake manifold, the burned gas concentration must be estimated.

3.4.6. Summary : control problems of the three case studies. —

Turbocharged gasoline engine. — In turbocharging conditions the control problem is SISO with constraints on the actuator and on the state. The goal is to avoid any oscillations while minimizing the response time of the system.

Diesel engine with two EGR loops. — In turbocharging conditions the control problem is SISO with constraints on the actuator and on the state. The goal is to minimize the response time of the system.

In EGR operating conditions the control problem is MIMO with constraints on the actuators. The intake gas composition has to be estimated. The goal is to minimize the pollutant emissions, therefore priority is given to the EGR control.

Diesel engine with two stage turbochargers. — The system is second order. In turbocharging conditions the control problem is MIMO with constraints on the actuators and on the states. The goal is to minimize the response time of the system.

3.5. Sate of the art

3.5.1. Conventional air systems control strategies. — Figure 3.7 below represents a conventional turbocharger control strategy for gasoline engines : the inputs are the manifold pressure measurement P_{man} and set-point $P_{man,sp}$ which is saturated to a maximum value in order to prevent turbocharger overspeed. The output of controller C is added to a feed forward term depending on the engine operating conditions. Variations of environmental conditions (P_{atm}, T_{amb} and P_{dt}) are taken into account via correction maps on the feed forward.

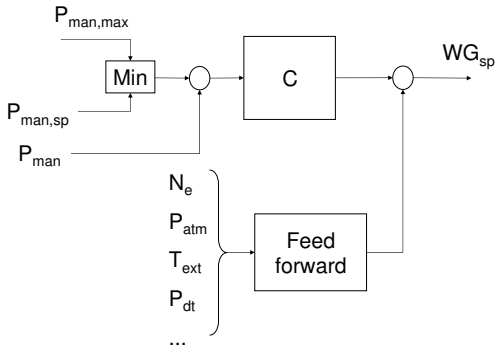

FIGURE 3.7. Turbocharger control strategies schematics.

Concerning Diesel engines with HP EGR and turbocharger, conventional control strategies consist of two decentralized PI controllers with gain scheduling and steady state maps for feedforward : the EGR controls the air mass flow and the VGT controls the boost pressure (this is considered as the basis in [**43, 44, 80, 34, 74, 71**]). The interactions between the two systems are not taken into account. In reality the operating zones are

often considered as separated and only one controller is active at a given time : in EGR zone the turbocharger actuator is given by steady state prepositioning maps, whereas in supercharging mode the EGR circuit is closed.

This type of strategies is possible for relatively small EGR circuits, corresponding to legislation Euro IV. It is not possible any more for the new technologies (for Euro VI) which either contain other sub systems or require to extend the operating zones of the two systems. This increased complexity has generated a lot of literature related to the topic of control for turbocharged air system.

The drawbacks of the conventional controllers mentioned above are linked to the application of linear control techniques to non-linear systems : the compromise obtained between performance and robustness is not satisfying on the whole operating range of the system (see [**78**]). Moreover, both feedforward based on maps and the gain scheduling technique require the definition of operating point. Besides the fact that this generates a heavy calibration task, the concept of operating point is not clear when the system is complex (two EGR loops, two stage turbochargers). Concerning the engine, an operating point is naturally defined in terms of engine speed and torque (see [**44**]), but it is not a good general referential when considering turbochargers in a complex air system. In fact, the operating conditions of turbocharger depend on the conditions at its boundaries : turbine and compressor inlet pressure and temperature and mass flow. These conditions define the influence of external variables (atmospheric pressure, ambient temperature) or the interactions with other subsystems (engine, EGR circuits, other turbocharger).

3.5.2. Advanced turbocharged air systems control. — A lot of works have been published on the subject of Diesel turbocharged air systems control consisting of a HP EGR circuit and a variable geometry turbine, because this problem is nonlinear and multivariable. The same approach can be applied to the control for a turbocharger on a gasoline engine. Most of the works propose a feedforward structure based on a model of the system and a feedback structure.

This model is sometimes based on identification techniques (see [**32, 33, 92**]), but more often on a physical representation of the system (see [**19, 53, 74, 34, 71, 70**]). This solution seems more appropriate given the complex interactions between the different subsystems and the high number of variables (states and inputs) that can influence the system (for example ambient temperature, atmospheric pressure, exhaust back pressure). A complete identification of the system would require a lot of experimental data.

Different approaches have been proposed concerning the feedback control laws. A large number of techniques have been tried, ranging from model based gain scheduling (in [**34**]), to sliding mode control (in [**90, 88**]), predictive control (in [**32, 33, 71, 42**]), H^∞ control (in [**92**] and [**52**]), fuzzy control in [**21**], or flatness based control in [**74**].

A lot of these works are based on linearized versions of the modeling of the system. Again, this requires an important calibration effort, and can be an issue given the strong nonlinearities of the system. Nonlinear control techniques seem more relevant, as shown in [**48, 89, 74**]. Also, [**27**] and [**26**] focused on the development and validation of advanced strategies for the estimation of intake manifold gas composition and the associated control in the case of HP EGR. These strategies exhibit good performances but require accurate turbocharger control which was not dealt with in these works. However this will be the basis of concerning the EGR control in this document. The new developments exposed in this thesis concern the connection between these strategies and the proposed turbocharger control strategies.

Concerning the extension of previous works to a Diesel engine with two EGR circuits, very few articles can be found in the literature and almost nothing specifically on the impact on the turbocharger control. Recently, Wang has proposed a LPV observer that estimates simultaneously the two EGR flows [**91**]. In [**42, 69, 81, 80**] the same engine setup is considered but the proposed control structures consist either of a decentralized structure with linear controllers or of a model predictive controller still too complex to be put in production. The work of [**27**] on HP EGR control was extended to this architecture in [**9**]. The global structure thus obtained is described in chapter 5.

Because of the novelty of the technology, very few papers are available for two stage turbochargers. Models are proposed in [**79**], [**93**] and [**75**] with a control oriented objective, but without any control strategy. In [**73**], [**76**] and [**77**], rather complex multivariable control strategies are proposed, showing only simulation results.

3.6. Claims of the proposed control strategies

The strategies proposed in this thesis are based on the reduction of the air system model. From this model the systems properties are analyzed, and a control strategy is designed for each setup. In chapters 4 and 5 this strategy consists of constrained motion planning and feedback linearization. This structure takes advantage of the proposed model both in the feed forward and the feed back part of the strategy. Concerning two stage turbochargers

(chapter 6), the control strategy still uses a similar model based feed forward structure to take account of state constraints in a second order system.

Thanks to the simplicity of the reduced model and of the control strategy, this approach enables to prove properties of the closed loop system : convergence, stability, constraints satisfaction. It would be possible to use a more complex and more accurate model for example by keeping some dynamics that are neglected in our approach. It would also be possible to use more complex controllers such as non linear model predictive control. However, in both cases it would be much more difficult to prove the stability of the closed loop system. We also show experimental validations of the strategies to demonstrate that the designed control strategies are fast and accurate in spite of the simplifications made.

The contributions and the novelty of the proposed approach are as follows :

– The structure of the model provides steady state and dynamic feedforward action taking account of constraints, with a limited calibration effort. It also naturally adapts to the interaction with other subsystems. For simple systems it takes account of variations of environmental conditions, but can also be generalized to more complex applications such as two EGR circuits or two stage turbocharger.
– As a consequence, the feedback action is also kept very simple and therefore easy to calibrate. It requires only a small number of parameters. The convergence and stability of the closed loop system are proved on the reduced model, and so is the constraints satisfaction when relevant. The strategies are validated experimentally.
– The novelty comes from the control strategy of each case study. In chapter 4 and 5 it consists in the combination of motion planning, feedback linearization, along with an anti windup scheme. The proposed approach takes account of the nonlinear dynamics, the actuator constraints, and the operating conditions in a simple and very efficient control law. This is illustrated by extensive experimental results for the cases studied.

The application of a similar model to three different architectures shows that the chosen representation is generic, and that the level of details is relevant. It allows the consideration of state and actuator constraints and can be adapted easily to different requirements (EGR priority, turbocharger speed limitation, ...). Therefore, the developments proposed in this document offer a useful basis for the consideration of future complex air systems.

We therefore answer to the main requirements of the air system control issues :

– A generic solution that can be adapted to various systems architectures
– A limited calibration effort
– Good transient performances
– Decoupling of the different subsystems

3.7. Conclusion

This chapter analyzes the control issues generic for air systems control, and deduces the specific objectives, requirements and constraints for the three different air systems that will be studied in the following chapters. New turbocharger control strategies will be developed and integrated in a global structure with existing EGR control and estimation strategies. For this purpose we use a reduced model for the design of constrained motion planning and feedback linearization. The stability and the convergence of the closed loop system are proved with the reduced model and validated experimentally on the real system.

The variety of the applications studied underlines the fact that the solutions proposed are flexible and generic, and reinforces the claims that the strategies well take account of the interactions between the turbocharger and other air subsystems. We therefore propose a structure that requires a limited calibration effort and gives good performances.

PART II

CASE STUDIES

CHAPTER 4

GASOLINE ENGINES WITH FIXED GEOMETRY TURBINES

The content of this chapter has been published in [**13, 11, 12**].

4.1. Introduction

4.1.1. Motivation. — This chapter concentrates on the control for single stage fixed geometry turbochargers because this system remains simple when considering the complexity of the air system : there is no EGR circuit and because the system is single input single output (SISO) in turbocharging operating mode. It is therefore a good starting point for the development of new turbocharger control strategies as long as the solution can be generalized to more complex applications.

The general context is the downsizing of gasoline engines, which requires the utilization of supercharging techniques in order to compensate for the consequent torque reduction. This technique has been detailed in various publications (see for example [**45, 61, 72, 58, 39**]). The chapter is organized in five sections. Section 4.2 describes a model of the system appropriate for the design of a model based control strategy. This model is analyzed in 4.3 in order to understand the system properties. Then, in section 4.4, a trajectory satisfying the actuator constraints is designed to provide a feasible setpoint, leading to the proposition of a feed forward strategy. A robustness study underlines the need for a feedback control strategy in order to compensate for model errors. This feedback is detailed in section 4.5. Finally, section 4.6 shows extensive simulation and experimental results of the proposed strategy.

4.1.2. Contributions of the chapter. — The strategy proposed in this paper is based on constrained motion planning and feedback linearization applied to a simplified model (for reference on motion planning see [**38**] and [**28**] for the application on an engine air system). In this combination, each element is important and will be detailed. In a first step, following [**13**], a control oriented model is developed. The model reduction keeps the main dynamics governing the behavior of turbochargers and the dependencies on environmental conditions. Then, a model based control strategy is presented, taking into account actuator constraints and integrator anti windup.

The contributions and the novelty of the proposed approach are as follows :

– The structure of the model provides steady state and dynamic feedforward action taking account of actuator constraints, with a limited calibration effort. It also naturally adapts to varying environmental conditions and can therefore be generalized to more complex applications.

– As a consequence, the feedback action is also kept very simple and therefore easy to calibrate. It requires only three gains kept constant on the overall operating range. Other control strategies can have performances relatively close to that presented, but at the price of considerable calibration effort. The results of the study demonstrate that constrained motion planning is an effective solution for controlling the air system. The control strategy is very aggressive, hits the constraints and convergence is guaranteed.

– Finally, the novelty comes from the combination of motion planning, feedback linearization, along with an anti windup scheme. The proposed approach takes account of the nonlinear dynamics, the actuator constraints, and the operating conditions in a simple and very efficient control law. This is illustrated by extensive experimental results.

4.2. Air system model reduction

This section proposes a simple description of the system in order to obtain a control oriented representation.

We start with the complete model (2.35) given in chapter 2. This model contains three states. Therefore the design of a model based control law is difficult. It is desirable to reduce this model and keep only the main dynamics and steady state effects for control purposes. We detail in this chapter the steps undertaken for the simplification. Different types of assumptions will be made and verified empirically.

The section also analyzes the main properties of the system, which will be used when designing the control strategy.

4.2.1. Model simplification by singular perturbation. — The third order nonlinear system (2.35) accurately describes the dynamics of the system. However, one can notice that the turbocharger speed is much slower than the pressure dynamics dynamics.

The reference dynamics (2.35) has the form of the following system where $u \triangleq S_{wg}$, $z_1 \triangleq a_1 N_t^2$, $z_2 \triangleq a_2 \begin{bmatrix} P_{ut} & P_{dc} \end{bmatrix}^T$ and $a_1 = 9e-9$, $a_2 = 1e-5$ are normalizing constants :

$$\begin{cases} \dot{z}_1 = f_1(z_1, z_2) \\ \dot{z}_2 = f_2(z_1, z_2, u) \end{cases} \tag{4.1}$$

The order of magnitude of f_1 is $a_1 \frac{2}{J_t} D_c c_p T_{uc} \phi_c(2) \simeq 3.2$ whereas that of the two components of f_2 are $a_2 \frac{RT_{ut}}{V_{ut}} \Psi \simeq 60$ and $a_2 \frac{RT_{dc}}{V_{dc}} \Psi \simeq 20$.

This suggests to simplify these dynamics by singular perturbation [**54**]. Let $\epsilon \triangleq \frac{1}{a_2} \frac{V_{ut}}{RT_{ut}} \frac{1}{\Psi}$ be a scalar that represents all the small parameters to be neglected. The reference dynamics (2.35) has the form of the standard singularly perturbed system

$$\begin{cases} \dot{z}_1 = \phi(z_1, z_2) \\ \epsilon \dot{z}_2 = \psi(z_1, z_2, u, \epsilon) \end{cases} \tag{4.2}$$

Noting the time constants $\tau_{dc} \frac{1}{a_2} \frac{V_{dc}}{RT_{dc}} \frac{1}{\Psi} = \mathcal{O}(\epsilon)$ i.e. $\tau_{dc} = k_{dc}(\epsilon)\epsilon$ with $\lim_{\epsilon \to 0} k_{dc}(\epsilon) = \bar{k}_{dc} > 0$, we have

$$\psi(z_1, z_2, u, \epsilon) = a_2 \begin{bmatrix} (1+\lambda_s)\eta_v \Pi_c \Psi - (\phi_{D_t}(\Pi_t, N_t)\Pi_t + u\phi_{wg}(\Pi_t)) \frac{P_{dt}}{\sqrt{T_{ut}}} \\ \frac{1}{k_{dc}(\epsilon)} \left(D_c - \eta_v \Pi_c \Psi\right) \end{bmatrix}$$

The equation $\psi(z_1, z_2, u, 0) = 0$ has a unique root of interest $z_2 = h(z_1, u)$. In details, it is

$$\begin{cases} (1+\lambda_s)\eta_v \Pi_c \Psi = (\phi_{Dt}(\Pi_t, N_t)\Pi_t + u\phi_{wg}(\Pi_t)) \frac{P_{dt}}{\sqrt{T_{ut}}} \\ D_c = \eta_v \Pi_c \Psi \end{cases}$$

To ensure the validity of the simplification, we can check the uniform stability of the Jacobian of ψ [**55**][Assumption 3.2 p11]. For that, we consider $\partial_{z_2} \psi_{|z_2 = h(z_1,u)}$ and compute its eigenvalues

$$\partial_{z_2} \psi_{|z_2 = h(z_1,u)} = a_2 \begin{bmatrix} -(\phi'_{Dt}\Pi_t + \phi_{Dt} + u\phi'_{wg}(\Pi_t)) \frac{P_{dt}}{\sqrt{T_{ut}}} & (1+\lambda_s)\eta_v \frac{1}{P_{uc}} \Psi \\ 0 & -\frac{1}{k_{dc}(\epsilon)} \eta_v \frac{1}{P_{uc}} \Psi \end{bmatrix}$$

Since ϕ_{Dt} is strictly increasing and positive, the fast system is stable : there exists $c > 0$ such that $\mathcal{R}e(\partial_{z_2}\psi_{|z_2=h(z_1,u)}) < -c$. The reduced dynamics write

$$\begin{cases} \dot{\bar{z}}_1 = \phi(\bar{z}_1, h(\bar{z}_1, u)) \\ \bar{z}_2 = h(\bar{z}_1, u) \end{cases} \tag{4.3}$$

From [**54**][Th 11.1], the following proposition holds

Proposition 4.1. — *Consider the singularly perturbed system* (4.2) *and* $z_2 = h(z_1, u)$ *the isolated root of* $\psi(z_1, z_2, u) = 0$. *There exists a positive constant* $\epsilon^\star > \epsilon > 0$ *such that* (4.2) *possesses a unique trajectory* $z_1(t, \epsilon)$, $z_2(t, \epsilon)$, *and*

$$z_1(t, \epsilon) - \bar{z}_1(t) = \mathcal{O}(\epsilon)$$

$$z_2(t, \epsilon) - h(\bar{z}_1(t), u) = \mathcal{O}(\epsilon)$$

hold when $\epsilon < \epsilon^\star$.

Thus, the new reference system writes

$$\begin{cases} \dfrac{d}{dt}(\dfrac{1}{2}J_t N_t^2) &= \phi_{D_t}(\Pi_t, N_t) c_p P_{dt} \sqrt{T_{ut}} \eta_t \phi_t(\Pi_t) - \eta_v \Pi_c \Psi c_p T_{uc} \dfrac{1}{\eta_c} \phi_c(\Pi_c) \\ (1 + \lambda_s)\eta_v \Pi_c \Psi &= (\phi_{D_t}(\Pi_t, N_t)\Pi_t + S_{wg}\phi_{wg}(\Pi_t)) \frac{P_{dt}}{\sqrt{T_{ut}}} \end{cases} \tag{4.4}$$

4.2.2. Turbine flow simplification. — The turbine can be considered as a restriction on the exhaust gas flow. However, the standard equation for compressible flow across an orifice cannot be applied in this case. Modified versions of this equation have been proposed which fit better the experimental results, based on various assumptions (see [**67**]). Most of them neglect the influence of the turbine speed. The formula kept in our case is given below, the justification being that it shows a good correlation with the characterization data (see Figure 4.1).

$$D_t = \frac{P_{dt}}{\sqrt{T_{ut}}} \phi_{turb}(\Pi_t)$$

where

$$\phi_{turb}(\Pi_t) \triangleq S_t \frac{\Pi_t^{\frac{3}{2}}}{\sqrt{R}} \sqrt{\frac{2\gamma}{\gamma - 1}\left(\Pi_t^{\frac{-2}{\gamma}} - \Pi_t^{\frac{-\gamma-1}{\gamma}}\right)}$$

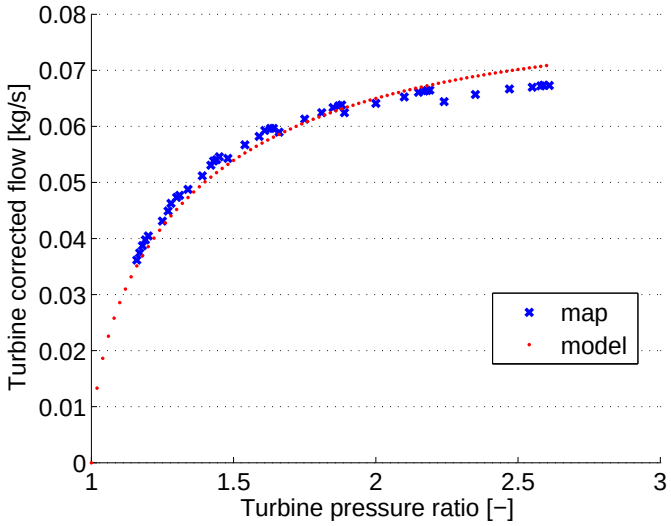

FIGURE 4.1. Comparison between turbine characterization data and simplified model.

4.2.3. Correlation between the turbocharger speed and compression ratio. — For given engine operating conditions, the turbocharger speed and the intake pressure are very correlated. Since we consider that the mass flow through the compressor is equal to the aspirated mass flow ($D_c = D_{asp}$), it is therefore interesting to consider the combination of (2.17) and (2.26). The corrected compressor flow depends on the compressor pressure ratio, the engine speed and the operating conditions, and :

$$\Pi_c = \phi_{\Pi,c}(\eta_v(\Pi_c P_{uc}, N_e)\Pi_c \Psi, \frac{N_t}{\sqrt{T_{uc}}}) \tag{4.5}$$

This expression is noticeable since it shows a direct dependency between compressor pressure ratio and engine speed. The influence of intake temperature is of second order and will be neglected. It is possible now to represent turbocharger speed as a function of pressure ratio. It can be observed in Figure 4.2 that the turbocharger speed square N_t^2 is a linear function of the compressor pressure ratio Π_c. In the sequel we will therefore use this simple representation and consider that

$$N_t^2 = a\Pi_c + b$$

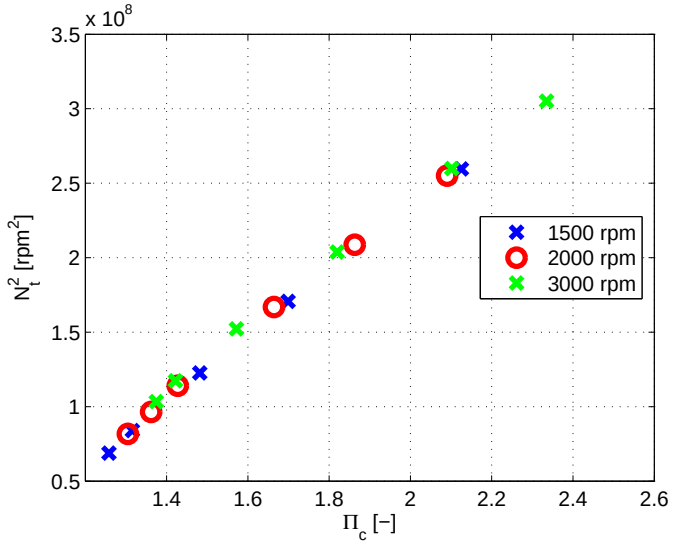

FIGURE 4.2. Experimental results at steady state. Variation of the turbocharger speed square N_t^2 w.r.t. the compressor pressure ratio Π_c.

4.2.4. Steady state assumptions. — The system dynamics described by 4.4 depend on a lot of different variables that physically are related to the engine (engine speed, volumetric efficiency) or the environment (compressor upstream pressure and temperature, turbine downstream pressure). Since they are external to the turbocharger, we will make the following assumptions :

- N_e, T_{uc}, T_{man}, P_{man} and P_{uc} are measured
- η_{vol} is a mapped function of N_e and P_{man}
- D_{air} is estimated as $\eta_{vol} P_{man} N_e \frac{V_{cyl}}{120 R T_{man}}$
- η_c and η_t are mapped functions of D_{air} and Π_c
- T_{ut} is a function of N_e and D_{fuel}
- P_{dt} and P_{uc} are estimated from P_{atm} and the assumption that pressure drops through the catalytic converter at the exhaust and the air filter at the inlet depend only on the engine aspirated air flow D_{air}.

These variables can either be measured or estimated based on steady state maps. Note that some dependencies on Π_c subsist in these computations. However, their effect on the behavior of the turbocharger is second order, and can therefore be neglected in the design of the control strategy.

4.2.5. Reference system. — The linear correlation between compressor pressure ratio and turbocharger kinetic energy (4.5) considerably simplifies the studied system. The state variable can be chosen as the compressor pressure ratio, and the turbocharger speed does not appear any more in the equations.

The reference system writes

$$\begin{cases} \dot{\Pi}_c &= \alpha_1 \psi_t(\Pi_t) - \alpha_2 \psi_c(\Pi_c) \\ \Pi_c &= \alpha_3(\phi_{turb}(\Pi_t) + uS_{wg,max}\phi_{wg}(\Pi_t)) \end{cases} \tag{4.6}$$

where the variables $\{\alpha_i\}_{i\in[1,3]}$ are given by :

$$\begin{cases} \alpha_1 \triangleq C_p\sqrt{T_{ut}}P_{dt}\eta_t\dfrac{2}{J_t a} \\ \alpha_2 \triangleq \eta_v \Psi C_p T_{uc}\dfrac{1}{\eta_c}\dfrac{2}{J_t a} \\ \alpha_3 \triangleq \dfrac{P_{dt}}{\sqrt{T_{ut}}(1+\lambda_s)\Psi\eta_{vol}} \end{cases} \tag{4.7}$$

with $\Psi \triangleq \frac{V_{cyl}P_{uc}N_e}{120RT_{man}}$.

Concerning the implementation of the strategy, these variables can be computed online, considering :

- N_e, T_{uc}, T_{man}, P_{man} and P_{uc} are measured
- η_{vol} is a mapped function of N_e and P_{man}
- D_{air} is estimated as $\eta_{vol}P_{man}N_e\frac{V_{cyl}}{120RT_{man}}$
- η_c and η_t are mapped functions of D_{air} and Π_c
- T_{ut} is a function of N_e and D_{fuel}
- P_{dt} and P_{uc} are estimated from P_{atm} and the assumption that pressure drops through the catalytic converter at the exhaust and the air filter at the inlet depend only on the engine aspirated air flow D_{air}.

Note that some dependencies on Π_c subsist in these computations. However, their effect on the behavior of the turbocharger is second order, and can therefore be neglected in the design of the control strategy.

In figures 4.3 the variables α_i are plotted for different engine operating points extracted from a test campaign corresponding to the complete turbocharging zone, for which the assumptions made before are valid. The α_i are represented as functions of engine speed because this variable is the most relevant to define the operating point of the system. It can be noticed that for a given engine speed the variation of these coefficients is limited.

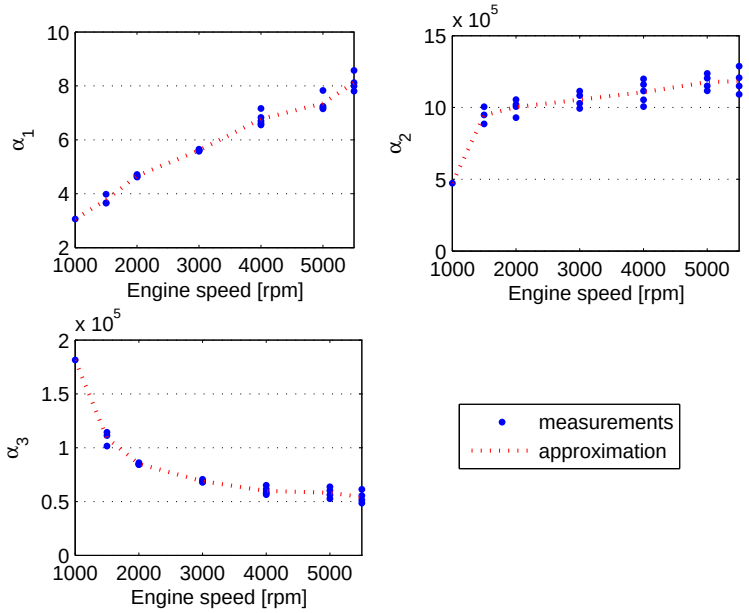

FIGURE 4.3. Coefficient α_i computed from test data for different turbocharging operating points.

Functions ϕ_{turb}, ϕ_{wg}, ψ_c and ψ_t are represented in Figure 4.4 and given by :

$$\begin{cases} \psi_c(\Pi) \triangleq \Pi(\Pi^{\frac{\gamma-1}{\gamma}} - 1) \\ \phi_{turb}(\Pi) \triangleq S_t \dfrac{\Pi^{\frac{3}{2}}}{\sqrt{R}} \sqrt{\dfrac{2\gamma}{\gamma-1}\left(\Pi^{-\frac{2}{\gamma}} - \Pi^{-\frac{\gamma+1}{\gamma}}\right)} \\ \psi_t(\Pi) \triangleq (1 - \Pi^{\frac{1-\gamma}{\gamma}})\phi_{turb}(\Pi) \\ \phi_{wg}(\Pi) \triangleq \dfrac{\Pi}{\sqrt{R}} \sqrt{\dfrac{2\gamma}{\gamma-1}\left(\Pi^{-\frac{2}{\gamma}} - \Pi^{-\frac{\gamma+1}{\gamma}}\right)} \end{cases} \tag{4.8}$$

The wastegate cross-section S_{wg}, the command of the system, has been normalized for simplification : $S_{wg} \triangleq u\bar{S}_{wg}$, with the constraints : $0 = u_m \leq u \leq u_M = 1$.

The first equation of system (4.6) represents the balance between compressor and turbine mechanical power, giving the main dynamics of the system. These dynamics are nonlinear and depend on the operating conditions. The second equation represents the mass conservation in the exhaust manifold, whose dynamics can be neglected.

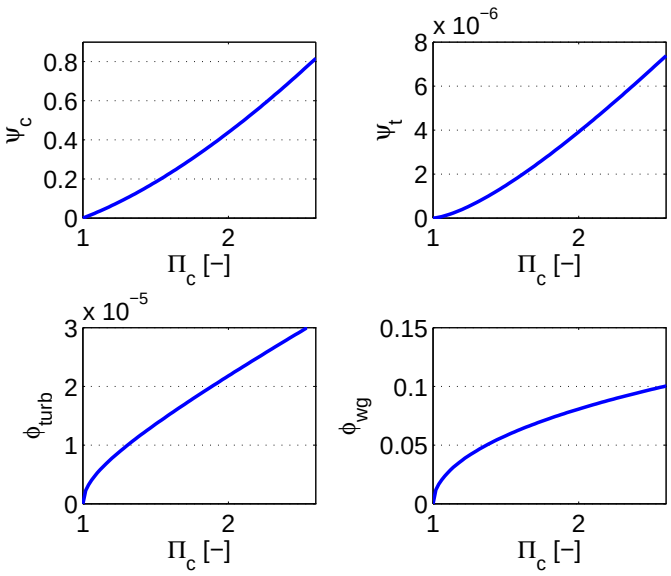

FIGURE 4.4. Functions ψ_c, ψ_t, ϕ_{turb}, ϕ_{wg}.

The compact representation (4.6) brings several advantages. First, functions ϕ_{turb}, ϕ_{wg}, ψ_c and ψ_t are non-linear, positive, strictly increasing, and thus invertible. This very important property will be used when designing the control law which can be based on the inversion of this model. Also, thanks to the choice of state variable and the simplifications made, the dependencies upon environmental variables are concentrated in the variables $(\alpha_1, \alpha_2, \alpha_3)$.

4.2.6. Model validation. — Figure 4.5 shows a comparison between the compressor and turbine powers computed from the expression given in the first equation of system (4.6) from experimental data measured in steady state. These two variables should be equal in order to ensure that the system is stable. The comparison shows only small differences.

Figure 4.6 shows a comparison between experimental data and results obtained from equations (4.6) during a turbocharger transient. The experiment was performed on an engine testbed, at a constant engine speed of 2000rpm. The input of the model are the sensors available on the engine, and the command applied on the wastegate. The model is valid after the throttle is closed ($t = 1$). The response time of the turbocharger is well represented, even if some higher dynamics are missing.

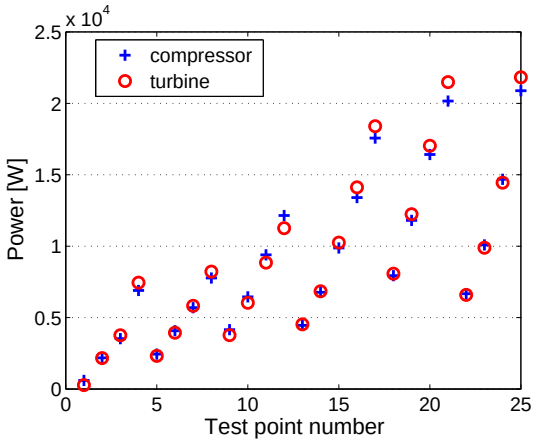

FIGURE 4.5. States of equilibrium : comparison between compressor turbine powers on steady state points measured on the test bench.

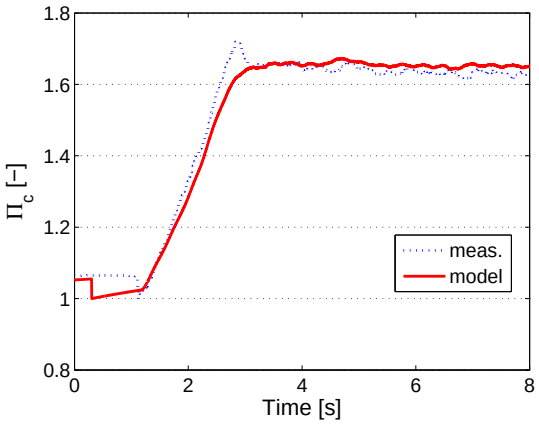

FIGURE 4.6. Transient validation : comparison between the compression ratio measured on a test bench and obtained from the dynamics equation of the model.

Additionally to these results, the figures presented in the last section also validate a posteriori the assumptions made, in particular the test made with the feedforward action alone (figures 4.20 and 4.21) which is based on the direct inversion of (4.6).

4.3. System analysis

4.3.1. System trajectories. — The simple representation provided by model (4.6) helps to better understand the system. Since it is particularly interesting to analyze its behavior with respect to engine speed, the coefficients α_i are approximated in the following by an average value at each engine speed. This does not affect the macroscopic analysis of the system but simplifies the study. First of all, we write Π_t as a function of Π_c and u by inverting the second equation of system (4.6) which is static, leading to

$$\dot{\Pi}_c = \alpha_1 \Psi_t(\Pi_c, u) - \alpha_2 \psi_c(\Pi_c)$$

It allows to look at the trajectories of the system when we consider a constant control input u. In Figure 4.7, we represent $\dot{\Pi}_c$ as a function of Π_c at an engine speed of 2000 rpm for different values of u. When the command is constant, the curves shown on the graph represent the trajectories of the system. The states of equilibrium correspond to the line

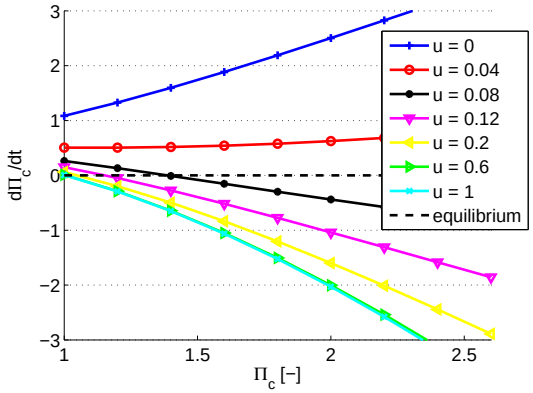

FIGURE 4.7. $\dot{\Pi}_c$ as a function of Π_c, at 2000rpm.

$\dot{\Pi}_c = 0$ (the dotted line of Figure 4.7). When a curve crosses this line, the system state corresponds to an equilibrium point. Above this line, the state derivative is positive, and the state is increasing, so the system moves on its trajectory towards the right of the graph. Below the line, the state derivative is negative, and the system moves on its trajectory towards the left of the graph. As a consequence, if the trajectory is increasing with respect to Π_c, the equilibrium point is unstable, otherwise it is stable. On the other hand, if the curve does not cross the line $\dot{\Pi}_c = 0$, the system is unstable (see **[20]** for the study of the dependence upon a parameter of systems trajectories). At 2000 rpm, several behaviors are noticeable. First, when the wastegate is closed ($u = 0$), the curve is increasing while never crossing the equilibrium point. The system is unstable in this case with no equilibrium point. Then, when the wastegate is more open (u closer to 1), the system has stable equilibrium points.

4.3.2. Equilibrium states of the system. — Since the functions of system (4.6) are invertible and increasing, there exists a unique Π_t such that the second equation is verified. The presented system is thus well posed. This value can be re-injected in the first part of the dynamics leading to a compact version of the dynamics. In the remainder of the paper, the dynamics are represented by $\dot{\Pi}_c \triangleq f(\Pi_c, u)$.
Moreover, this system is fully actuated and invertible. Based on **[38]**, an analytical expression for the command u can be derived from the state variable and their first derivative

histories. Indeed, from $(\Pi_c, \dot{\Pi}_c)$, it is possible to compute

$$\Pi_t = \psi_t^{-1}(\frac{1}{\alpha_1}(\dot{\Pi}_c + \alpha_2\psi(\Pi_c))) \tag{4.9}$$

The input u can then be computed using the static equality

$$u = \frac{\Pi_c - \alpha_3\phi_{turb}(\Pi_t)}{\alpha_3 S_{wg,max}\phi_{wg}(\Pi_t)} \tag{4.10}$$

Combining (4.9) and (4.10) leads to an expression of u as a function of Π_c and $\dot{\Pi}_c$. This inverse model is noted g.

$$u \triangleq g(\Pi_c, \dot{\Pi}_c) \tag{4.11}$$

Notice that $u = g(\Pi_c, f(\Pi_c, u))$. From (4.11), the unique input (u^{r}) corresponding to any desired (Π_c^{r}) trajectory is in fact

$$u^r = g(\Pi_c^r, \dot{\Pi}_c^r) \tag{4.12}$$

The states of equilibrium of the system correspond to the solutions of a system of two equations with three variables ($\Pi_{c,eq}$, $\Pi_{t,eq}$, and u_{eq}). It corresponds to the inversion described above, with a state derivative equal to zero :

$$u_{eq} = g(\Pi_{c,eq}, 0) \tag{4.13}$$

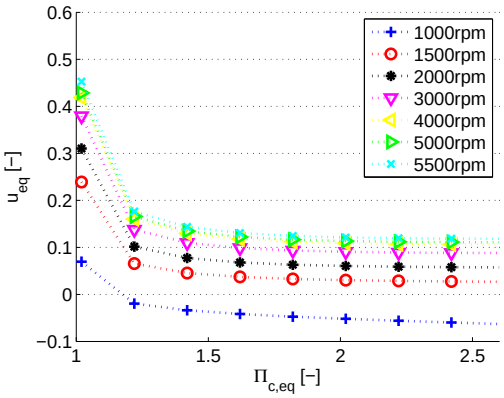

FIGURE 4.8. States of equilibrium : u_{eq} as a function of $\Pi_{c,eq}$, for different engine speeds.

Figure 4.8 shows the different values of command u_{eq} depending on $\Pi_{c,eq}$, for different engine speeds. Since the command represents the section of the wastegate valve, negative

values are not physically possible. At a given engine speed the maximum Π_c achievable corresponds to a command $u_{eq} = 0$. At 1000 rpm this value is lower than 1.2, whereas at higher speeds it is possible to reach 2.6, which is the limit allowed by the system.

From this analysis, it is also possible to compute the minimum input maintaining the pressure ratio at an equilibrium point lower than the maximum value allowed by the system, corresponding to a maximum turbocharger speed (set at a compression ratio of 2.6 in this case). Figure 4.9 shows this minimum command as a function of engine speed. At low engine speed the maximum pressure ratio can not be reached even with the actuator fully closed ($u = 0$).

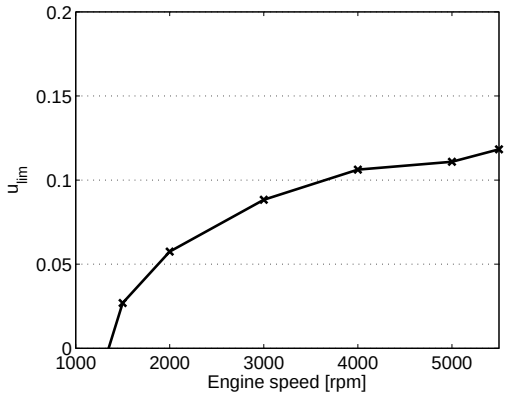

FIGURE 4.9. Input limit to have a pressure ratio equilibrium less that 2.6 bar with respect to the engine speed.

4.3.3. Stability of the system. —

4.3.3.1. Stability around an equilibrium state. — System (4.6) can be linearized around the states of equilibrium (defined by (4.13)) leading to the following representation (the command u_{eq} is considered constant) :

$$\left\{ \begin{array}{rcl} \dot{x}_1 & = & a_1 x_2 - a_2 x_1 \\ x_1 & = & a_3 x_2 + a_4 u_{eq} x_2 \end{array} \right. \tag{4.14}$$

where $x_1 \triangleq \Pi_c - \Pi_{c,eq}$, $x_2 \triangleq \Pi_t - \Pi_{t,eq}$, and a_i are coefficients depending on the engine operating points :

$$\left\{ \begin{array}{rclcrcl} a_1 & = & \alpha_1 \frac{d\psi_t}{d\Pi_t}(\Pi_{t,eq}) & , & a_2 & = & \alpha_2 \frac{d\psi_c}{d\Pi_c}(\Pi_{c,eq}) \\ a_3 & = & \alpha_3 \frac{d\phi_{turb}}{d\Pi_t}(\Pi_{t,eq}) & , & a_4 & = & \alpha_4 \frac{d\phi_{wg}}{d\Pi_t}(\Pi_{t,eq}) \end{array} \right.$$

System (4.14) can be rewritten as a first order linear system with a time constant depending of the constant input:

$$\dot{x}_1 = \tau(u_{eq}) x_1 \quad \text{with} \quad \tau(u_{eq}) = \frac{a_1}{a_3 + a_4 u_{eq}} - a_2 \tag{4.15}$$

The stability of the system around the equilibrium states is guaranteed if τ is negative (see [**20**]). Figure 4.10 represents the value of τ as a function of $\Pi_{c,eq}$ for different engine speeds. It can be checked that τ remains always negative, and thus, all the equilibrium points are stable. However, τ is increasing : as the compressor ratio (and thus the engine load) increases, the system becomes closer to instability.

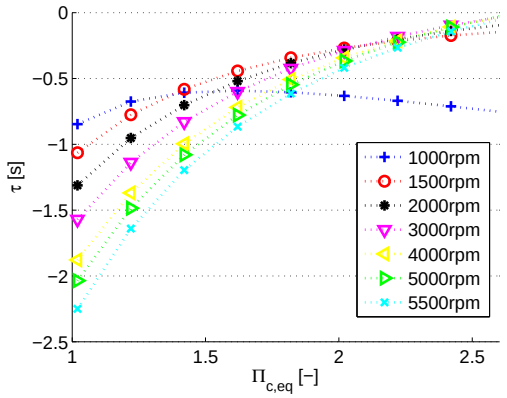

FIGURE 4.10. States of equilibrium : $\tau(u_{eq})$ as a function of $\Pi_{c,eq}$, for different engine speeds.

4.3.3.2. Stability around trajectories. — Let $\mathcal{X} \triangleq [1, \bar{\Pi}]$ and $\mathcal{U} \triangleq [u_m, u_M]$ the state and the input constraints. (Π_c^r, u^r) is said to be a feasible reference trajectory if

$$\forall t \quad (u^r(t), \Pi_c^r(t)) \in \mathcal{U} \times \mathcal{X} \text{ and } \dot{\Pi}_c^r = f(\Pi_c^r, u^r)$$

Let (Π_c^r, u^r) be a feasible reference trajectory. Applying the open loop control law u^r to (4.6) with any initial condition $\Pi_c(0) \in \mathcal{X}$, system (4.6) gives $\dot{\Pi}_c = f(\Pi_c, u^r)$. We note

$\tilde{\Pi}_c \triangleq \Pi_c^r - \Pi_c$. Linearizing around the reference trajectory leads to

$$\begin{cases} \dot{\tilde{\Pi}}_c = \alpha_1 \psi_t^{'}(\Pi_t^r)\tilde{\Pi}_t - \alpha_2 \psi_c^{'}(\Pi_c^r)\tilde{\Pi}_c \\ \tilde{\Pi}_c = \alpha_3(\phi_{turb}^{'}(\Pi_t^r) + u^r \bar{S}_{wg}\phi_{wg}^{'}(\Pi_t^r))\tilde{\Pi}_t \end{cases}$$

with the notation $\phi^{'}(x) = \frac{d\phi(x)}{dx}$. Then, we have $\dot{\tilde{\Pi}}_c = \tau^r(t)\tilde{\Pi}_c$ where

$$\tau^r(t) \triangleq \frac{\alpha_1}{\alpha_3}\frac{\psi_t^{'}(\Pi_t^r)}{\phi_{turb}^{'}(\Pi_t^r) + u^r \bar{S}_{wg}\phi_{wg}^{'}(\Pi_t^r)} - \alpha_2 \psi_c^{'}\left(\alpha_3(\phi_{turb}(\Pi_t^r) + u^r \bar{S}_{wg}\phi_{wg}(\Pi_t^r))\right)$$

From the analysis above concerning the stability around the states of equilibrium, the system is exponentially stable around any feasible steady state trajectory. It could be numerically verified that this property can be extended to any feasible trajectory.

4.4. Feed forward and Motion planning: design of a feasible trajectory

4.4.1. Feasible trajectory generation. From $\Pi_c^{\mathbf{sp}}$ to $\Pi_c^{\mathbf{mp}}$. — Since P_{uc} can be measured or estimated, the setpoint P_{dc}^{sp} is transformed into Π_c^{sp} such as $\Pi_c^{\mathrm{sp}} \triangleq \frac{P_{dc}^{\mathrm{sp}}}{P_{uc}}$. Equation (4.12) can therefore be used in order to design the feedforward strategy :

$$u^{\mathrm{sp}} = g(\Pi_c^{\mathrm{sp}}, \dot{\Pi}_c^{\mathrm{sp}}) \tag{4.16}$$

However, in order to fulfill the requirements in terms of safety and feasibility, the following constraints must be considered

- Since the speed of the turbocharger shaft is directly linked to the compressor pressure ratio, a limit on the setpoint will ensure the safety of the system by maintaining the shaft speed below a maximum value, i.e. $\Pi_c \leq \bar{\Pi}$.
- The state setpoint has to be continuously differentiable in order to compute $\dot{\Pi}_c^{\mathrm{sp}}$.
- Finally, the actuator is limited between u_m and u_M, which is not guaranteed by (4.16).

The purpose of this section is to compute a feasible setpoint trajectory Π_c^{mp} such that the state and actuator constraints are satisfied. The notation $sat(u, u_m, u_M)$ is used for the function defined by

$$sat(u, u_m, u_M) = \begin{cases} u_m & \text{if} \quad u \leq u_m \\ u & \text{if} \quad u_m \leq u \leq u_M \\ u_M & \text{if} \quad u_M \leq u \end{cases}$$

The new reference setpoint, called Π_c^{mp} is obtained from the filter defined by

$$\dot{\Pi}_c^{mp} = sat\big(\beta(\min\{\Pi_c^{sp}, \bar{\Pi}\} - \Pi_c^{mp}), f(\Pi_c^{mp}, u_M), f(\Pi_c^{mp}, u_m)\big) \tag{4.17}$$

where β is a gain tuning the dynamics of the trajectory. When the actuator constraints are not reached, this filter corresponds to a first order low pass filter with a time constant $1/\beta$. The gain β provides the possibility of dampening the system dynamics and of controlling the actuator solicitation. This can be very useful when considering unmodelled dynamics, modeling errors, or noise. The feedforward strategy becomes finally :

$$u = g(\Pi_c^{\mathrm{mp}}, \dot{\Pi}_c^{\mathrm{mp}}) \tag{4.18}$$

The new strategy is obtained by the succession of (4.17) (schematized in figure 4.11) and (4.18) . Since function g is the inverse of f the constraints are respected and the system is brought towards the setpoint. Experimental results of this strategy are presented in section 4.6.3.

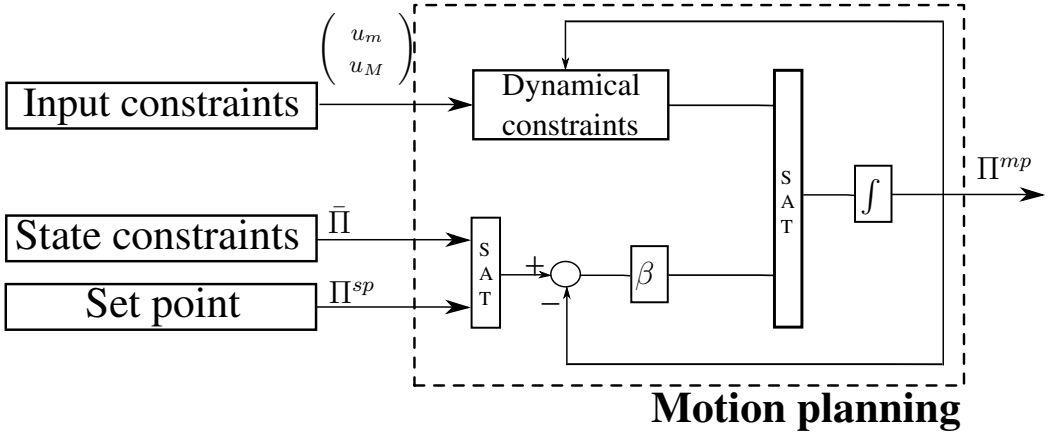

FIGURE 4.11. Constrained motion planning in order to obtain a feasible trajectory as defined by (4.17).

4.4.2. Robustness with respect to parameters variations. — Since the system is open loop stable (as discussed in subsection 4.3), the application of the control input $u^{mp} = g(\Pi_c^{mp}, 0)$ implies that $|\Pi_c - \Pi_c^{mp}|$ will asymptotically converge toward 0. However, this is true if and only if the model inversion is perfect, which is not the case experimentally because the coefficients α_i depend on environmental conditions and on systems characteristics that are known with an error margin. In order to evaluate the modeling error impact on the steady state error, dispersions can be added to the reduced model (4.6) to represent errors on the system characteristics. The dispersed model is called f_Δ. Application of the control input $u^{mp} = g(\Pi_c^{mp}, 0)$ results in an equilibrium state $\Pi_{c,\Delta}$ corresponding to $f_\Delta(\Pi_{c,\Delta}, g(\Pi_c^{mp}, 0)) = 0$.

The difference between $\Pi_{c,\Delta}$ and Π_c^{mp} gives the steady state error of the open loop system for a given dispersion. It is possible to compute this error for a high number of dispersed systems in order to deduce the dispersion of the equilibrium state of the open loop system. Figure (4.12) shows the results of this approach applied at 3000 rpm.

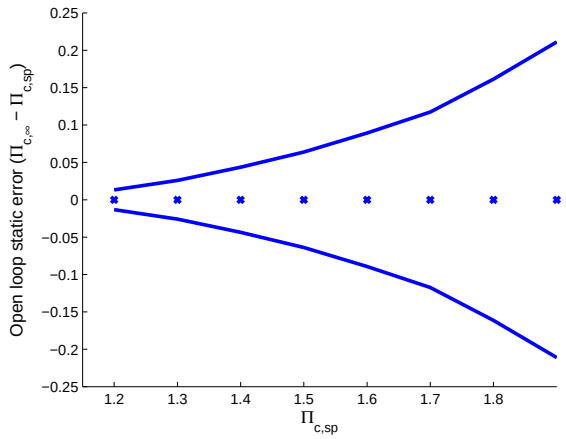

FIGURE 4.12. Steady state error of the dispersed system.

Dispersions with a Gaussian distribution have been added on compressor and turbine efficiencies, on compressor upstream pressure and temperature, and on turbine upstream temperature. One thousand tests have been performed in order to obtain a representative output. The bold lines on the graph represent three times the variance of the steady state error, corresponding in a Gaussian distribution to the area where 97.5% of the population should be found.

Undesired behaviors appear at high compression ratios, when the state of equilibrium can be very different from the set-point. In some cases, the maximum compression ratio is higher than the maximum value allowed by the system. This lack of robustness of the open loop system comprising only an inversion of the steady state part of the model as a feed forward underlines the necessity of a feedback term in the strategy. This dispersion will be used further to assess the robustness of the closed loop strategy.

4.5. Control strategy

4.5.1. Feedback linearization. — A feedback strategy is designed in order to improve the robustness of (4.18). The control strategy can be decomposed into two terms. The

first term is obtained by feedback linearization through dynamic inversion of the model (see **[82]** for more details). Moreover, an integral action is added to guarantee convergence even in case of disturbance.
The desired dynamics for the system can be written

$$\dot{\Pi}_c^{mp} - \dot{\Pi}_c = -\mu_p(\Pi_c^{mp} - \Pi_c) - \mu_i \int (\Pi_c^{mp} - \Pi_c)$$

With the non-linear model, $\dot{\Pi}_c = f(\Pi_c, u)$. Thus, in order to fulfill the desired dynamics,

$$f(\Pi_c, u) = \dot{\Pi}_c^{mp} + \mu_p(\Pi_c^{mp} - \Pi_c) + \mu_i \int (\Pi_c^{mp} - \Pi_c)$$

The closed loop command can be deduced

$$\left\{ \begin{array}{rcl} u^{mp} & = & g\left(\Pi_c, \dot{\Pi}_c^{mp} + \mu_p(\Pi_c^{mp} - \Pi_c) + \mu_i z\right) \\ \dot{z} & = & \Pi_c^{mp} - \Pi_c \end{array} \right.$$

Moreover, to improve the robustness, decrease the measurement noise dependency and keep the feedforward strategy, Π_c is replaced by Π_c^{mp} in the first term of g. Convergence speed is slightly impacted but robustness is highly improved.

$$\left\{ \begin{array}{rcl} u^{mp} & = & g\big(\Pi_c^{mp}, \dot{\Pi}_c^{mp} + \mu_p(\Pi_c^{mp} - \Pi_c) + \mu_i z\big) \\ \dot{z} & = & \Pi_c^{mp} - \Pi_c \end{array} \right. \tag{4.19}$$

Notice that when the controller parameters are tuned down to 0, u^{mp} becomes the feedforward control law (4.18).

The designed control strategy satisfies the requirements and constraints :
– The compressor downstream pressure is controlled to the manifold pressure setpoint, which ensures that in steady state the throttle is open.
– The environment conditions are taken into account.

The actuator and state constraints are taken into account in the trajectory generation, but not in the feedback control law. Moreover, when the calibration gains (μ_p and μ_i) are tuned to 0, the input is guaranteed to be feasible. When these are not tuned to 0, this is no longer the case. Addition of the integral term may lead to integrator windup. The control strategy must therefore be modified to include an anti windup scheme. This is the purpose of the next subsection.

4.5.2. Anti windup design. — The anti windup scheme proposed in **[86]** for nonlinear systems and detailed in **[87]** for the linear case can be applied to the application studied

here. The integral term z in equation (4.19) is modified as below :

$$\begin{cases} \dot{z} &= \Pi_c^{mp} - \Pi_c - e\mu_{aw}z \\ \dot{w} &= |u^{mp} - sat(u^{mp}, u_m, u_M)| - w \\ e &= sat(w, 0, 1) \end{cases} \tag{4.20}$$

When the command u^{mp} reaches its limits, the state w integrates the difference between u^{mp} and the limit, and is used to discharge the integrator z. Proof of the stability of the anti windup scheme for Euler Lagrange systems is given in **[86]**.

4.5.3. Complete control law. — The complete control law, considering actuator constraints and including an anti windup term is then defined by the system

$$\begin{cases} u^{mp} &= g(\Pi_c^{mp}, \dot{\Pi}_c^{mp} + \mu_p(\Pi_c^{mp} - \Pi_c) + \mu_i z) \\ \dot{z} &= \Pi_c^{mp} - \Pi_c - e\mu_{aw}z \\ u^{sat} &= sat(u^{mp}, u_m, u_M) \\ \dot{w} &= |u^{mp} - u^{sat}| - w \\ e &= sat(w, 0, 1) \end{cases} \tag{4.21}$$

The command u^{sat} is applied to the system. This strategy corresponds to the sketch shown in Figure 4.13, where

- The motion planning block corresponds to the setpoint filtering presented in (4.17).
- The feedback linearization corresponds to the computation of u^{mp} in (4.21).
- Finally, the anti windup corresponds to the computation of the integral term z in (4.21) that takes into account the input constraints.

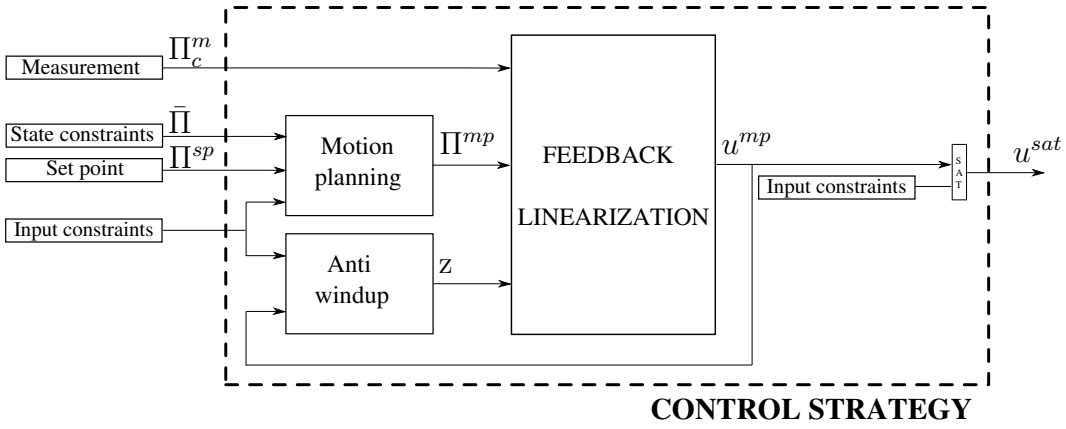

FIGURE 4.13. Control strategy schematics.

4.5.4. Robustness and calibration. — The approach described in subsection 4.4.2 has been performed with the feedback strategy. Figure 4.14 shows the dispersion of the steady state error of the closed loop system for various values of the proportional gain μ_p. The integral gain μ_i was kept equal to zero. It shows the decreasing relationship between proportional gain and steady state error.
Figure 4.15, however, shows the level of overshoot obtained during a transient test (set-point step), computed with the same approach. In this case, the relationship between proportional gain and overshoot is increasing.
Following this analysis, a pragmatic approach has been adopted for calibration of the feedback strategy. Calibration of the proportional gain can naturally result from a trade off between steady state error and overshoot in case of dispersions when the integral action is removed. The integral gain can then correct the remaining steady state error. It is tuned experimentally with a focus on stability and settling time.

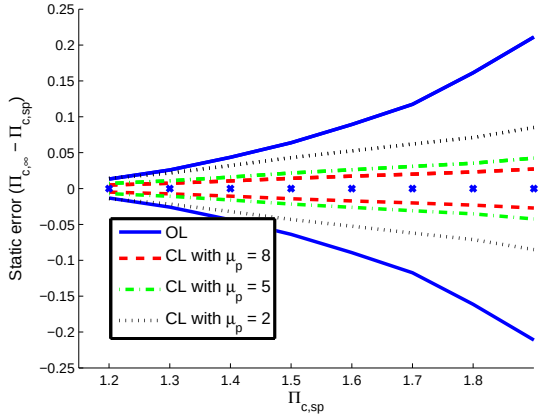

FIGURE 4.14. Steady state error of the dispersed system for various proportional gains (OL=open loop, CL=closed loop).

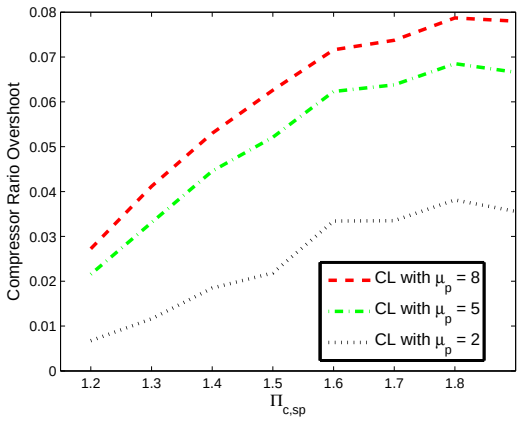

FIGURE 4.15. Overshoot of the dispersed system for various proportional gains (CL=closed loop).

4.5.5. Simulation results and analysis. — Control strategy (4.21) has been implemented in simulation in closed loop with a system modeled by (4.6). Since the strategy contains the inverse of the model the results are expected to be very good. However, this approach highlights the different features of the strategy : the advantages of each part and their robustness in presence of modeling errors.

First, figures 4.16 and 4.17 show results when unmodeled dynamics are introduced on the actuator (first order filter with a time constant of $0,1s$), and when an additional error is added on the turbocharger inertia (multiplied by $1,5$). The control strategy still behaves well in both cases, but the balance between the different terms of the strategy is modified dramatically. In the nominal case, the feedforward term is dominant and the other terms have a negligible impact. When errors are introduced on the dynamic terms of the system, the proportional term compensates for the inaccuracy of the feedforward term. The integral term remains low thanks to the anti windup strategy. The strategy performance is maintained thanks to a high proportional gain.

In a second time, the unmodeled actuator dynamics are still present, but the anti windup term and the setpoint filter are removed in order to underline their respective effects. Only a small first order filter is applied to the setpoint so that it is differentiable. The results are shown in figures 4.18 and 4.19, and can be compared to the corresponding tests in 4.16 and 4.17. When only one of these terms is removed the system still behaves correctly, but the results are catastrophic when both terms are removed. Again, the results could be expected but provide interesting insight into the strategy. The anti windup reduces the overshoot, but so does the setpoint filtering which takes into account the actuator constraint. Again in this case the effect of the feedforward is counterbalanced by a high proportional gain.

This analysis can be used in order to better tuned the strategy :

– When the proportional gain cannot be tuned very high, the setpoint filtering is necessary in order to generate an accurate feedforward.
– The anti windup strategy is necessary when the trajectory is inaccurate.

4.6. Experimental validation

4.6.1. Implementation. — The proposed strategy was integrated in a torque control structure (described in **[63]** for the airpath control and in **[60]** concerning the fuel path and high level vehicle control). The rapid prototyping tool chain provided by Mathworks was used : the strategies were coded using Matlab / Simulink, compiled and executed in real time on the operating system XPC Target. The air path control tasks, including the turbocharger control strategies, are triggered at every engine top dead center.

The computation of variables α_i is detailed in the appendix. The wastegate position is directly linked with the control variable u. When the wastegate is equal to 0%, the

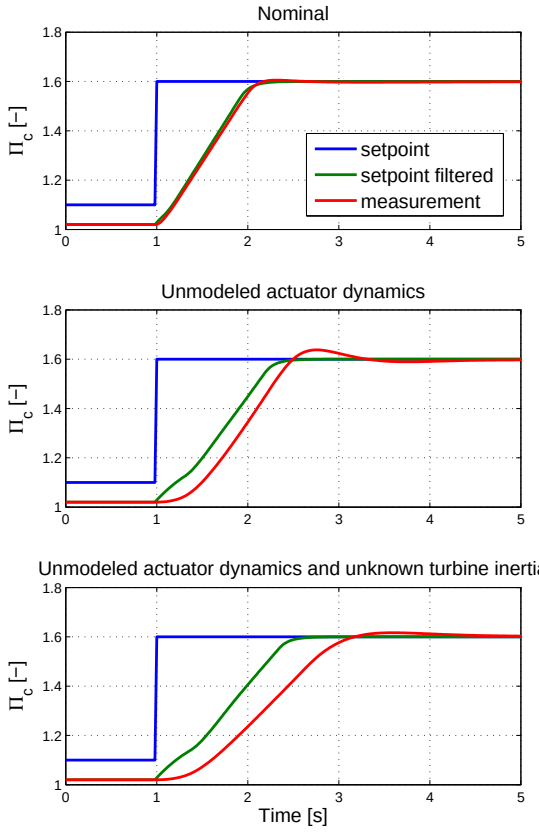

FIGURE 4.16. Performance of the strategy in presence of modeling errors : Π_c raw and filtered setpoint, and measurement.

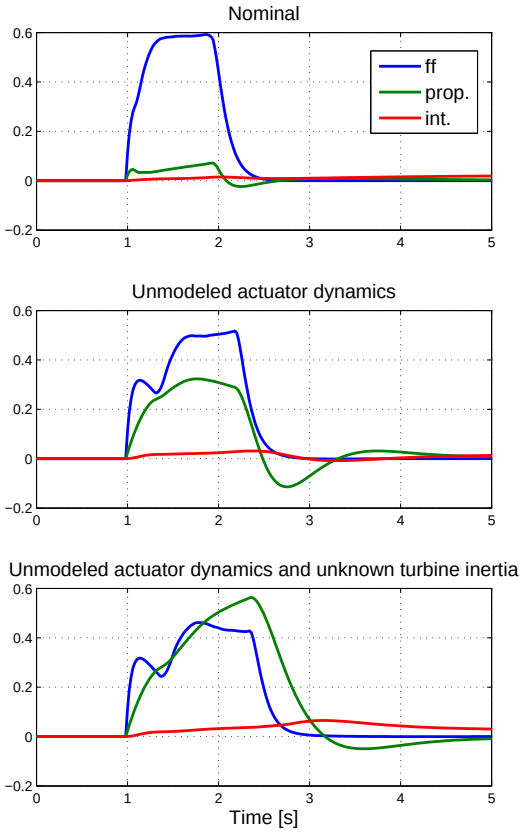

FIGURE 4.17. Performance of the strategy in presence of modeling errors : different terms of the controller.

wastegate is fully open, i.e. $u = 1$. On the contrary, when the wastegate is equal to 100%, the wastegate is fully closed, i.e. $u = 0$.

4.6.2. Experimental setup and validation approach. — The validation tests were performed on a dynamic engine test bench, capable of running at constant speed but also of representing vehicle transient behavior. In this case, the dynamometer control embeds a vehicle model which determines an engine speed setpoint from the measurement of engine torque. The vehicle model represents the main elements of the load seen by an engine

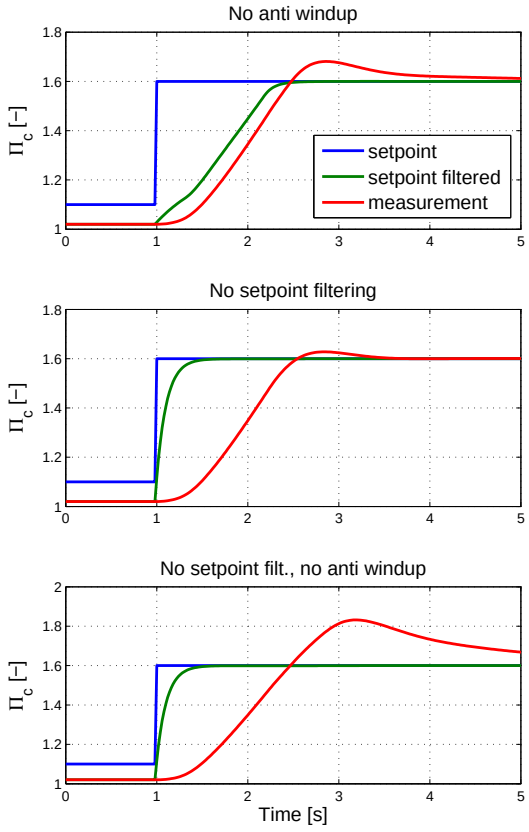

FIGURE 4.18. Comparison between different tuning of the control strategy : Π_c raw and filtered setpoint, and measurement.

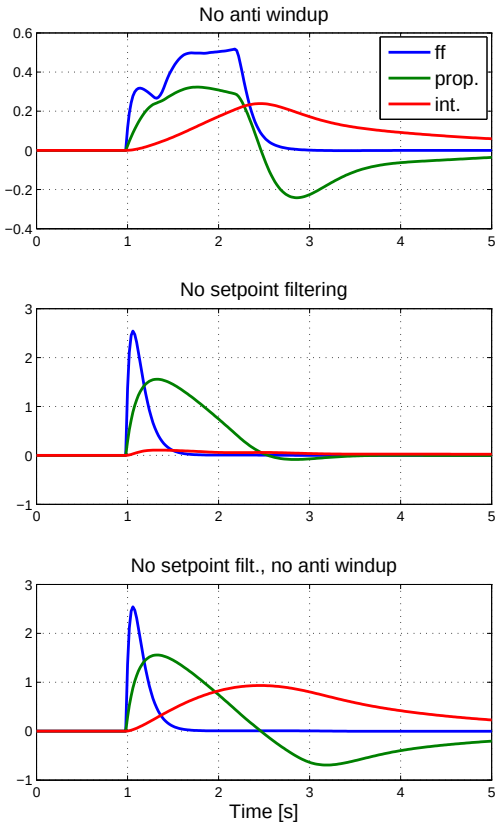

FIGURE 4.19. Comparison between different tuning of the control strategy : different terms of the controller.

mounted in a vehicle : transmission ratio, vehicle mass, road resistive force. It is run in real time and managed by the bench supervision system. More details on the test setup can be found in [**16**].

When validating the turbocharger control strategies, some important features have to be considered.

- The overshoot of the compressor downstream pressure has to be minimized in order to avoid a closing of the throttle.
- The pressure oscillations that might occur when reaching the setpoint are undesirable because they would generate torque oscillations that would be felt by the driver.
- The wastegate has to be actuated as much as possible in transient in order to take advantage of the whole system bandwidth.

The most relevant tests are high load transients, from low load when operating under throttle control, to high load in supercharging conditions. They correspond in fact to high solicitation of the system, and can be used to assess the pressure overshoot, the oscillations and the wastegate actuation. For these reasons, slower transients are less interesting and will not be presented in this paper.
It is important to validate the strategy on the whole engine operating range. Both load transients at constant engine speed and vehicle representative tests are interesting. Concerning tests at constant speed, the relevant operating zone corresponds to an engine speed sufficiently high for the turbocharger to provide some boost, but sufficiently low to remain representative of normal driving conditions. These maneuvers are commented in subsections 4.6.3, 4.6.4 and 4.6.5, which describe first the results of the feedforward alone in order to validate both the structure of the feedforward and the assumptions made in the modeling part, and then the whole control strategy. Load transients on vehicles from low engine speed to high speed highlight the influence of engine speed on turbocharger dynamics. These tests are discussed in subsection 4.6.6.

4.6.3. Experimental transient on test bench : feedforward control strategy. — Before showing the results of the complete control strategy, this subsection describes experimental tests when only the feedforward is activated. This corresponds to setting the gains to 0 in (4.21). The setpoint filter is parameterized so that only the constraint consideration is active because this is part of the feedforward strategy. The constant β that corresponds to a tuning parameter is set to a very high value in order to remove its effect.

Experimental results obtained during a load step (tip-in) at constant speed (2000 rpm) are shown in Figures 4.20 and 4.21 which represent respectively the input (wastegate position) and the output (intake pressure).

Before $t = 0$ s, the pressure setpoint is lower than atmospheric pressure. The throttle therefore controls the pressure (more details can be found in **[63]**). At time $t = 0$ s,

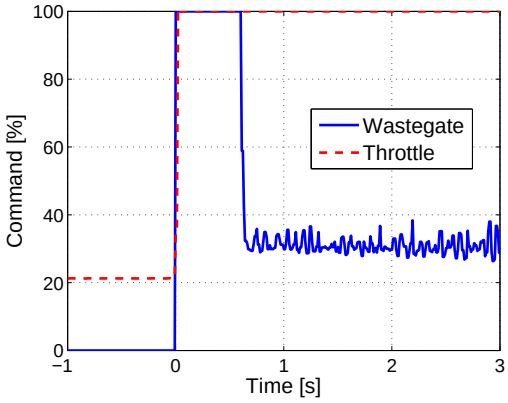

FIGURE 4.20. Wastegate command and throttle position with the feedforward strategy.

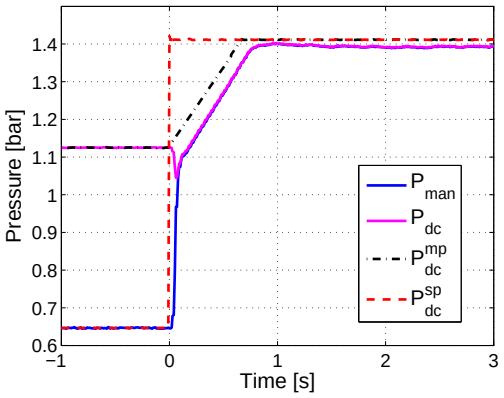

FIGURE 4.21. Intake manifold, downstream compressor, setpoint and motion planning pressure.

the torque demand goes from 90 to 225 Nm implying a pressure demand P_{man}^{sp} from 0.65 to 1.42 bar, which activates the turbocharger control strategy. Due to the turbocharger inertia, the pressure change is not possible instantaneously. P_{dc}^{sp} is filtered as described by (4.17) in order to generate a feasible trajectory P_{dc}^{mp}. The wastegate then closes to provide the maximum power to the turbine and thus to the compressor, resulting in rapid evolution of the system. Around $t = 0.75$ s, the wastegate opens in order to take into account the turbocharger dynamics. The control strategy is very aggressive and hits the constraints.

The feedforward control strategy provides very good transient results due to the explicit consideration of the input constraints in the trajectory generation. If the raw setpoint was used, the control input would directly go to the same steady state value $\bar{u}^{sp} \triangleq g(\Pi_c^{\text{sp}}, 0)$ because the derivative of the setpoint becomes 0. Since the system is stable, the pressure would reach the same steady state value but the convergence rate would be much lower.

These results also validate the assumptions made to design model (6.1). Indeed, the good accuracy obtained between the filtered setpoint and the measured pressure both in transient and in steady state confirms that the model complexity is well adapted for control design. A slight steady state error still remains, due to the modeling errors and simplifications. In the next subsection, the feedback part of the strategy is activated to correct these errors.

4.6.4. Experimental transient on test bench : feedback strategy. —

μ_k	μ_i	μ_{aw}	β
4	1	20	10

TABLE 4.1. Controller gains for experimental tests

The same test as in the previous subsection was performed with the feedback part of the strategy activated. The controller gains used for the experimental results are given in table 4.1. In this case, the integrator brings the system to its setpoint with no steady state error. In this example, the wastegate remains fully closed for a long time but the throttle stays open because no pressure overshoot can be noticed. The amplitude of the pressure oscillations is very small compared to the transient amplitude. The control strategy is very aggressive, hits the constraints and convergence is guaranteed. The robustness and performances on the overall operating range will be discussed in the next subsection.

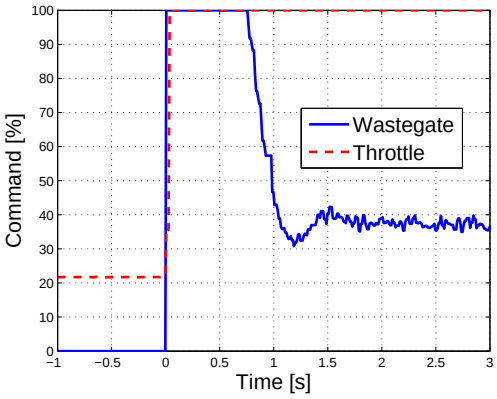

FIGURE 4.22. Wastegate command and throttle position.

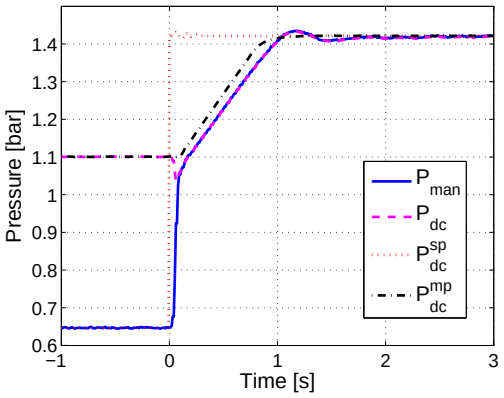

FIGURE 4.23. Intake manifold, downstream compressor, setpoint and motion planning pressure.

A decrease in compressor downstream pressure can be observed at the beginning of the transient, due to the throttle opening time and the balance of pressure between heat exchanger and intake manifold. Since these dynamics are not taken into account in the motion planning, the pressure does not follow the planned trajectory perfectly even though the actuator is at its constraint. This anticipation generates a constant tracking error which could result in integrator windup, but is taken into account by the anti windup strategy.

4.6.5. Load steps at constant engine speed. —

The compression ratio (Π_c) and the wastegate command are represented respectively in Figures 4.24 and 4.25 for different load steps (air mass flow from 650 to 800 mg per stroke) at a constant engine speed of 2000 rpm, and in Figures 4.26 and 4.27 for a load step at different engine speeds, showing similar behavior. The non-linear nature of the system is thus illustrated by the dependency on engine speed of the system response time and steady state position. The efficiency of the proposed control strategy is demonstrated by the high solicitation of the actuator during the transient when it is limited by its constraint. For all the load steps, the strategy takes advantage of the full capacity of the system dynamics with a very short stabilizing time on the setpoint. The command is both fast and accurate, suppressing the need for throttle action to compensate for an overshoot of its upstream pressure. These tests validate the control strategy on the overall operating range.
Some undesired effects remain. When the engine speed increases an overshoot appears clearly on Figure 4.26 (about 50 mbar at 3000 rpm). This phenomenon can be explained by the fact that, at this speed, the turbocharger dynamics are close to dynamics neglected in the strategy, in particular on the actuators (throttle and wastegate). Consideration of these dynamics in the strategy is not desirable since it would increase the complexity considerably. A better way of correcting overshoots would be to modify β at high speed (even if this is not shown in this paper).

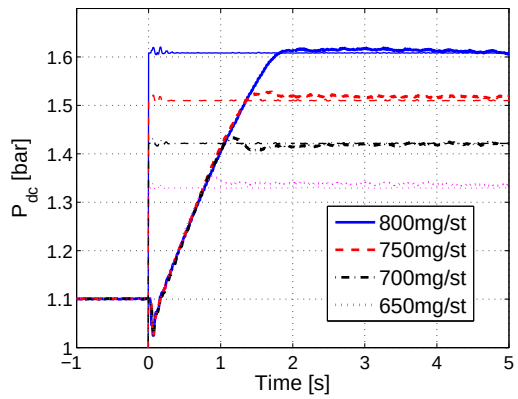

FIGURE 4.24. Compressor downstream pressure for different load steps (the corresponding airflow is indicated in mg per engine stroke) at constant engine speed (2000rpm).

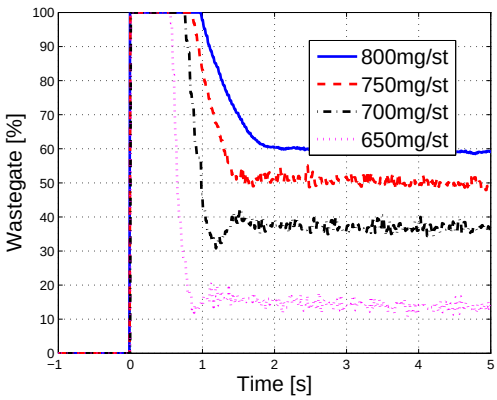

FIGURE 4.25. Wastegate command for different load steps (the corresponding airflow is indicated in mg per engine stroke) at constant engine speed (2000rpm).

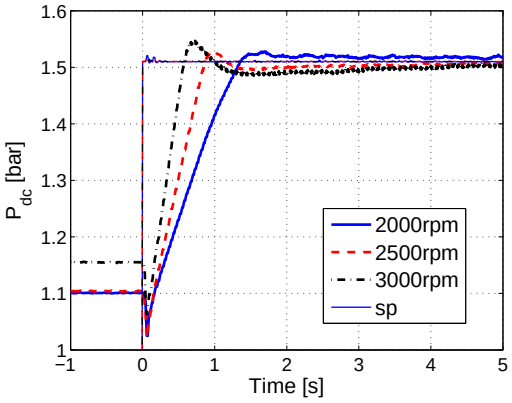

FIGURE 4.26. Compressor downstream pressure for a load step at different engine speeds.

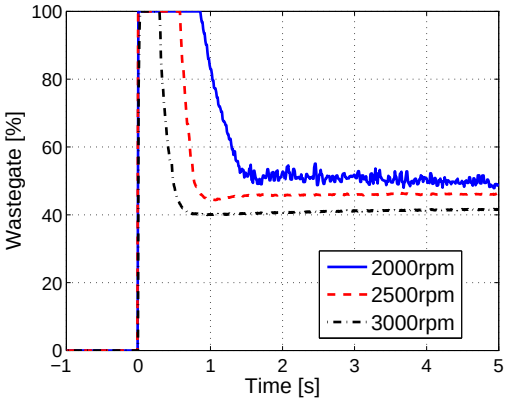

FIGURE 4.27. Wastegate command for a load step at different engine speeds.

4.6.6. Vehicle transients. — Figures 4.28 and 4.29 show a test representative of a vehicle transient. The turbocharger transient is very slow, due to a low engine speed at the start of the maneuver, but the actuator is commanded to its maximum and the pressure stabilization is fast.
The pressure setpoint following is not perfect during the vehicle test. However, the global performance is very promising and it is believed that these drawbacks could be improved by more work on the calibration, particularly on the steady state part.
These tests demonstrate the validity of the approach evaluated in a global engine control structure on the whole operating range of the system. These tests have been performed with the same set of tuning parameters and therefore required a very limited calibration effort. The assumptions made in the design of the strategy are verified a posteriori. In particular, the vehicle test shows the relevance of considering only the turbocharging operations in the model and assuming that the throttle remains open.

4.7. Conclusion

This chapter describes the development of a model based control for a turbocharger in a gasoline engine. It presents a simple control strategy based on feedback linearization and constrained motion planning. It consists in a dynamic inversion of a physical simplified

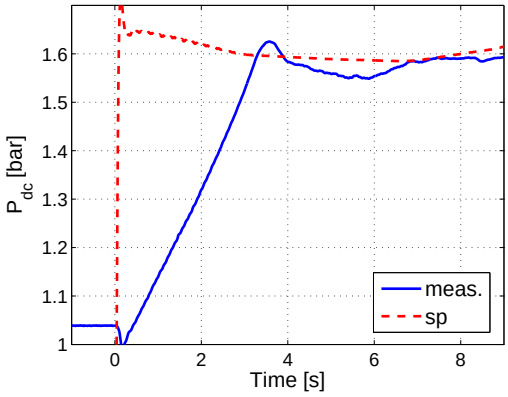

FIGURE 4.28. Compressor downstream pressure for a vehicle transient.

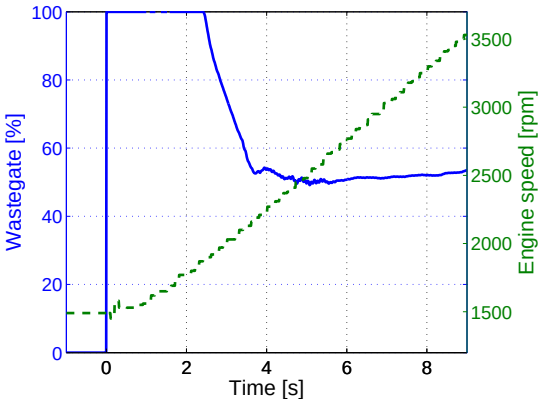

FIGURE 4.29. Wastegate command for a vehicle transient.

model of the system and an anti windup scheme. Practical issues such as actuator constraints and integrator wind up are taken into account in both feedforward and feedback terms of the controller.

Experimental results representative of vehicle transients illustrate the validity of the approach and the relevance of the different assumptions. The results show very good dynamic performances with a limited calibration effort : only one set of gains is used on the whole engine operating range. The strategy takes account explicitly of the variation in environmental conditions.

This approach is believed to be generic enough to be extended to the new turbocharging technologies whose complexity increases the difficulties encountered. For example, some works on double stage turbochargers have been published in [**5**], with modeling assumptions similar to those presented in this paper but with a simpler control structure.

CHAPTER 5

DIESEL ENGINES WITH TWO EGR LOOPS AND VGT

Part of the content of this chapter has been published in [**18, 9, 6**]. The analysis of the impact of EGR on the system trajectories has been submitted for publication in [**14**]. The control strategy is partially patented in [**17**].

5.1. Introduction

In the automotive industry, the necessary reduction of pollutant emissions involves drastic evolution of engines, and in particular Diesel engines. Exhaust Gas Recirculation (EGR) and turbocharging have been the major evolution of Diesel engines in the recent past. They allow to increase the quantity of burned gas in the intake manifold, which helps reducing the NOx production during the combustion. Two types of EGR systems have been investigated : high pressure (HP) and low pressure (LP) systems, named after their position on the air system with respect to the turbocharger. When both systems are combined, the operating conditions of the turbochargers are highly dependent on the use of either of these two systems. This must be taken into account in the turbocharger control strategy which determines the Variable Geometry Turbocharger (VGT) position corresponding to a required pressure at the outlet of the compressor.

On this topic, few publications can be found. In [**80**] the same engine setup is considered but no details are given for the turbocharger control whereas in [**91**] deals with the control and estimation of the EGR system, with no regard to the turbocharger control.

As explained in chapter 3 the control problem is SISO outside the EGR operating zone and similar to that studied in chapter 4. But in the EGR zone the global control problem is

multi variables, strongly non linear, with a lot of interactions between the different subsystems. The performance of the turbocharger control does not affect the torque production but it has a strong impact on the pollutant emissions. Therefore we focus mainly on this zone. For this kind of issue, an interesting solution consists of model based techniques which decouple the subsystems and therefore simplify the problem.

The present chapter describes the design of turbocharger control strategies adapted for an engine architecture with two EGR loops and their integration in a global air system control structure. We show how it is possible to decouple the EGR and turbocharger control problems. The EGR control is not the main concern, but it is mentioned because both systems are highly dependent. The approach proposed is the extension of chapter 4 for gasoline engines fitted with fixed geometry turbines. The application to variable geometry turbines was first tried in **[18]** where it was validated mostly outside the EGR operating area. It was then completed in **[6]** which shows that the model proposed can easily be adapted for a system with two EGR circuits. The EGR control and estimation is described in **[9]** which also proposes a global control structure.

The chapter is organized as follows. First a model of the system is designed. It is then shown that the dynamics of the different subsystems can be separated : the EGR system is fast whereas the turbocharger is slower. Therefore we can split the control problems. We first describe the control strategy used for the EGR system. We then concentrate on the development of a control strategy for the slow system : the turbocharger. It is studied on the basis of a reduced model which is used for the design of a model based strategy. A global control structure is then designed. Experimental results are provided to validate the different assumptions.

5.2. Comprehensive engine model

The system considered is shown in figure 2.15. A complete model is proposed in (2.36). This section recalls the main assumptions made for obtaining these equations.

5.2.1. Turbocharger model. — The description of the model is detailed in chapter 2. In figure 5.1 we verify that the measured operating points fit with the compressor pressure ratio map in LP and HP EGR modes.

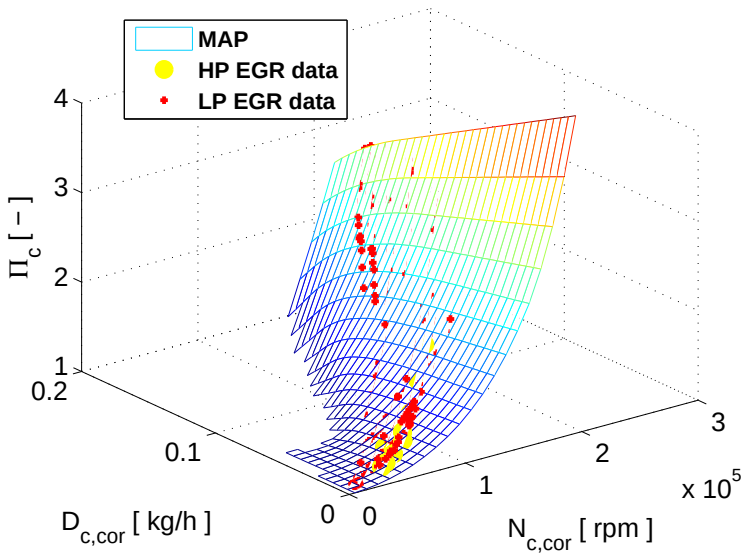

FIGURE 5.1. Compressor map. Pressure ratio Π_c at the compressor w.r.t. the corrected flow through the compressor $D_{c,cor}$ and the corrected turbine crankshaft speed $N_{c,cor}$. Measurements are shown for both the HP and LP EGR mode.

5.2.2. EGR flows. — The EGR mass flow (HP loop or LP loop) depends on the upstream temperature T_u and the pressure drop across the valve $\Pi = P_d/P_u$ as described by the standard equation for compressible gas flow through an orifice (appendix A) :

$$D_{egr} = \frac{S(u_{egr})P_u}{\sqrt{RT_u}}\Pi^{\frac{1}{\gamma}}\sqrt{\frac{2\gamma}{\gamma-1}\left(1-\Pi^{\frac{\gamma-1}{\gamma}}\right)} \tag{5.1}$$

5.2.3. Intake and exhaust model. — We consider the exhaust and intake manifolds as receivers with constant volumes with two gas species (fresh air and burned gas). The systems are assumed isothermal because heat exchangers are located on both EGR circuits and downstream from the compressor. From the equations in chapter 2 the system dynamics in the intake system are given by (5.2) where the first two equations result from the mass balances upstream the compressor applied to the total gas and to the burned gas. The last two equations represent the same phenomena downstream from the compressor (in the intake manifold).

$$\begin{cases} \dfrac{dP_{uc}}{dt} &= \dfrac{RT_{uc}}{V_{uc}}(D_{in} + D_{egr,lp} - D_c) \\ \dfrac{dF_{uc}}{dt} &= \dfrac{RT_{uc}}{P_{uc}V_{uc}}\left(D_{egr,lp}\left(F_{exh} - F_{uc}\right) - D_{air}F_{uc}\right) \\ \dfrac{dP_{dc}}{dt} &= \dfrac{RT_{dc}}{V_{dc}}(D_c + D_{egr,hp} - D_{asp}) \\ \dfrac{dF_{dc}}{dt} &= \dfrac{RT_{dc}}{P_{dc}V_{dc}}\left(D_{egr,hp}\left(F_{exh} - F_{dc}\right) - D_c\left(F_{uc} - F_{dc}\right)\right) \end{cases} \tag{5.2}$$

Similarly in the exhaust system, we have system (5.3) upstream and downstream from the turbine. The burned gas fraction in the exhaust manifold can be measured using the AFR sensor.

$$\begin{cases} \dfrac{dP_{ut}}{dt} &= \dfrac{RT_{ut}}{V_{ut}}(D_{asp} + D_f - D_t - D_{egr,hp}) \\ \dfrac{dP_{dt}}{dt} &= \dfrac{RT_{dt}}{V_{dt}}(D_t - D_{out} - D_{egr,lp}) \\ \dfrac{dF_{exh}}{dt} &= \dfrac{RT_{exh}}{P_{exh}V_{exh}}\left(D_{asp}\left(F_{dc} - F_{exh}\right) + D_f\left(PCO + 1 - F_{exh}\right)\right) \end{cases} \tag{5.3}$$

5.2.4. Summary. — Model (2.36) combines all the equations representing the studied system. This model is comprehensive for turbocharger and EGR systems description. However, all these equations are not necessary when considering either one of these systems. The last three equations concern only gas fractions in the receivers, they do not affect the turbocharger. On the contrary, the first equations describe the turbocharger behavior. They account for parameters external to the turbocharger itself (temperatures upstream the compressor and turbine, pressure downstream the turbine) and represent the interactions with the EGR circuits.

This system contains eight states. It is too complex for the design of a model based control law, for which further simplifications have to be undertaken. Different types of assumptions will be made and verified experimentally.

5.3. Dynamics separation and EGR control

5.3.1. Singular perturbation. — The eighth order nonlinear system (2.36) accurately describes the dynamics of the system. The difference between the turbocharger speed dynamics and the pressure dynamics suggests the application of the singular perturbations method. The justification is the same as in chapter 4.

As a consequence, the EGR control and the turbocharger control are dealt with independently. For the turbocharger control problem we consider only the slow dynamics and the steady state equations corresponding to the faster dynamics. The slow reference system for the turbocharger becomes :

$$\left\{\begin{array}{rcl} \frac{d}{dt}(\frac{1}{2}J_tN_t^2) & = & \phi_{D_t}(\Pi_t, \frac{N_t}{\sqrt{T_{ut}}}, u_{vgt})c_pP_{dt}\sqrt{T_{ut}}\eta_t\phi_t(\Pi_t) - (\eta_v\Pi_c\Psi - D_{egr,hp})c_pT_{uc}\frac{1}{\eta_c}\phi_c(\Pi_c) \\ \eta_v\Pi_c\Psi & = & \phi_{D_t}(\Pi_t, \frac{N_t}{\sqrt{T_{ut}}}, u_{vgt})\frac{P_{dt}}{\sqrt{T_{ut}}} - D_f + D_{egr,hp} \end{array}\right. \tag{5.4}$$

This system is not affected by LP EGR, but only by HP EGR. The stationary part of system (2.36) also gives :

$$\left\{\begin{array}{rcl} D_{air} + D_{egr,lp} + D_{egr,hp} - \eta_v\Pi_c\Psi & = & 0 \\ D_{egr,lp}(F_{exh} - F_{uc}) - D_{air}F_{uc} & = & 0 \\ D_{egr,hp}(F_{exh} - F_{dc}) + (\eta_v\Pi_c\Psi - D_{egr,hp})(F_{uc} - F_{dc}) & = & 0 \\ \eta_v\Pi_c\Psi(F_{dc} - F_{exh}) + D_f(PCO + 1 - F_{exh}) & = & 0 \end{array}\right. \tag{5.5}$$

In the case where the LP EGR circuit is closed ($D_{egr,lp} = 0$ and $F_{uc} = 0$), this can be simplified into (5.6) that links $D_{egr,hp}$, F_{dc} and F_{exh}.

$$\left\{\begin{array}{rcl} D_{egr,hp}F_{exh} - \eta_v\Pi_c\Psi F_{dc} & = & 0 \\ \eta_v\Pi_c\Psi(F_{dc} - F_{exh}) + D_f(PCO + 1 - F_{exh}) & = & 0 \end{array}\right. \tag{5.6}$$

5.3.2. EGR observation and control. — The complete description of the strategies to observe and control the EGR systems is given in [**9**]. We expose here the main results in order to understand the impact on the turbocharger control strategies which are the main concerns of this chapter and are described further in the following sections.

5.3.2.1. Assumptions and limits. — We consider now that only one EGR circuit is used at a given time. The mixing of the two EGR loops is a more complex problem that will need further work. The dynamics of the system can be simplified and it is shown in **[9]** that the LP EGR operation is very similar to the HP EGR one, except that the intake volume downstream from the EGR circuit is different. We therefore give here only the equations used for HP EGR, the LP EGR ones are deduced directly.

5.3.2.2. Observation. — The production engines are not usually fitted with differential pressure sensors, thus, the direct computation of EGR flows using the standard equation of flow through a restriction (5.1) is not possible. Even if the sensor is available it provides a poor estimation due to the sensor accuracy and the very low pressure drop across the LP EGR system (see **[30]**). For these reasons, the HP and LP EGR flows are estimated using a closed-loop observer proposed in **[29]**. The main measurements required for the closed-loop observer are provided by the standard sensors fitted on Diesel engines : the exhaust equivalence ratio F_{exh}, the air mass flow, and the intake manifold pressure P_{dc} which allows the estimation of the aspirated gas flow. The proposed observer uses the dynamical equations derived from the reference systems (2.36) augmented by a third state for the normalized EGR flows $\theta_{egr,hp}$ defined as follow :

$$D_{egr,hp} = u_{egr,hp}\ \theta_{egr,hp} \tag{5.7}$$

Let $x_{hp} = [P_{dc}\ F_{dc}\ \theta_{egr,hp}]$ be the observer state and $y = P_{dc}$ be the measurement. If we note $\alpha_{hp} = (RT_{dc})/V_{dc}$, and $\beta = (1/RT_{dc})V_{cyl}(N/120)$, the proposed observer is as follows :

$$\begin{cases} \dfrac{d\widehat{P}_{dc}}{dt} &= \alpha_{hp}\left(D_{air} + u_{egr,hp}\widehat{\theta}_{egr,hp} - \beta\eta_{vol}\widehat{P}_{dc} - \alpha_{hp}\left(l_1 - \eta_{vol}\right)\beta(\widehat{P}_{dc} - P_{dc})\right) \\ \dfrac{d\widehat{F}_{dc}}{dt} &= \dfrac{\alpha_{hp}}{P_{dc}}\left(-(D_{air} + u_{egr,hp}\widehat{\theta}_{egr,hp})\widehat{F}_{dc} + F_{exh}u_{egr,hp}\widehat{\theta}_{egr,hp}\right) \\ \dfrac{d\widehat{\theta}_{egr,hp}}{dt} &= -l_3\alpha_{hp}u_{egr,hp}(\widehat{P}_{dc} - P_{dc}) \end{cases} \tag{5.8}$$

The constant values of the tracking terms, (l_1, l_3), are computed in order to ensure the observer convergence. This was previously proved in **[29]**.

5.3.3. EGR control strategy. — The setpoint for the EGR control strategy has been chosen as the intake manifold burned gas ratio F_{dc} (BGR) because it is a variable that

influences directly the gas composition in the cylinder and hence the combustion (chapter 1). Since we have considered that the turbocharger and EGR systems dynamics are different, we deal independently with the control strategies of these two systems.

We apply a motion planning strategy to transform the intake manifold and burned gas rate set points into air flow (D_{air}^{mp}) and EGR flow trajectories ($D_{egr,hp}^{mp}$ or $D_{egr,lp}^{mp}$). The HP and LP EGR valves positions are controlled in order to track their respective EGR flow trajectories. The exhaust throttle position is controlled in order to track the air flow trajectory (in LP EGR mode only).

From the system of equations (2.36) the following equations can be extracted :

$$\begin{cases} \dfrac{dP_{dc}}{dt} = \alpha_{hp}\left(D_{air} + D_{egr,hp} - \beta\eta_{vol}P_{dc}\right) \\ \dfrac{dF_{dc}}{dt} = \dfrac{\alpha_{hp}}{P_{dc}}\left(F_{exh}D_{egr,hp} - (D_{air} + D_{egr,hp})F_{dc}\right) \end{cases} \tag{5.9}$$

The computation of the motion planning for flows is an implicit inversion of the systems of equations (5.9). This inversion is demonstrated in [**28**] for the HP EGR mode and is easily transposed to the LP EGR mode. As a result, the desired air and EGR flow trajectories are derived from the measurements, the set points and their first-derivatives. For the HP EGR mode :

$$D_{egr,hp}^{mp} = f_1(T_{dc}, N_e, F_{exh}, P_{dc}^{mp}, \dot{P_{dc}^{mp}}, F_{dc}^{mp}, \dot{F_{dc}^{mp}}) \tag{5.10}$$

This approach is valid as long as the turbocharger control strategy manages to respect its setpoint P_{dc}^{mp}. In the following we will develop a motion planning approach consisting in the computation of a feasible trajectory P_{dc}^{mp} and the determination of the actuator setpoint in order to track this trajectory. The development of this strategy is the purpose of the following sections. Alternatively we could also use the pressure measurement P_{dc} thanks to the assumption that the turbocharger dynamics are much slower.

5.4. Model reduction for turbocharger control

The same approach as in chapter 4 is applied. As mentioned before, the model dynamics are simplified by singular perturbations. Other steady state assumptions allow a further reduction. The purpose is to keep only the relevant dynamics of the system, and parameters that can be measured or estimated from the available sensors.

5.4.1. Dynamics simplification. — As mentioned in section 5.3, the eighth order nonlinear system (2.36) can be simplified by singular perturbations. For the turbocharger control problem we consider only the slow dynamics and the steady state equations corresponding to the faster dynamics. The dynamics considered for the turbocharger control issues are summarized in (5.4) which is independent of LP EGR. Also, since we consider that either one of the EGR circuits is used at a given time, only HP EGR mode is of interest. In this case, we can keep only the stationary part of the faster dynamics summarized in (5.6) which can be transformed into (5.11).

$$\left\{\begin{array}{rcl} D_{egr,hp}F_{exh} & = & \eta_v \Pi_c \Psi F_{dc} \\ F_{exh}(\eta_{vol}\Pi_c\Psi + D_f) & = & D_f(PCO+1) + F_{dc}\eta_{vol}\Pi_c\Psi \end{array}\right. \tag{5.11}$$

System (5.11) enables to express the HP EGR flow from Π_c and available sensors. We can introduce variable δ_{HP} to characterize the choice of EGR circuit : when HP EGR is used δ_{HP} is equal to 1, it is equal to 0 otherwise. With this notation, we have :

$$D_{egr,hp} = \frac{F_{dc}\delta_{HP}}{F_{exh}}\eta_{vol}\Pi_c\Psi \tag{5.12}$$

The exhaust burned gas fraction can be considered as an input because it is measured. Alternatively, we can also compute the exhaust burned gas fraction F_{exh} from intake burned gas fraction F_{dc}, engine gas flow and injected fuel flow D_f as suggested by the second equation of (5.11) :

$$F_{exh} = \frac{D_f(PCO+1) + F_{dc}\eta_{vol}\Pi_c\Psi}{\eta_{vol}\Pi_c\Psi + D_f} \tag{5.13}$$

To conclude, (5.4) is combined either with (5.12) or with (5.13). The simplified dynamics write now as a first order nonlinear dynamics with an algebraic equation representing the steady state solution of the intake and exhaust dynamics.

5.4.2. Steady state assumptions. —

5.4.2.1. Turbine flow simplification. — The turbine can be considered as a restriction on the exhaust gas flow. However, the standard equation for compressible flow across an orifice cannot be applied in this case. Modified versions of this equation have been proposed which fit better the experimental results, based on various assumptions (see [**83, 37**]). Most of them neglect the influence of the turbine speed. The formula kept in the present case is given below, the justification being that it shows a good correlation with

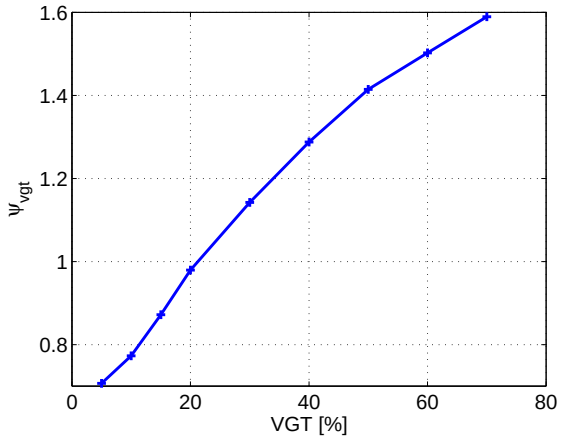

FIGURE 5.2. Function ψ_{vgt} with respect to the control input u_{vgt}.

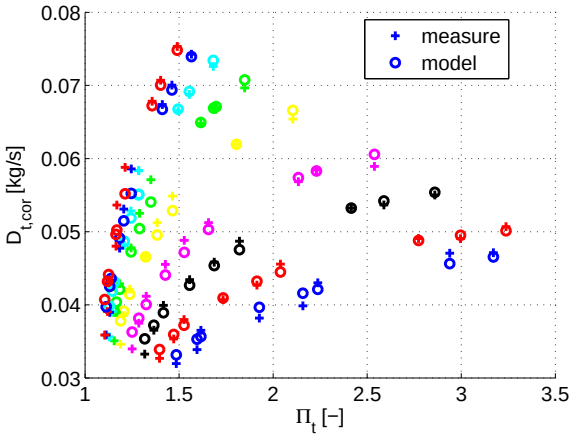

FIGURE 5.3. Comparison between the measured corrected turbine flow $D_t \frac{\sqrt{T_{ut}}}{P_{dt}}$ and its simplified model for several value of the VGT position.

the characterization data (see Figure 5.3).

$$D_t = \frac{P_{dt}}{\sqrt{T_{ut}}} \phi_{turb}(\Pi_t) \psi_{vgt}(u_{vgt})$$

where $\psi_{vgt}(u_{vgt})$ is equivalent to an effective area (represented in Figure 5.2) and

$$\phi_{turb}(\Pi_t) \triangleq \frac{\Pi_t^{\frac{3}{2}}}{\sqrt{R}} \sqrt{\frac{2\gamma}{\gamma - 1} \left(\Pi_t^{\frac{-2}{\gamma}} - \Pi_t^{\frac{-\gamma-1}{\gamma}} \right)}$$

5.4.2.2. Correlation between the turbocharger speed and compression ratio. — For given engine operating conditions, the turbocharger speed and the intake pressure are very correlated. It is therefore interesting to consider the combination of (2.17) and (2.26). The corrected compressor flow depends on the compressor pressure ratio, the engine speed and the operating conditions, and :

$$\Pi_c = \phi_{\Pi,c}(\eta_v(\Pi_c P_{uc}, N_e)\Pi_c \Psi, \frac{N_t}{\sqrt{T_{uc}}}) \tag{5.14}$$

As in chapter 4 this expression is noticeable since it shows a direct dependency between the compressor pressure ratio and the engine speed. The influence of the intake temperature is of second order and will be neglected. These assumptions must be verified. Figure 5.4

shows experimental measurements on a large engine operating range. We can therefore estimate the turbocharger speed square N_t^2 linearly w.r.t. the compressor pressure ratio Π_c, i.e.

$$N_t^2 = a\Pi_c + b$$

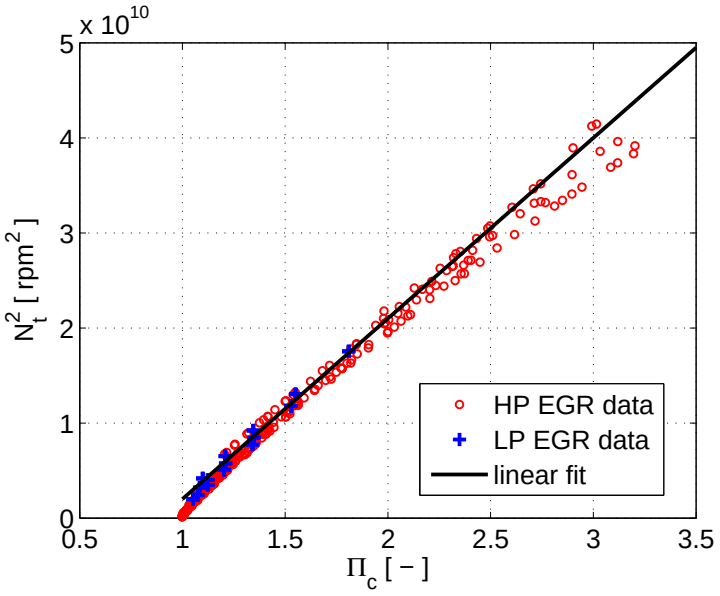

FIGURE 5.4. Experimental results at steady state. Variation of the turbocharger speed square N_t^2 w.r.t. the compressor pressure ratio Π_c.

5.4.3. Reference system for turbocharger control. — The state variable can now be chosen as the compressor pressure ratio. The reference system writes

$$\left\{ \begin{array}{rcl} \dot{\Pi}_c & = & \alpha_1(\beta\Pi_c + D_f)\psi_t(\Pi_t) - \alpha_2\beta\psi_c(\Pi_c) \\ \Pi_c & = & \alpha_3(\phi_{turb}(\Pi_t)\psi_{vgt}(u_{vgt}) - \alpha_4) \end{array} \right. \tag{5.15}$$

where $\{\alpha_i\}_{i\in[1,\ 4]}$ depend on the engine operating conditions :

$$\left\{ \begin{array}{c} \beta = (1 - \frac{F_{dc}\delta_{HP}}{F_{exh}})\eta_v\Psi \\ \alpha_1 = c_pT_{ut}\eta_t\frac{2}{J_ta} \quad \text{and} \quad \alpha_2 = c_pT_{uc}\frac{1}{\eta_c}\frac{2}{J_ta} \\ \alpha_3 = \frac{P_{dt}}{\beta\sqrt{T_{ut}}} \quad \text{and} \quad \alpha_4 = \frac{\sqrt{T_{ut}}D_f}{P_{dt}} \end{array} \right.$$

The first equation of system (5.15) represents the balance between compressor and turbine mechanical power, giving the dynamics of the system. The second equation represents the mass conservation in the exhaust manifold, the dynamics being neglected.

Functions ϕ_{turb}, ψ_{vgt}, ψ_c and ψ_t are nonlinear but strictly increasing and invertible. This property is very important and will be used when designing the control law.

Coefficients α_i can be computed from sensors available on the engine. The variable β represents the gas mass flow through the compressor and through the turbine. Only this variable depends on the EGR loop choice.

The validation of this representation will be justified by a comparison between its states of equilibrium and steady state measurements in the following section, and by the experimental results of the control strategy based on the inversion of this model.

5.5. Reduced model analysis

The representation (5.15) is well adapted for the analysis of the system properties. As for turbocharged gasoline engines with fixed geometry turbines studied in chapter 4, the system can be inverted because the functions of (5.15) ϕ_{turb}, ψ_{vgt}, ψ_c and ψ_t are invertible. This enables to manipulate the equations in order to compute the trajectories and the states of equilibrium of the system for a given operating point.

We first need to define the operating point of the system. With the approach of chapter 2, it corresponds to the thermodynamic conditions at the boundaries of the air system P_{uc}, T_{uc}, P_{dt}, and the flows through the engine D_f, T_{ut} and Ψ. These variables are exogenous to the turbocharger. The coefficients α_i can be computed from them.

This section is organized in two subsections. In subsection 5.5.1 model (5.15) is inverted. The states of equilibrium are deduced. A comparison with the states of equilibrium obtained experimentally validates the model. The system trajectories are analyzed in 5.5.2 which highlights the influence of the EGR on the system behavior. This section ends with a discussion of the impact of the actuator constraints on the system trajectories.

5.5.1. System inversion. —

First, from the algebraic equation of (5.15) it is possible to compute Π_t as a function of Π_c and u_{vgt} :

$$\Pi_t = \phi_{turb}^{-1}\left(\frac{\Pi_c + \alpha_4\alpha_3}{\alpha_3\psi_{vgt}(u_{vgt})}\right)$$

Then, the computation of $\dot{\Pi}_c$ follows from the first equation. We note f the combination of these two computations. We have : $\dot{\Pi}_c = f(\Pi_c, u_{vgt})$.

Similarly, we can compute the unique u^r_{vgt} corresponding to a given trajectory $(\dot{\Pi}^r_c, \Pi^r_c)$:

$$\Pi^r_t = \psi_t^{-1}\left(\frac{1}{\alpha_1(\beta\Pi^r_c + D_f)}(\dot{\Pi}^r_c + \alpha_2\beta\psi(\Pi^r_c))\right) \tag{5.16}$$

and

$$u^r_{vgt} = \psi^{-1}_{vgt}\left(\frac{\Pi^r_c - \alpha_4\alpha_3}{\alpha_3\phi_{turb}(\Pi^r_t)}\right) \tag{5.17}$$

The combination of these two equations is noted g : $g \triangleq g(\Pi_c, \dot{\Pi}_c)$. This function is the inverse of f. Indeed we have $u = g(\Pi_c, f(\Pi_c, u))$. As in chapter 4 we can use g to compute a feedforward control for a feasible trajectory. Indeed, for a desired feasible trajectory $(\Pi_c)^r$ there exists a unique input trajectory u^r defined by :

$$u^r = g(\Pi^r_c, \dot{\Pi}^r_c) \tag{5.18}$$

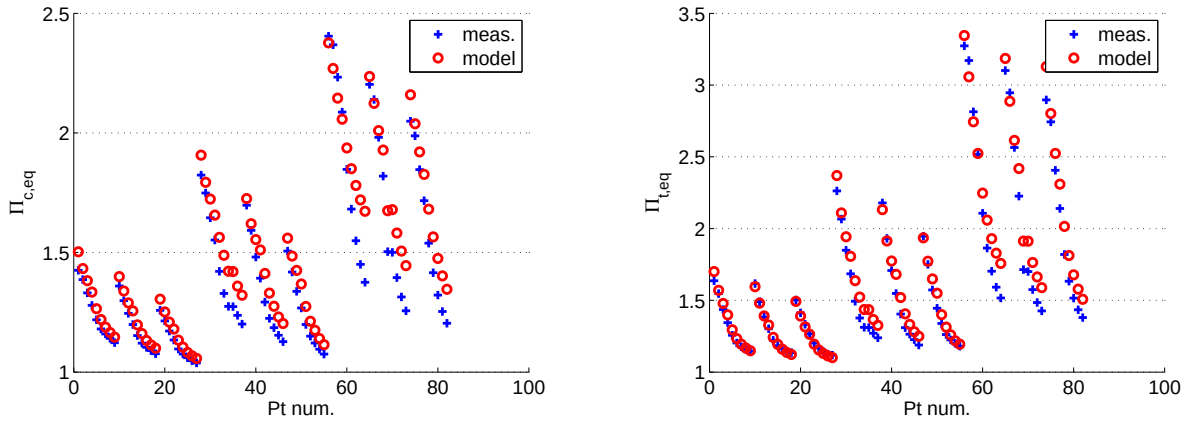

FIGURE 5.5. States of equilibrium for experimental operating points : comparison between prediction and measurement for $\Pi_{c,eq}$ and $\Pi_{t,eq}$.

The states of equilibrium correspond to the stationary part of the system ($\dot{\Pi}_c = 0$). This can be computed from $u_{eq} = g(\Pi_{c,eq}, 0)$.

The model (5.15) can be validated by comparing its states of equilibrium with steady state experimental measurements. This is shown in figures 5.5 for $\Pi_{c,eq}$ and $\Pi_{t,eq}$ for different engine operating points with variations of the VGT actuator positions on its complete range. The results show a good accuracy between model and experimental data.

5.5.2. System trajectories. —

The analysis exposed in the following concerns two operating points described by table 5.1. They are chosen because they correspond to a medium speed at high load for point 1 and at medium load for point 2 for which EGR is needed. We can therefore study the influence of different parameters on the trajectories, particularly the dependence upon the EGR valve or the BGR setpoint ($F_{dc,sp}$) is of interest.

	N_e	P_{uc}	T_{uc}	P_{dt}	T_{ut}	D_f	η_c	η_t	η_v
Point	[rpm]	[bar]	[K]	[bar]	[K]	[kg/s]	-	-	-
1	2000	1	300	1.1	1000	0.0037	0.55	0.6	0.85
2	2000	1	300	1.1	800	0.0015	0.55	0.65	0.85

TABLE 5.1. Operating points for trajectory analysis

Trajectories at high load without EGR. — Figure 5.6 shows the trajectories $\dot{\Pi}_c = f(\Pi_c, u_{vgt})$ for operating point number 1 defined in table 5.1. The different lines correspond to different actuator positions u_{vgt}. The states of equilibrium are defined by $\dot{\Pi}_c = 0$. They are located at the intersection between the trajectories and the abscissa axis. As expected, the system is always stable because the trajectories at the states of equilibrium are decreasing with respect to Π_c. When the VGT actuator is closed the system stabilizes at a higher compression ratio. Contrary to the observation made in chapter 4, the system is never unstable. For a given operating point it is safe to choose any actuator position as long as the states of equilibrium remain below a reasonable compression ratio $\Pi_{c,eq}$ (and hence below a maximum turbocharger speed).

In 5.7 the engine speed is changed while the other values are kept the same. The system is still stable, but the value of $\Pi_{c,eq}$ is greatly modified for a given command. For a control point of view this means that the command u_{vgt} must be modified with an adequate feedforward when the operating point changes.

Dependence upon the EGR circuit. — We now consider operating point number 2 defined in table 5.1. It is chosen because it corresponds to medium conditions for which EGR is needed. Therefore this point is relevant for the study of the influence of EGR on the system trajectories.

Figure 5.8 shows the influence of the turbocharger actuator on the system trajectories when the EGR valve is closed. The results are very similar to figure 5.6.

However, the trajectories are modified when the EGR valve is opened. System (5.15) contains a dependency on the burned gas rate downstream from the compressor F_{dc}.

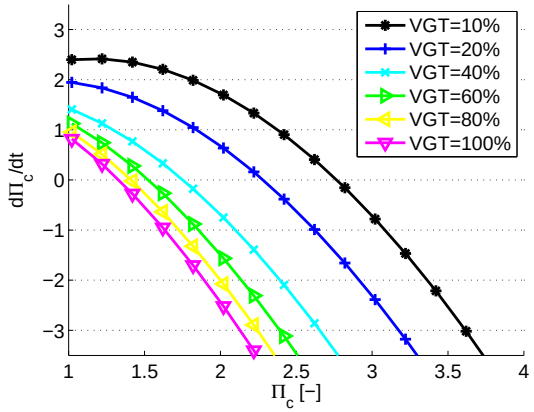

FIGURE 5.6. System trajectories at high load.

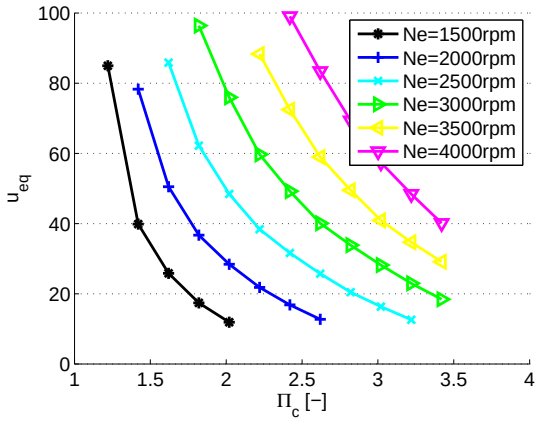

FIGURE 5.7. Dependence of the states of equilibrium upon engine speed.

From (5.11) and (5.1) it is possible to compute directly the impact of the EGR valve on the system.

Figure 5.9 shows the behavior of the system with respect to the EGR valve opening when the VGT actuator is constant (here at 10%). Again, the system remains stable but the states of equilibrium are affected : they are translated to the left side of the graph until the trajectory is limited to a very small region around the origin. In this case the command u_{vgt} looses all authority on the system.

Since the EGR control uses the intake manifold BGR (F_{dc}) as a setpoint, it is also interesting to consider the influence of the BGR rather than EGR valve. The trajectories shown on figure 5.10 represent the effect of a change in BGR setpoint for a constant VGT actuator (10%). Again, the system remains stable and the trajectory of the system are translated to the left side of the graph when the BGR increases.

These considerations emphasize the impact of the EGR circuit on the turbocharger, and the need for taking these effects into account in the turbocharger control strategies.

Constraints consideration. — In fact, the system trajectories are restricted to a limited region due to constraints. They are of two types. First, the VGT actuator is physically limited between maximum and minimum values. But there is also a limitation linked with the maximum position of the EGR valve (fully open). This position implies a constraint on the turbocharger trajectory : in order to ensure that the BGR setpoint is feasible with a fully opened EGR valve, the relationship between Π_c and Π_t implied by (5.1) has to

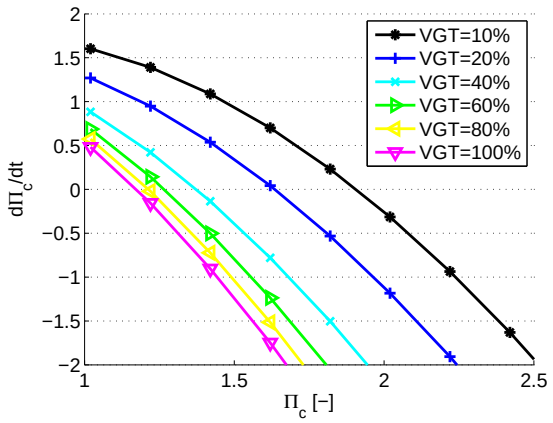

FIGURE 5.8. Trajectories at medium load.

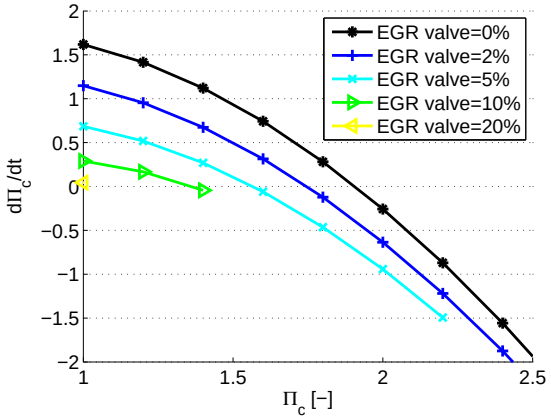

FIGURE 5.9. Dependence of the trajectories upon the EGR valve.

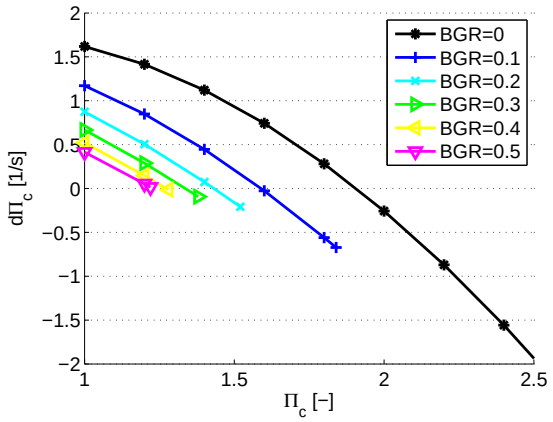

FIGURE 5.10. Dependence of the trajectories upon the BGR.

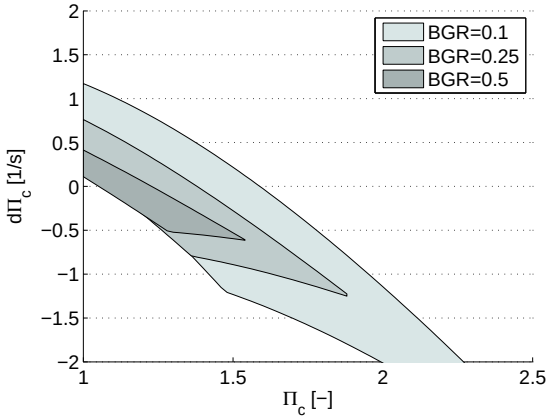

FIGURE 5.11. Admissible operating region.

be respected. This trajectory gives a priority to the EGR requirement rather than to the pressure requirement. This is a relevant choice because it does not affect the torque production but minimizes the pollutant emissions (see chapter 1 for the impact of EGR on the pollution). The constraints can be computed as follows.

From (5.11) and (5.1) it is possible to compute directly the impact of the EGR valve on the system. These equations are not very accurate when the pressure difference across the considered system is low (see A). However, since it is used here for the computation

of a constraint we will consider it is sufficient. This assumption will be confirmed by the experimental results in section 5.8.

The pressure ratio across the EGR valve is noted Π_{egr}. We have :

$$\Pi_{egr} = \frac{\Pi_t}{\Pi_c}\frac{P_{dt}}{P_{uc}} \tag{5.19}$$

The maximum EGR flow $D_{egr,max}$ is given by :

$$D_{egr,max} = \frac{S(u_{egr,max})\Pi_{egr}P_{dt}}{\sqrt{RT_{ut}}}\Pi_{egr}^{\frac{1}{\gamma}}\sqrt{\frac{2\gamma}{\gamma-1}(1-\Pi_{egr}^{\frac{\gamma-1}{\gamma}})} \tag{5.20}$$

On the other hand, we have

$$D_{egr} = \frac{F_{dc}}{F_{exh}}\eta_{vol}\Pi_c\Psi \tag{5.21}$$

$$F_{exh} = \frac{D_f(PCO+1) + F_{dc}\eta_{vol}\Pi_c\Psi}{\eta_{vol}\Pi_c\Psi + D_f} \tag{5.22}$$

So it is possible for each Π_c and F_{dc} to compute the required EGR flow $D_{egr,sp}$ from (5.22) and (5.21). Then, equations (5.19) and (5.20) give a minimum $\Pi_{t,min}$ that ensures that $D_{egr,sp}$ does not exceed $D_{egr,max}$.

The limit $\Pi_{t,min}$ can be transformed into a limit $\dot{\Pi}_{c,egr}$ on the trajectory via the first equation of system (5.15).

The constraints on the trajectory can be represented on the plane $(\dot{\Pi}_c, \Pi_c)$, as shown on figure 5.11 which represents the regions corresponding to trajectories for the system that satisfy a BGR request and the VGT actuator constraints. For each region, there are two minima values defined by the constraints on the VGT actuator $f(\Pi_c, u_{vgt,min})$ and on the BGR feasibility $\dot{\Pi}_{c,egr}$, and there is one maximum value $f(\Pi_c, u_{vgt,max})$.

5.6. Turbocharger control strategy

As for gasoline engines with fixed geometry turbines studied in chapter 4 we design a control strategy based on motion planning and feedback linearization techniques. The following subsections therefore describe the construction of a feasible trajectory, a feedforward strategy consisting in the inversion of system (5.15) and a feedback strategy.

5.6.1. Motion planning : design of a feasible trajectory. — The setpoint P_{dc}^{sp} is transformed into Π_c^{sp} such as $\Pi_c^{\text{sp}} \triangleq \frac{P_{dc}^{\text{sp}}}{P_{uc}}$.

Function g defined in 5.5.1 can therefore be used in order to design the feedforward strategy :

$$u^{\text{sp}} = g(\Pi_c^{\text{sp}}, \dot{\Pi}_c^{\text{sp}}) \tag{5.23}$$

However, the following constraints must be considered :

1. A limit on the setpoint will ensure the safety of the system by maintaining the shaft speed below a maximum value, i.e. $\Pi_c \leq \bar{\Pi}$.
2. The state setpoint has to be continuously differentiable in order to compute $\dot{\Pi}_c^{\text{sp}}$.
3. The actuator is limited between u_{min} and u_{max}, which is not guaranteed by (5.23).
4. The trajectory must respect the BGR requirement with a fully opened EGR valve $u_{egr,max}$.

The purpose of this section is to compute a feasible setpoint trajectory Π_c^{mp} such that these constraints are satisfied. The constraints 3, and 4 have been explained above. The other ones are trivial.

The notation $sat(u, u_m, u_M)$ is used for the function defined by

$$sat(u, u_m, u_M) = \begin{cases} u_m & \text{if} \quad u \leq u_m \\ u & \text{if} \quad u_m \leq u \leq u_M \\ u_M & \text{if} \quad u_M \leq u \end{cases}$$

We define $\dot{\Pi}_{c,min} \triangleq \max\{f(\Pi_c^{mp}, u_{max}), \dot{\Pi}_{c,egr}\}$ and $\dot{\Pi}_{c,max} \triangleq f(\Pi_c^{mp}, u_{min})$. We choose a positive parameter $\dot{\Pi}_m$. The new reference setpoint, called Π_c^{mp} is obtained from the filter defined by

$$\dot{\Pi}_c^{mp} = sat\big(\beta_f(\min\{\Pi_c^{sp}, \bar{\Pi}\} - \Pi_c^{mp}), \min\{\dot{\Pi}_{c,min}, -\dot{\Pi}_m\}, \max\{\dot{\Pi}_{c,max}, \dot{\Pi}_m\}\big) \tag{5.24}$$

where β_f is a gain tuning the dynamics of the trajectory. The parameter $\dot{\Pi}_m$ is necessary in order to ensure that the trajectory converges to the steady state $\dot{\Pi}_c = 0$, which is not guaranteed by the BGR constraint.

5.6.2. Robustness of the feedforward strategy. — The feedforward strategy becomes finally :

$$u = g(\Pi_c^{\text{mp}}, \dot{\Pi}_c^{\text{mp}}) \tag{5.25}$$

The new strategy is obtained by the combination of (5.24) and (5.25). Since function g is the inverse of f the system is brought towards the setpoint while respecting the constraints.

In the case of modeling errors, this feedforward is erroneous and produces a steady state error. This can be estimated by introducing errors in the coefficients α_i. Figure 5.6.2 shows the difference between the state of equilibrium obtained for a required Π_c when the turbine efficiency and the turbine upstream temperatures are known with an uncertainty. Contrary to the gasoline case described in chapter 4, the steady state error remains low. However, this confirms the necessity to introduce a feedback strategy.

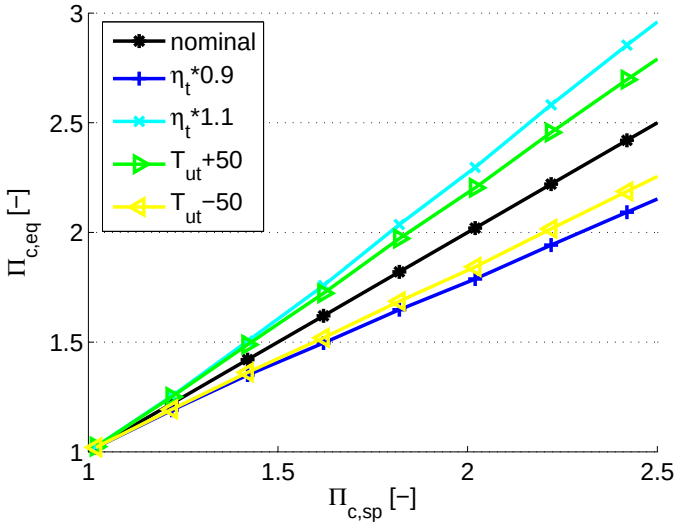

FIGURE 5.12. Robustness of the feedforward strategy in the presence of modeling errors.

5.6.3. Feedback control strategy. —

Model (5.15) was inverted and implemented in a control strategy. The basic structure of the strategy is represented in figure 5.13. Controller C consists in a linear PI controller. Its output is added to a feedforward term and transformed into an actuator setpoint in M^{-1}. Controller C is built via feedback linearization. We want that :

$$\dot{\Pi}_c^{mp} - \dot{\Pi}_c = -\mu_p(\Pi_c^{mp} - \Pi_c) - \mu_i \int (\Pi_c^{mp} - \Pi_c)$$

Where μ_p and μ_i are proportional and integral gains.

The actuator setpoint is computed by :

$$\left\{\begin{array}{rcl} \dot{z} & = & \Pi_c^{mp} - \Pi_c \\ C & = & \mu_p(\Pi_c^{mp} - \Pi_c) + \mu_i z \\ u_{vgt}^{mp} & = & g(\Pi_c^{mp}, C + \dot{\Pi}_c^{mp}) \end{array}\right. \tag{5.26}$$

Controller C follows from the two first lines, whereas the last line is the inversion of (5.15) given in (5.16) and (5.17). Variable z is the state of the controller. In steady state when the intake manifold pressure is controlled to the setpoint, an indication of the accuracy of model 5.15 is given by the relative importance of C with respect to the feedforward term $\alpha_2\beta\psi_c(\Pi_c^{mp})$. This criterium will be used to assess the experimental results.

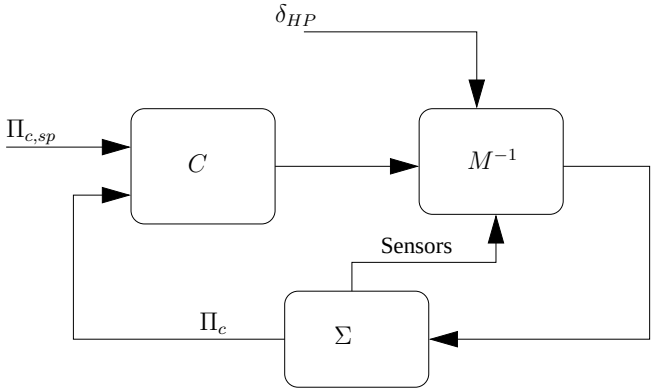

FIGURE 5.13. Turbocharger control structure

5.6.4. Anti windup strategy. — A similar anti windup scheme as that used in chapter 4 can be applied to strategy (5.26). It is indeed necessary when the constraints are active. It is the case both for actuator constraints and for the constraint on the turbine expansion ratio $\Pi_{t,min}$. This limit can indeed be transformed into an actuator limit via equation (5.17). The saturated actuator command is obtained by :

$$u_{vgt}^{sat} = sat(u_{vgt}^{mp}, u_m, \min\{u_M, \psi_{vgt}^{-1}(\frac{\Pi_c^{mp} - \alpha_4\alpha_3}{\alpha_3\phi_{turb}(\Pi_{t,min})})\}) \tag{5.27}$$

The antiwindup scheme is given by :

$$\left\{\begin{array}{rcl} \dot{z} & = & \Pi_c^{mp} - \Pi_c - e\mu_{aw}z \\ \dot{w} & = & (\Pi_c^{mp} - \Pi_c)(u_{vgt}^{sat} - u_{vgt}^{mp}) - w \\ e & = & sat(w, 0, 1) \end{array}\right. \tag{5.28}$$

5.7. Complete air system control strategy

A global air system control structure is built from the combination of the EGR and turbocharger control strategies described in the previous sections. Figure 5.14 represents the global strategy finally obtained. The first layer corresponds to the engine mapping resulting from the calibration phase. The gas composition (F_{dc}^{sp}) and pressure (P_{dc}^{sp}) targets are mapped according to the IMEP set point and the engine speed N_e. The engine speed is measured and the IMEP depends on the driver's demand. The map μ determines the engine operating range where HP or LP EGR must be applied (according to the engine operating conditions once again defined as a function of the engine speed and IMEP set point).

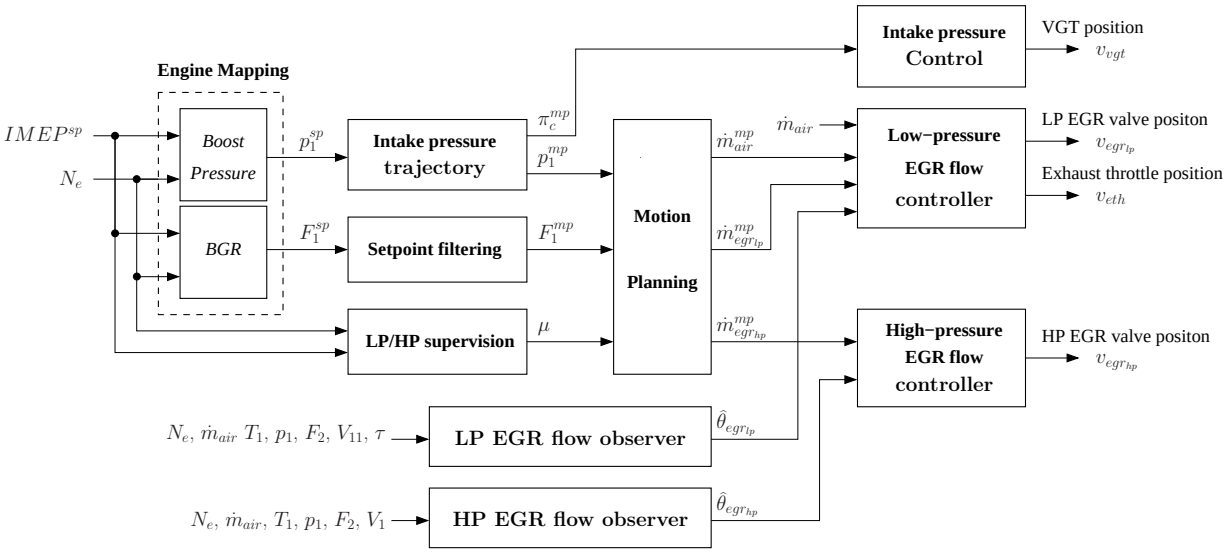

FIGURE 5.14. Principle of the air system control.

The two set points (F_{dc}^{sp} and P_{dc}^{sp}) cannot be applied directly to the input of the control system, thus two feasible trajectories (P_{dc}^{mp} and F_{dc}^{mp}) are computed in order to respect the system dynamics and the constraints. Then, the EGR and air systems are separated by singular perturbations :

The flow control related HP or LP loop. In our case, we apply a motion planning strategy which transforms the intake pressure and the burnt gas rate set points into air flow (D_{air}^{mp}) and EGR flow trajectories ($D_{egr,hp}^{mp}$ and $D_{egr,lp}^{mp}$). The HP and LP EGR valves positions are controlled in order to track their respective EGR flow trajectories. The exhaust

throttle position is controlled in order to track the air flow trajectory (in LP EGR mode only).

The pressure control. The turbocharger has a slower dynamics than the EGR circuits due to its inertia. The actuator constraints are included into the compression ratio trajectory Π_c^{mp} which is also computed so that the EGR requirements can be satisfied.
The intake system is treated as separated control loops : the EGR gas flow trajectories are tracked with the fast actuators (EGR valves), the pressure control is achieved by the turbocharger which has a slower dynamics. The multivariable problem is solved by including the dynamics into the different trajectories. One advantage of the structure is that the feasible pressure trajectory P_{dc}^{mp} can be included into the EGR flow trajectories generation.

5.8. Experimental results

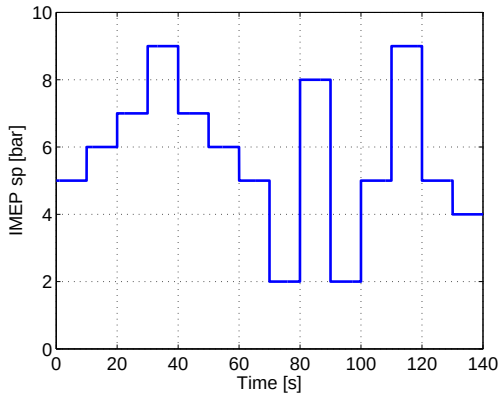

FIGURE 5.15. Reference load trajectory in EGR operating zone

We want to verify that the turbocharger control offers the following advantages :
– The strategy does not depend on the calibration of the engine. If the BGR or pressure setpoints are changed, the turbocharger control strategy does not need any modification because it naturally takes this change into account. This is an advantage with respect to conventional strategies where the feedforward positions are given by maps depending on engine speed and torque setpoint.

– The global air system control structure shows good performances in the EGR zone with respect to pollutant emissions.
– The constraints taken into account in the trajectory planning are efficient.
– Outside the EGR zone, the turbocharger control exploits the whole dynamics of the actuator, with minimum overshoot, undershoot and oscillations.

The tests consisted of load steps performed at a constant engine speed. The load trajectory shown on figure 5.15 is used as a reference in the EGR operating zone because it covers most of the area.

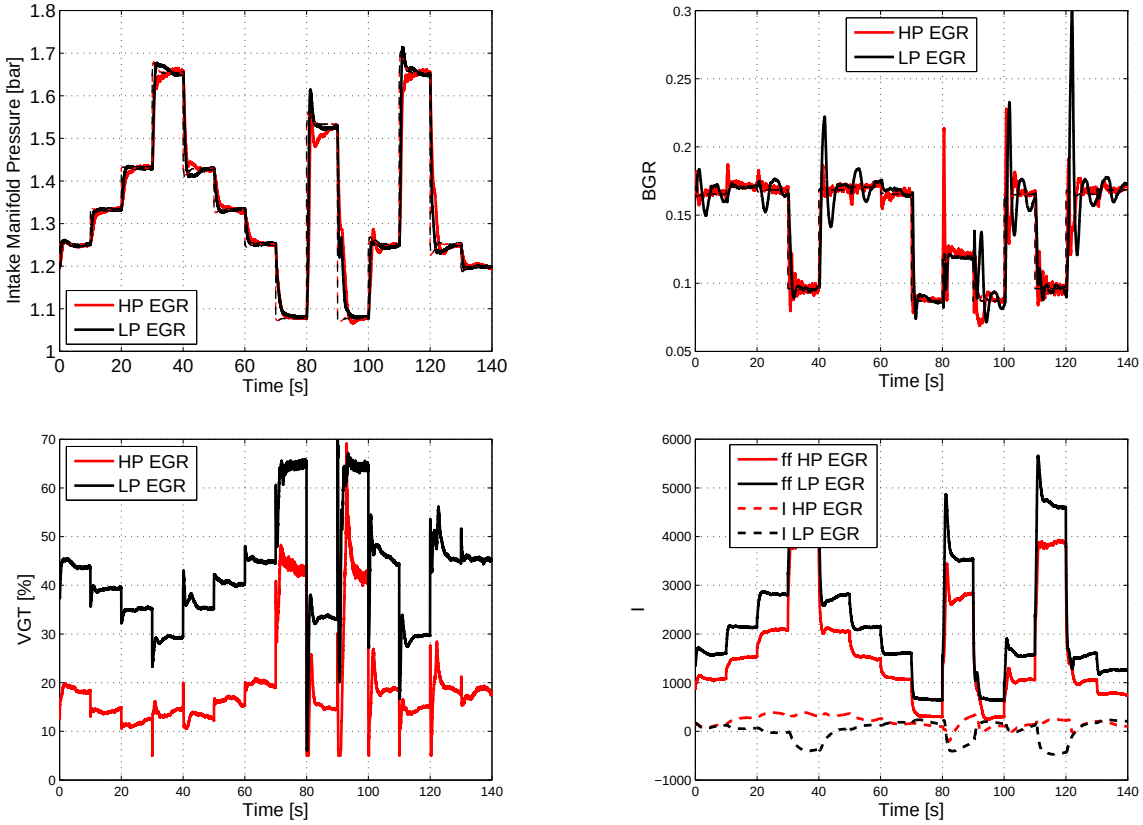

FIGURE 5.16. Transient results in HP or LP EGR : load trajectory of figure 5.15 at 2500rpm. I : integral term represented by C in (5.26) , ff : feedforward term equal to $\alpha_2\beta\psi_c(\Pi_{c,sp})$ in (5.26)

5.8.1. Influence of the EGR. — Load transients at constant speed have been performed in HP or LP EGR configurations. The results are reported in figures 5.16 which show the intake manifold pressure, the intake manifold burned gas rate, the turbocharger actuator (VGT) and the controller output compared to the feedforward term. On each figure a test performed with HP EGR is compared with a test in LP EGR mode. The intake manifold conditions (composition and pressure) are controlled to the same values, but the VGT has to be actuated at very different positions due to the differences in mass flow through the turbine and the compressor. However, the correction necessary from controller C is similar in each mode and stays at low levels compared to the feedforward term (see section 5.6.3). This validates the control strategy, the reduced model chosen for the control design and the assumptions made in its design.

The model provides a feedforward structure that takes into account the interactions between the turbocharger and other components, in particular the EGR circuit. The calibration of the turbocharger controller is independent of the choice of EGR loop, which reduces dramatically the calibration effort required.

5.8.2. Impact of the BGR constraint. — Figure 5.17 zooms on a transient where the BGR constraint is necessary in the computation of the intake manifold pressure trajectory. It consists of a step from high load to low load (see figure 5.15, at time $t = 10$s). The BGR requirement increases abruptly while the fuel injected quantity and hence the burned gas rate in the exhaust manifold decreases. This transient generates a high demand of flow through the EGR valve and therefore a high differential pressure is necessary. The intake manifold pressure decay is slowed down in order to maintain a high exhaust manifold pressure and the possibility to respect the BGR requirements during the transient. The graphs show the difference in pressure trajectory, the consequence on the VGT actuator that remains closed, the beneficial impact on the BGR trajectory and eventually on the NOx emissions.

This graph illustrates the beneficial effect of the strategy and demonstrates how the priority can be given to the EGR circuit in transient in order to account for a pollution requirement. Even if the improvement is small on the NOx emissions, it comes at no cost : it is made possible by a control strategy that does not require any additional sensor or actuator.

5.8.3. Comparison with conventional control. — A conventional control structure for the air system consists of two decentralized PI controllers. The air mass flow D_{air} is

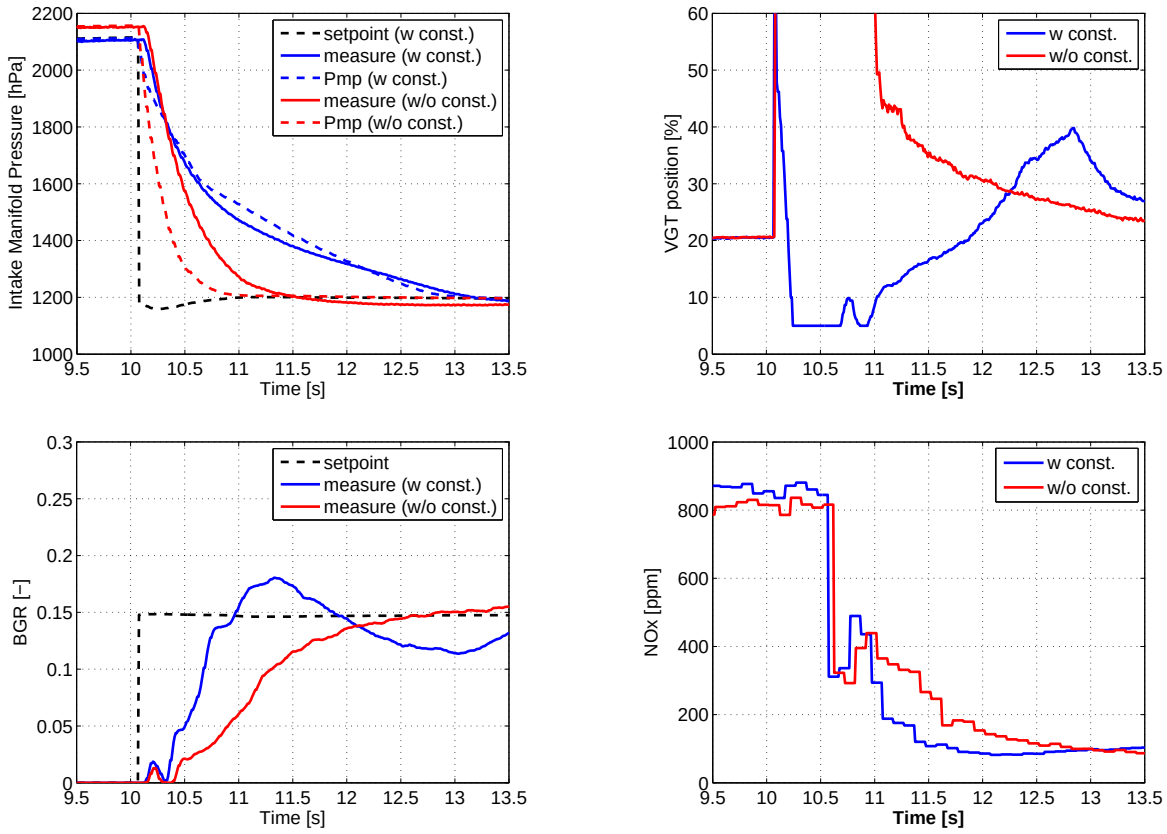

FIGURE 5.17. Effect of the consideration of BGR constraints in the pressure trajectory on the NOx emissions in transient : zoom on part of the load trajectory defined in figure 5.15 at 2000rpm.

controlled by the EGR valve and the intake manifold pressure by the VGT actuator. The comparison between this strategy and that proposed in this chapter is shown in figure 5.18.

As expected, the controls are faster with the proposed strategy and the actuator is more solicited. The most important aspect is that the NOx emissions are reduced in transient, with no deterioration of the opacity measurement. Big NOx excursions observed in transient with the conventional strategy have been removed because the BGR control is more efficient. The turbocharger control helps by ensuring a correct setpoint tracking while respecting a BGR feasibility constraint, as can be seen during the transients at $t = 60s$ and $t = 140s$ where the improvement brought by the consideration of the BGR constraint is highlighted.

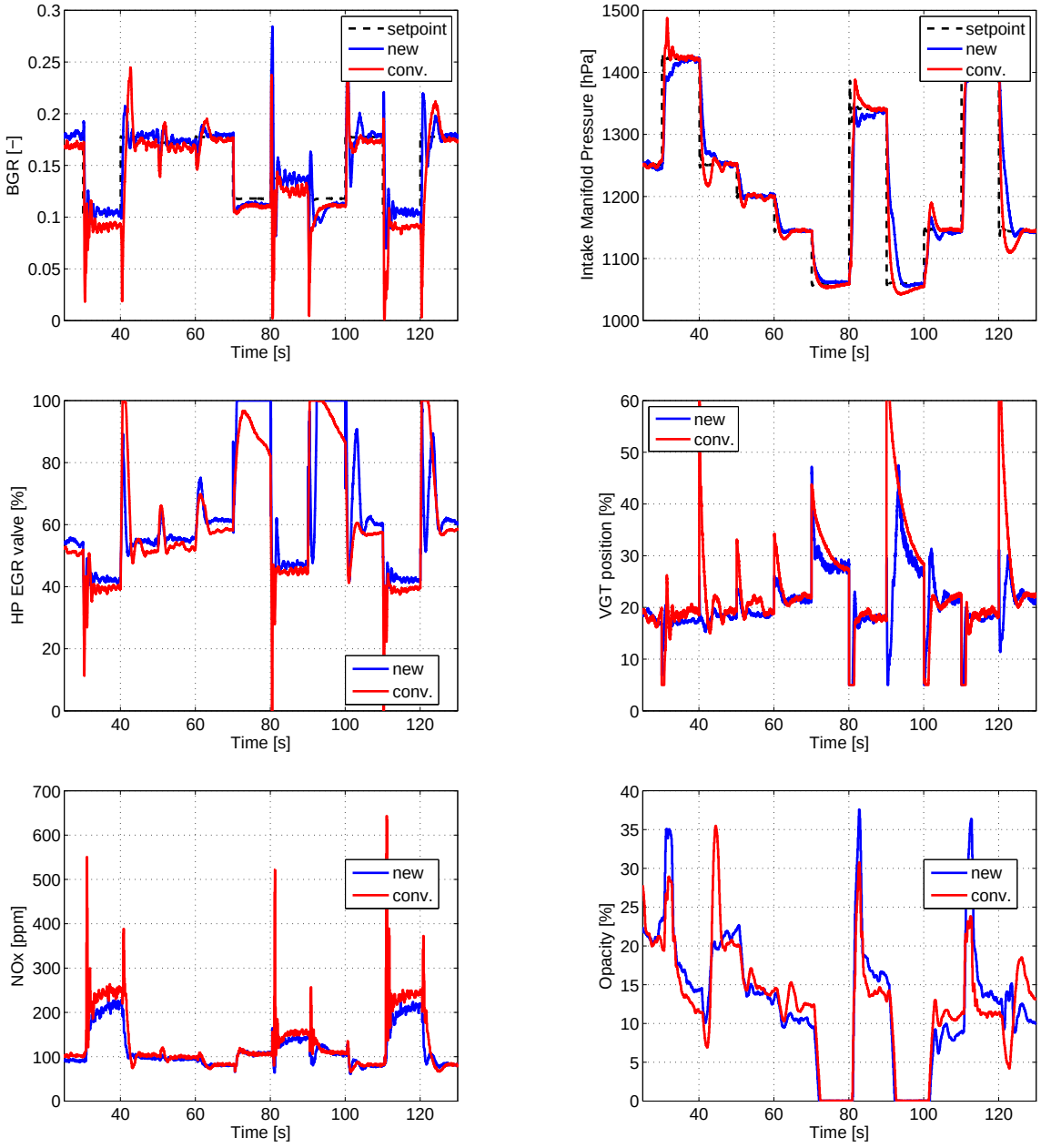

FIGURE 5.18. Comparison between conventional and proposed strategy. Zoom on part of the load trajectory defined in figure 5.15 at 2000rpm.

5.8.4. Outside the EGR operating zone. — Figure 5.19 shows results obtained during load steps where the final operating point is outside the EGR zone. The intake manifold pressure is shown, as well as the command and the controller outputs : integral term and feedforward term (see section 5.6.3). The same transient is performed for different pressure setpoints. At the start of the transient the actuator is fully closed, so the full dynamics of the system are used. The integral term remains low, which shows the accuracy of the feedforward for various pressures setpoints and therefore its independence on the calibration.

The pressure trajectory is not well handled after $t = 1.5s$ where the system could be accelerated for some of the tests presented. As discussed in chapter 3 this is not an issue because the smoke limit is active only at the start of the transient. However, this aspect could be improved and more work could be done on the strategy.

5.9. Limits of the approach and potential improvements

5.9.1. Turbocharger / EGR dynamics separation. — The assumption that the dynamics between turbocharger and EGR circuits are very different can be questionable for certain operating points. It is indeed possible to accelerate the turbocharger close to the time constant of the EGR. In this case some oscillations might appear in the behavior of the system. The tuning constant β_f introduced in (5.24) allows to compensate for this drawback by artificially slowing down the turbocharger via its setpoint trajectory. We can use this approach safely as long as it has an impact on the system time response but not on NOx emissions. More investigations could be done on this aspect.

5.9.2. Actuator dynamics. — Depending on the actuator technology a decentralized controller can be in charge of tracking the actuator to its setpoint. In some cases this can generate effects (dynamics and constraints) that should not be neglected by the high level turbocharger controller (this is probably the source of the issues highlighted in section 5.8.4). The proposed structure is flexible enough to compensate for this. It requires the implementation of a cascaded controller for the turbocharger. This should be investigated.

5.10. Conclusion

This chapter describes the development of a turbocharger model in a Diesel engine fitted with LP and HP EGR loops, its reduction in order to provide a control oriented model, its analysis and the development of an adequate control strategy. Experimental validation results justify the assumptions made in the model reduction process and show that the

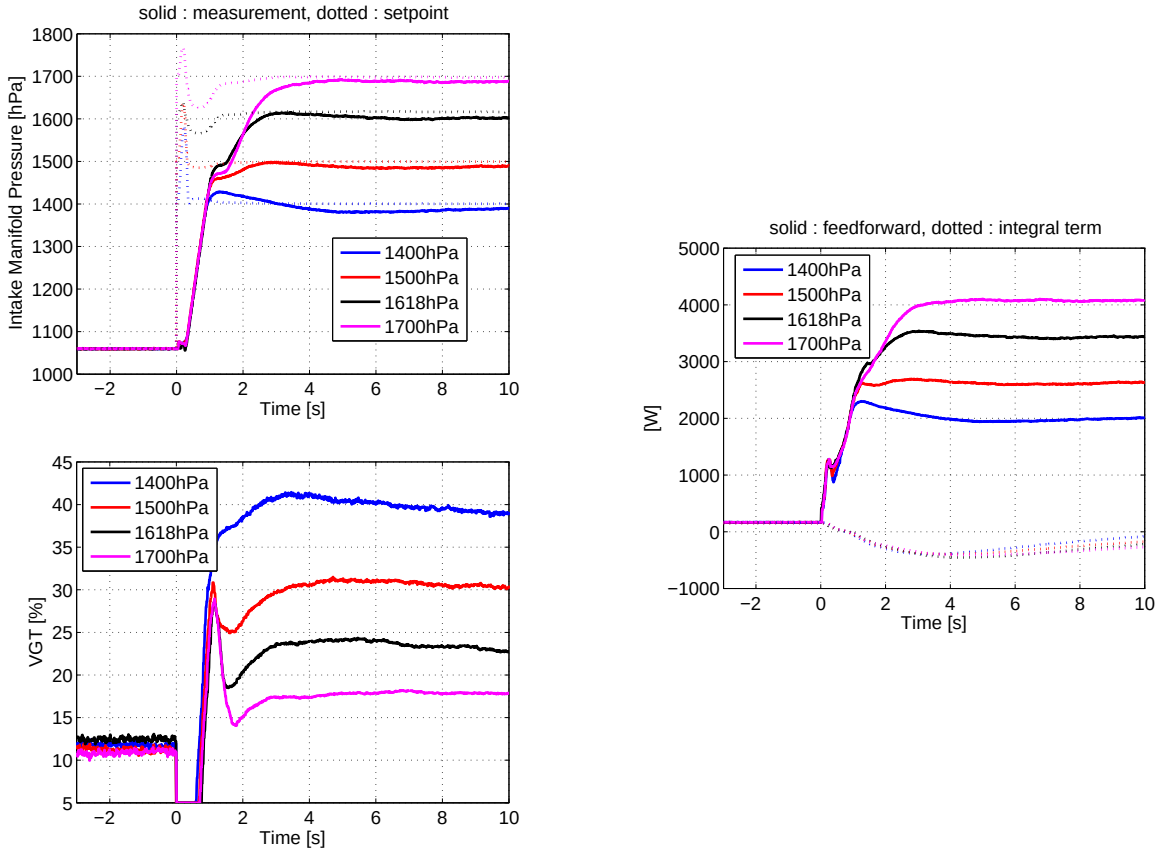

FIGURE 5.19. Transient results outside EGR zone : load steps (IMEP setpoint from 2bar to 12bar at 2000rpm) with different pressure setpoints. Intake manifold pressure, VGT setpoint and turbocharger controller terms (integral term represented by C in (5.26) and feedforward term equal to $\alpha_2\beta\psi_c(\Pi_{c,sp})$ in (5.26)

strategies have a positive impact on the pollutant emissions of the engine when compared to the standard decentralized control structure.

This work complements chapter 4. It shows that the strategy proposed for gasoline engines with fixed geometry turbines can be simply extended to more complex architectures with variable geometry turbines, while taking into account interactions with other subsystems in the form of constraints.

The turbocharger control strategies designed from this model combined with an adequate EGR control and estimation provide a solid basis for the management of modern Diesel

engines. In particular, the calibration of a complex air system could be a daunting task. In the proposed structure the effort required is greatly reduced thanks to an adequate physical representation of the system.

CHAPTER 6

TWO STAGE TURBOCHARGERS ON DIESEL ENGINES

Part of the content of this chapter has been published in [**5, 15**]. However, the papers have been restructured around the stability analysis and the study of the trajectories in the phase plane. Simplified versions of the control strategy have been patented in [**10**].

6.1. Introduction

A major issue in the development of future engines (Diesel or gasoline) concerns in the architecture and the control of the air intake system. Many setups are investigated, and in particular turbocharging systems are becoming more and more complex : variable geometry turbines, two stage turbochargers, maybe variable geometry compressors. For these new architectures, the engine control strategies need to be modified in order to address specific issues related either to the new system in itself or to its integration in the complete engine.

Among the technologies mentioned, two stage turbochargers offer many advantages, because they improve the performances of Diesel engines in terms of power, consumption, pollutant emissions and dynamic behavior (see [**31**]). This chapter presents the development of control strategies for a two stage turbocharged air system in a Diesel engine.

Many publications can be found on the topic of single stage turbocharger control. Because of the novelty of the technology, very few papers are available for two stage turbochargers. In [**73**] and [**77**], complex multivariable control strategies are proposed, and only simulation results.

Papers [**8**] and [**5**] describe respectively a simulator of the system studied, and an analysis of the specific control issues leading to the proposition of a control structure. We propose here to better formalize the problem through the approach already described in

chapter 4 for the simpler problem of single stage turbochargers. An analysis of the system underlines the similarities and differences between single stage and two stage turbochargers control issues and shows that the control problem can be simplified as a single input single output (SISO) problem. Two different control structures are then proposed, analyzed and compared experimentally in terms of performance and robustness.

The chapter is organized as follows. The turbocharger control objectives are presented in Section 6.2, and a strategy adapted for single stage turbochargers is described. This section is followed by an analysis of the system in 6.3 highlighting the issues specific to two stage turbochargers. This leads to the proposition of two different control structures capable of dealing with these issues. These two controllers are compared experimentally in section 6.5.

6.2. Reference single stage turbocharger control

We present in this section the single stage turbocharger control issues that will be considered specifically in this chapter, and propose an adapted control structure that will be taken as reference. Notice that when the HP actuators are open, system 2.16 is a single stage turbocharger.

6.2.1. System representation. — Using an approach similar to that explained in chapter 4, the system can be represented in a reduced form. The following assumptions are made :

- The air dynamics in the manifolds are faster than the turbocharger dynamics.
- The dependency between turbocharger kinetic energy and compression ratio is linear. A more complex relationship is proposed in **[83]**. Its utilization would imply a modification of the functions introduced in (6.1) without changing the main properties of the system on which is based the analysis made in the sequel.
- The relationship between turbine expansion ratio and mass flow does not depend on turbocharger speed.

Noting $x_1 = \Pi_c$, $x_2 = \Pi_t$, and u the wastegate command, the following equations capture the most important characteristics of the system :

$$\left\{ \begin{array}{rcl} \dot{x_1} & = & \alpha_1 \psi_t(x_2) - \alpha_2 \psi_c(x_1) \\ x_1 & = & \alpha_3(\phi_{turb}(x_2) + u\phi_{wg}(x_2)) - \alpha_4 \end{array} \right. \tag{6.1}$$

where the functions and parameters α_i are given in the appendix in (6.20) and (6.21).

The first equation represents the turbocharger dynamics. The second equation represents the mass balance in the exhaust manifold. Variables $\{\alpha_i\}_{i\in[1,4]}$ are positive, they depend on the engine operating conditions, and they are measured by sensors or can be estimated directly from sensor measurements. Indeed, we have $P_{uc,1} = P_{atm}$, $T_{uc,1} = T_{amb}$, $P_{dt,1} = P_{atm} + \Delta P_{pf}$, $T_{ut,1} = T_{exh}$. The compressor and turbine efficiencies can be mapped against measurements : air flow and pressure ratio for compressor, compressor pressure ratio (through turbocharger speed) and expansion ratio for turbine. Notice that α_i depend also on the pressures upstream compressor and downstream turbine. This will make the system more complex when considering two stage turbochargers in section 6.3.

Functions ψ_t, ψ_c, ϕ_{turb} and ϕ_{wg} are monotonic, increasing, invertible and defined for $x > 1$.

This reduced model is not exactly the same as in chapter 4 because the engine is not operated at stoechiometry and therefore the injected fuel flow is not proportionnal to the air flow. However, the main properties are kept : the system is stable around the equilibrium states, can be inverted and controlled in a similar way as proposed in chapter 4.

6.2.2. Control problem. — As explained in chapter 3, the objective of the turbocharger control strategies is to track an intake manifold pressure setpoint. In this chapter we pay particular attention to high load operating zone because this is where the system is really specific. For this reason, the interactions with the EGR circuit are not studied here. In fact, on the engine considered, the calibration resulted in closing both turbochargers wastegates in the EGR operating zone, suppressing the need for any work on this topic. However the interactions between EGR and turbochargers could probably be dealt with similar solutions as proposed in chapter 5.

On the contrary, it is very important to verify that the constraints on maximum turbocharger speed and maximum exhaust manifold pressure are respected for safety reasons. These constraints are active when the engine operate close to high loads.

System of equations (6.1) is convenient when formulating the control problem. The boost pressure is in fact equal to $x_1 P_{uc}$, where P_{uc} is the atmospheric pressure, measured by a sensor. The setpoint $P_{man,sp}$ can therefore be transformed into $x_{1,sp}$. The constraints on the turbocharger speed and on the exhaust pressure can be expressed directly through variables x_1 because the compressor map is invertible and x_2 because the pressure downstream from turbine is measured.

6.2.3. Reference single stage turbochargers control structure. — Figure 6.1 shows the implementation of a strategy for a single stage system which was considered as the reference for the work presented here. This structure consists of two cascaded controllers. The input of the first controller c_1 is the compression ratio. It computes a turbine expansion ratio setpoint for the second controller c_2. For each controller a feed forward term is added to the contribution of the feedback term. In this structure, each controller is in charge of the inversion of each equation of system (6.1). It is possible to compute the feedforward terms by inverting the static parts of system (6.1). Choosing c_1 and c_2 as two first order controllers, the feedback and feedforward parts of the strategy are given respectively by (6.2) and (6.3). Anti windup schemes are usually necessary, but not mentioned here.

$$\left\{\begin{array}{rcl} e_1 & = & x_{1,sp} - x_1 \\ \dot{z_1} & = & e_1 \\ x_{2,cl} & = & c_1(e_1, z_1) \\ x_{2,sp} & = & min(x_{2,max}, x_{2,cl} + x_{2,ff}) \\ e_2 & = & x_{2,sp} - x_2 \\ \dot{z_2} & = & e_2 \\ u_{cl} & = & c_2(e_2, z_2) \\ u & = & u_{cl} + u_{ff} \end{array}\right. \tag{6.2}$$

and

$$\left\{\begin{array}{rcl} x_{2,ff} & = & \psi_t^{-1}\big(\dfrac{\alpha_2}{\alpha_1}\psi_c(x_{1,sp})\big) \\ u_{ff} & = & \dfrac{x_{1,sp} + \alpha_4 - \alpha_3\phi_{turb}(x_{2,sp})}{\alpha_3\phi_{wg}(x_{2,sp})} \end{array}\right. \tag{6.3}$$

This structure is well adapted to the requirements. Limits on the setpoints of each controller $x_{1,sp}$ and $x_{2,sp}$ ensure that the speed and exhaust pressure limitations are respected if controllers c_1 and c_2 do not generate any overshoot. A way of solving this problem is to use PI controllers for c_1 and c_2 and to set the integral terms z_1 and z_2 to 0 when the constraints are hit. In this case the controllers contain in fact only proportional actions which do not generate overshoots when applied to a stable first order system.

Compression and expansion ratios are used to be independent on the variation in atmospheric pressure and turbine downstream pressure. This structure brings two main drawbacks : an exhaust pressure sensor is needed, and the calibration of two controllers in cascade is difficult.

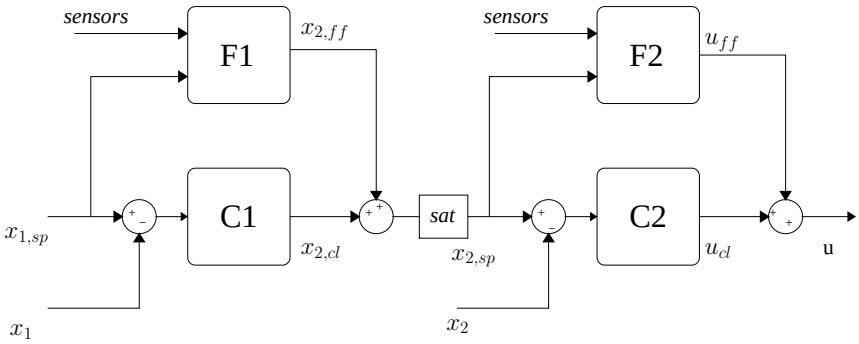

FIGURE 6.1. Single stage control strategy.

6.3. Analysis of two stage turbocharger control issues

In the sequel, we use respectively subscripts 1 and 2 for LP and HP turbocharger.

6.3.1. Specific control issues. —

Two stage turbochargers are represented as the succession of twice system (6.1), except that the pressures between the compressors and between the turbines are not measured. We use the notations : $x_1 = \Pi_{c,1}$, $x_2 = \Pi_{t,1}$, $x_3 = \Pi_{c,2}$, $x_4 = \Pi_{t,2}$, and u_1, u_2 and u_3 are respectively the LP and HP wastegate command and the HP compressor bypass (expressed as a fraction of the mass flow through the compressor over the total air flow). The system becomes :

$$\left\{\begin{array}{rcl} \dot{x_1} & = & \alpha_1\psi_t(x_2) - \alpha_2 x_3\psi_c(x_1) \\ x_1x_3 & = & \alpha_3(\phi_{turb,1}(x_2) + u_1\phi_{wg1}(x_2)) - \alpha_4 \\ \dot{x_3} & = & \alpha_5 x_2\psi_t(x_4) - u_3\alpha_6 x_1\psi_c(x_3) \\ x_1x_3 & = & \alpha_7 x_2(\phi_{turb,2}(x_4) + u_2\phi_{wg2}(x_4)) - \alpha_4 \end{array}\right. \tag{6.4}$$

with $\{\alpha_i\}_{i\in[1,4]}$ given as above for single stage turbochargers but applied to LP turbocharger, and $\{\alpha_i\}_{i\in[5,7]}$ given in (6.22) in the appendix.

We still have measurements for $P_{uc,1} = P_{atm}$, $T_{uc,1} = T_{amb}$, $P_{dt,1} = P_{atm} + \Delta P_{pf}$ and $T_{ut,2} = T_{exh}$. However, $T_{ut,1}$ and $T_{uc,2}$ are not measured.

The objective of the control strategy is still to control the intake manifold pressure, which now is equal to $x_1x_3P_{uc1}$. There is a constraint for each turbocharger speed and for the exhaust manifold pressure. The problem is more complex because the system is second order, it has three actuators u_1, u_2 and u_3, and because it consists in controlling

x_1x_3 while limiting x_1, x_3 and x_2x_4. The cross dependencies between the variables x_i add even more complexity. We will have to simplify it before trying to find solutions.

6.3.2. Simplification based on system analysis. — Pragmatic considerations can help to simplify the control problem. An important observation is that a closed position of the LP wastegate is always beneficial to the system. It makes the global system dynamics faster in transient (intake pressure and air flow rate), whereas it decreases in steady state the difference between exhaust and intake pressure, hence reducing engine pumping losses. These effects are illustrated on figure 6.2 which shows on the top left graph the engine differential pressure as a function of LP wastegate for a given engine operating point, and on the other graphs a load transient at constant speed for two different positions of the LP wastegate command (0% is open, 100% is closed).

Furthermore, when HP compression is positive (i.e. $\Pi_{c,hp} > 1$), the compressor bypass should be closed. Otherwise the gas would in fact flow backward, from the compressor outlet to its inlet. This would result in an increase of the compressor flow with no benefits for the engine. Therefore, the HP compressor bypass has to be open in the choke area of the compressor and closed outside this zone.

As a consequence of these two assumptions, the complex control problem can be reduced to a single input single output problem. The boost pressure is the input of the controller. The output is either the HP or the LP wastegate, defining two different operating modes HP or LP. These two modes are not equivalent from a control point of view. In LP mode, the system is similar to a single stage turbocharger, so the control issues are not specific and are included in the scope of section 6.2.

In the sequel we will consider mainly HP mode. In this case the control issues are specific. The system behavior depends on the two sequential turbochargers.

From the analysis above, u_1 is set to zero, u_3 is set to 1, and the system becomes :

$$\left\{\begin{array}{rcl} \dot{x_1} & = & \alpha_1\psi_t(x_2) - \alpha_2 x_3\psi_c(x_1) \\ x_1x_3 & = & \alpha_3\phi_{turb,1}(x_2) - \alpha_4 \\ \dot{x_3} & = & \alpha_5 x_2\psi_t(x_4) - \alpha_6 x_1\psi_c(x_3) \\ x_1x_3 & = & \alpha_7 x_2(\phi_{turb,2}(x_4) + u_2\phi_{wg2}(x_4)) - \alpha_4 \end{array}\right. \tag{6.5}$$

Finally, the system is second order, and the control problem is SISO but with constraints on the states. The global compression ratio x_1x_3 cannot be controlled without taking into account the trajectory of x_1 and x_3. This is the main control issue for this system. It is illustrated in 6.2 where the HP turbocharger speed exceeds its limit in transient when the system is controlled with a simple PI strategy.

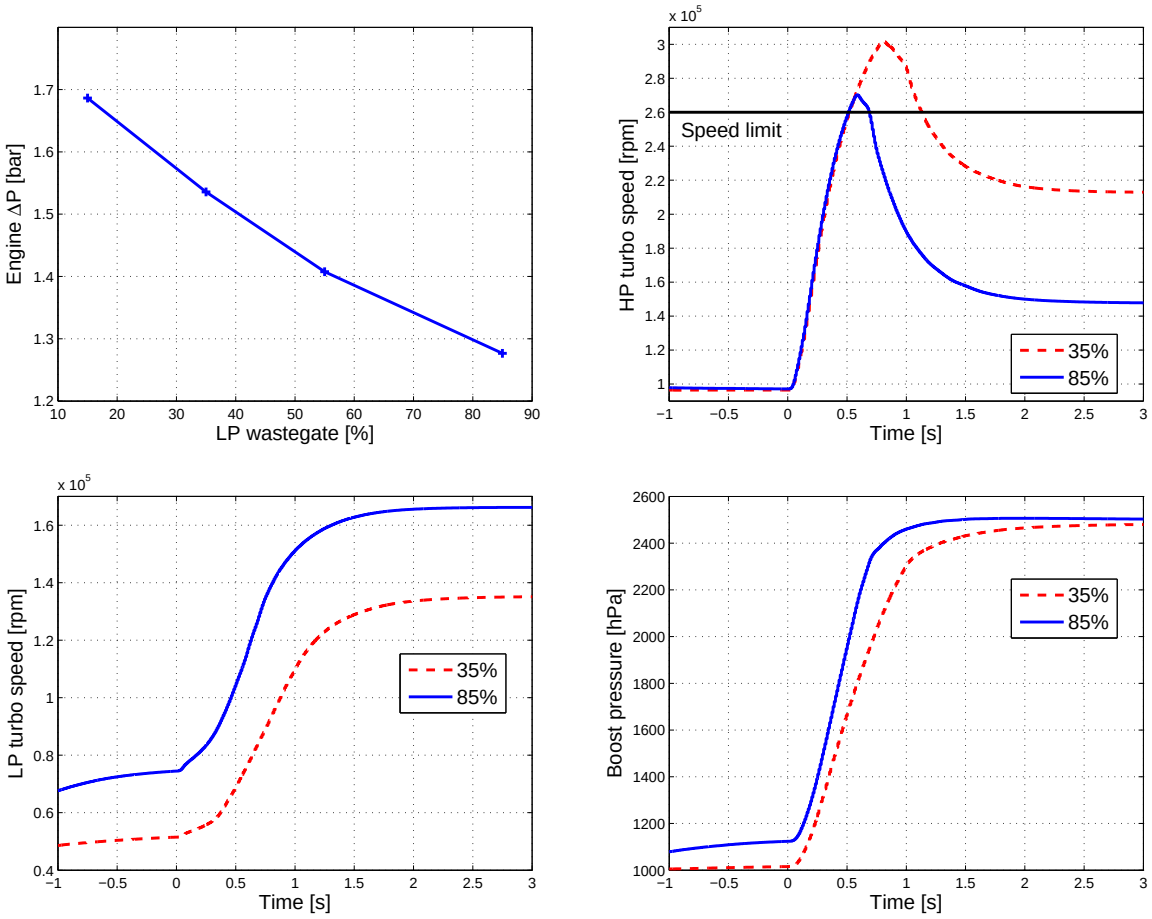

FIGURE 6.2. Impact of LP wastegate command on the system in steady state (top) and during transient.

The properties of the system will be discussed in 6.4 where we will design a control with an approach consisting in estimating x_1 and controlling x_3.

We first discuss briefly the mode transition.

6.3.3. Mode transition. — Two different operating modes can be identified : the HP mode and the LP mode. The transition between these modes is decided by a manager based on the conditions at the boundaries of the controlled turbocharger.

Transition from HP mode to LP mode (condition c1). — To change from HP mode to LP mode, the HP compression ratio must be lower than one. That means that the HP

compressor does not provide any enthalpy to the gas. The compression ratio is calculated from the measurement of the supercharging pressure and the estimation of the pressure before HP compressor.

Transition from LP mode to HP mode. — To change from LP mode to HP mode, the following conditions have to be respected :

- condition c2 : the pressure set point cannot be reached when the LP waste gate is closed
- condition c3 : the use of HP compressor allows to reach the intake pressure set point. If the HP compressor was used on the current point, then its compression ratio would be greater than one. This condition prevents operating in the choke area.

To test if the HP compressor ratio would be greater than 1 while using the HP compressor, it is possible to use the compressor map.

The second condition for the transition LP-HP is contradictory with the condition HP-LP. The first condition LP-HP plays the role of a hysteresis that stabilizes the system. However, the stability of this strategy is not proved. We will only notice that experimentally there was no specific issue on this topic.

The scheme of Figure 6.3 illustrates the mode transition. From top to bottom, the graphs show the engine speed, the pressures (setpoint, outlet of LP compressor and outlet of HP compressor), the three transition conditions described above, and the operating mode. The system starts at low speed in LP mode. Then the following events occur :

- t1 : setpoint step. The LP wastegate is fully closed. Condition c2 becomes true. The controller switches to HP mode and closes the HP wastegate. Since the engine speed is low, the HP compressor is in its normal operating range. The HP compression ratio becomes greater than one and condition c1 becomes false. The controller stays in HP mode.
- t2 : the setpoint is reached by the LP compressor. The condition c1 becomes true. The controller switches to LP mode. The LP wastegate is opened because the system is on its setpoint. Condition c2 becomes false and the controller stays in LP mode.
- t3 : the current operating point corresponds to HP choking conditions, because the engine speed (and thus the compressor mass flow) is increasing. Condition c3 becomes false.
- t4 : setpoint step. The LP wastegate is closed and condition c2 becomes true. However, condition c3 is still false and prevents from switching to HP mode because the HP compressor would be in choking conditions. The controller stays in LP mode.

– t5 : the setpoint is reached. The LP wastegate is opened. Condition c2 becomes false.
– t6 : the engine speed decreases, the system leaves HP choking conditions. Condition c3 becomes true. Since the LP compressor provides enough pressure the controller stays in LP mode.
– t7 : same as t1, the controller switches to HP mode.
– t8 : same as t2, switch to LP mode.

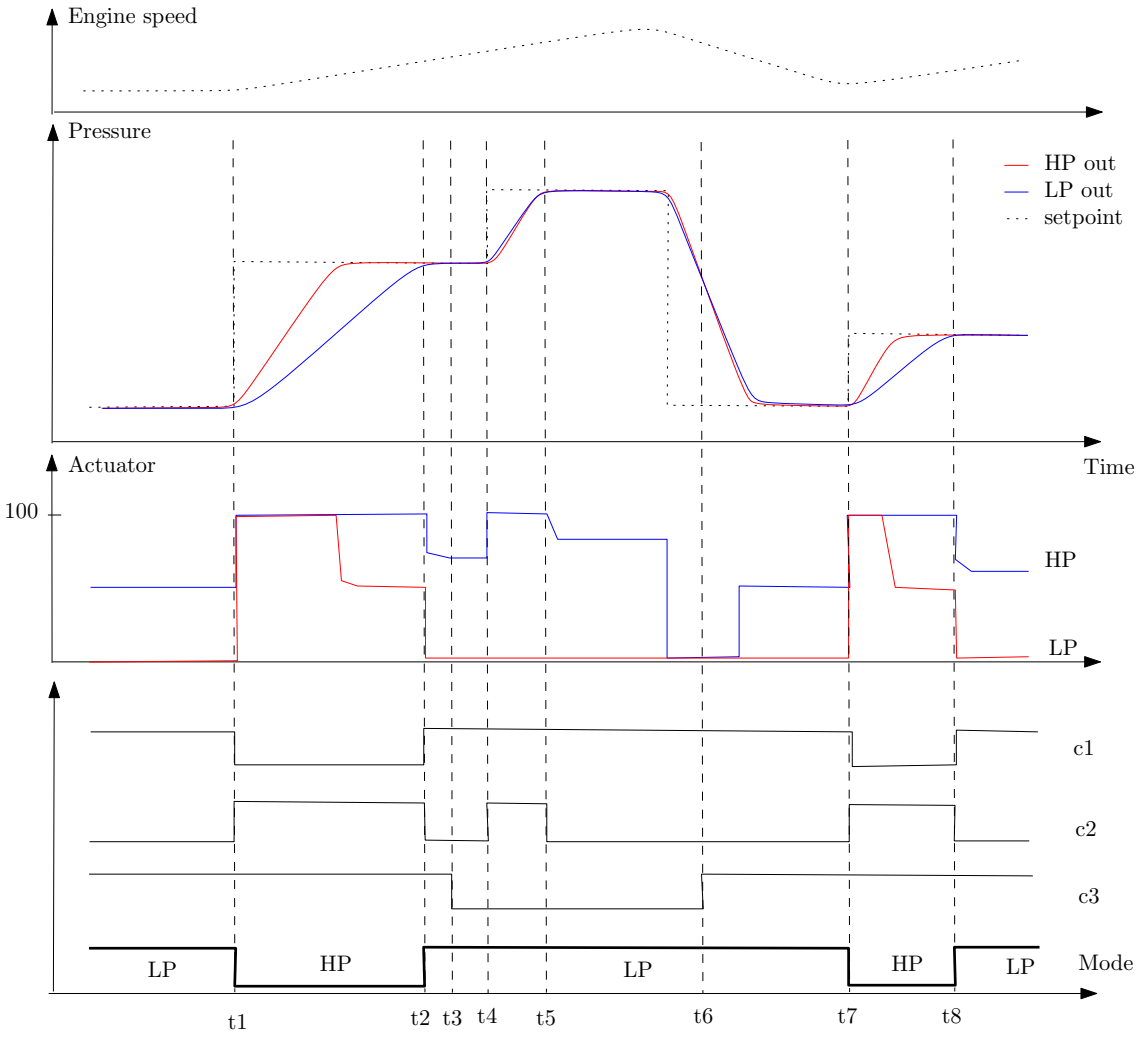

FIGURE 6.3. Illustration of mode transition

6.3.4. System properties in HP mode with proportional controller. —
We analyze in this section the properties of system (6.5) for a given operating point. We choose the operating point defined in table 6.1. At the chosen engine speed, the LP stage can provide some boost but usually not enough to reach the setpoint. For these conditions there may be a risk of HP turbocharger over speed. The following analysis could be made in exactly the same way for other operating points.

N_e	P_{uc}	T_{uc}	P_{dt}	T_{ut}	D_f	$\eta_{c,1}$	$\eta_{t,1}$	$\eta_{c,2}$	$\eta_{t,2}$	η_v
[rpm]	[bar]	[K]	[bar]	[K]	[kg/s]	-	-	-	-	-
2000	1	300	1.1	1000	0.0027	0.55	0.65	0.5	0.6	0.85

TABLE 6.1. Operating points for trajectory analysis

6.3.4.1. System inversion. — We use the notation : $x_{sp} = \frac{P_{man,sp}}{P_{uc}}$, and the function $\Psi_c(x) = \dfrac{\psi_c(x)}{x}$. This function is invertible (see appendix), so the steady state part of system (6.5) can be inverted. For a given setpoint we can compute :

$$\begin{cases} x_2 &= \phi_{turb,1}^{-1}(\dfrac{x_{sp}+\alpha_4}{\alpha_3}) \\ x_1 &= \Psi_c^{-1}(\dfrac{\alpha_1\psi_t(x_2)}{\alpha_2 x_{sp}}) \\ x_3 &= \dfrac{x_{sp}}{x_1} \\ x_4 &= \psi_t^{-1}(\dfrac{\alpha_6 x_1\psi_c(x_3)}{\alpha_5 x_2}) \\ u_2 &= \dfrac{x_{sp}+\alpha_4-\alpha_7 x_2\phi_{turb,2}(x_4)}{\phi_{wg,2}(x_4)} \end{cases} \tag{6.6}$$

Since functions $\phi_{turb,1}$, Ψ_c, ψ_t are invertible, positive and defined for $x > 1$, the command u_2 exists and is unique as long as $x_3 > 1$. This restrictive condition means that the setpoint x_{sp} must be greater than the value of x_1 at steady state. This is true when the HP mode is active.

There is only one equilibrium state. It is defined by (6.6).

6.3.4.2. Stability of the states of equilibrium. — For a given command u_2 it is possible to inverse the static equations of (6.5). We thus obtain a system with two states that can be expressed in the form :

$$\begin{cases} \dot{x}_1 &= f_1(x_1, x_3) \\ \dot{x}_3 &= f_2(x_1, x_3, u_2) \end{cases} \tag{6.7}$$

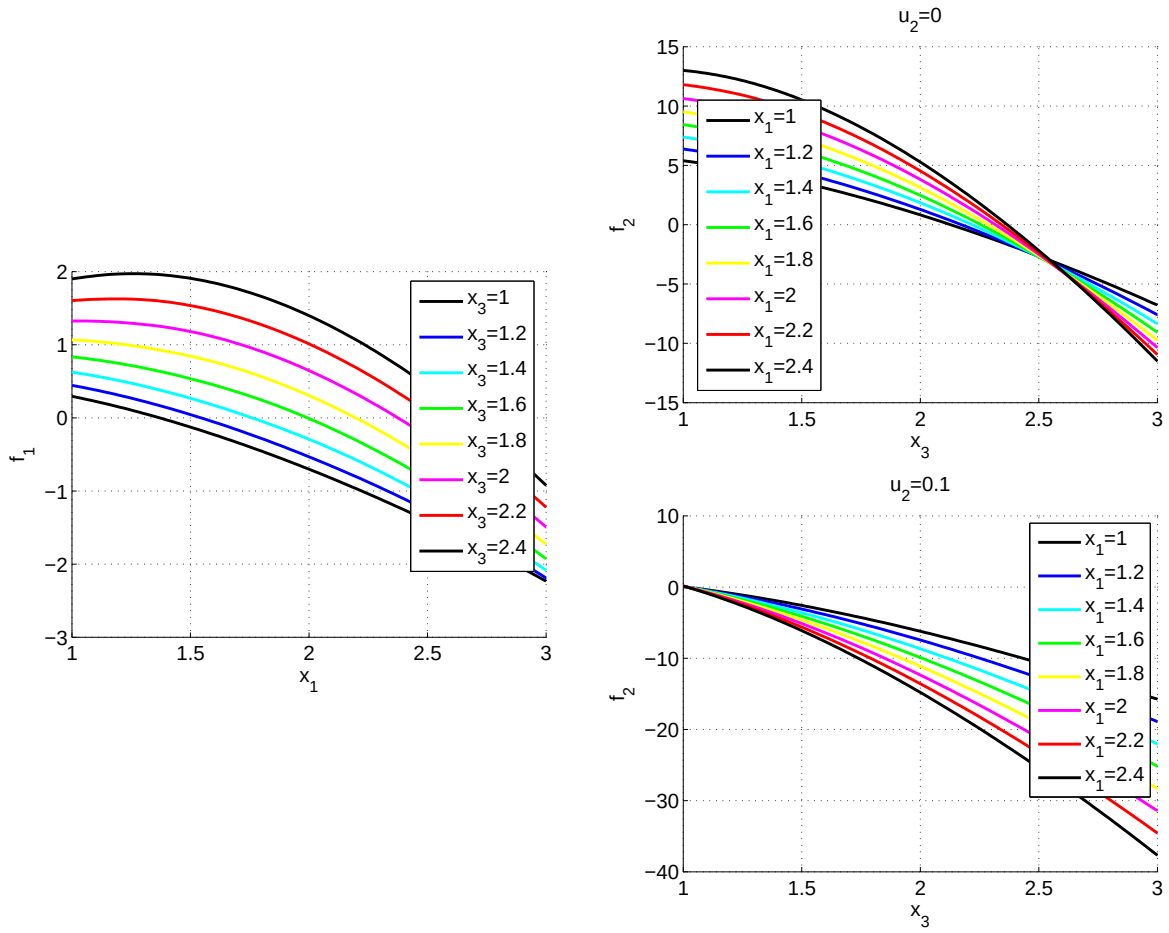

FIGURE 6.4. Functions f_1 and f_2.

The function f_1 is represented in figure 6.4 as a function of x_1 for various x_3. Similarly, f_3 is shown for various x_1 when $u_2 = 0$ and $u_2 = 0.1$. These functions have the following properties :

i $\forall (x_1, x_3), \dfrac{\partial f_1}{\partial x_1} < 0$. f_1 is always strictly decreasing with respect to x_1. The stability of the LP turbocharger does not depend on the HP turbocharger.

ii $\forall(x_1, x_3), \dfrac{\partial f_1}{\partial x_3} > 0$. We can observe that f_1 is strictly increasing with respect to x_3.

iii $\forall(x_1, x_3, u_2), \dfrac{\partial f_2}{\partial x_3} < 0$. For the two values of u_2 shown, f_2 is strictly decreasing with respect to x_3. We will therefore assume it is always the case. The stability of the HP turbocharger does not depend on the LP turbocharger.

iv $\forall(x_1, x_3, u_2), \dfrac{\partial f_2}{\partial u_2} < 0$. We also assume that f_2 is strictly decreasing with respect to u_2. The HP turbocharger accelerates when the wastegate is closed (this was shown in the previous chapters).

v Concerning the last partial derivative $\dfrac{\partial f_2}{\partial x_1}$ we cannot conclude for all the operating range since it depends on the command u_2.

This system can be linearized around the state of equilibrium $(x_{1,eq}, x_{3,eq})$. We call $\tilde{x}_1 \triangleq x_1 - x_{1,eq}$ and $\tilde{x}_3 \triangleq x_3 - x_{3,eq}$. We have the following linear system :

$$\begin{pmatrix} \dot{\tilde{x}}_1 \\ \dot{\tilde{x}}_3 \end{pmatrix} = A \begin{pmatrix} \tilde{x}_1 \\ \tilde{x}_3 \end{pmatrix}, A = \begin{pmatrix} \dfrac{\partial f_1}{\partial x_1}(x_{1,eq}, x_{3,eq}) & \dfrac{\partial f_1}{dx_3}(x_{1,eq}, x_{3,eq}) \\ \dfrac{\partial f_2}{\partial x_1}(x_{1,eq}, x_{3,eq}, u_{eq}) & \dfrac{\partial f_2}{dx_3}(x_{1,eq}, x_{3,eq}, u_{eq}) \end{pmatrix} \tag{6.8}$$

The stability of the system depends on the sign of the roots of the characteristic equation of A, and therefore on its coefficients. These coefficients are shown in figure 6.5 as a function of x_{sp} when $x_{sp} > x_{1,eq}$.

We can verify, as suggested before that $\forall x_{sp}$: $\dfrac{\partial f_1}{\partial x_1}(x_{1,eq}, x_{3,eq}) < 0$, $\dfrac{\partial f_1}{\partial x_3}(x_{1,eq}, x_{3,eq}) > 0$, and $\dfrac{\partial f_2}{\partial x_3}(x_{1,eq}, x_{3,eq}, u_{eq}) < 0$. We can also observe that at the equilibrium state, $\dfrac{\partial f_2}{\partial x_1}(x_{1,eq}, x_{3,eq}, u_{eq}) < 0$. Therefore we can deduce the sign of the determinant and trace of matrix A. Since :

$$det(A) = \frac{\partial f_1}{\partial x_1}(x_{1,eq}, x_{3,eq})\frac{\partial f_2}{\partial x_3}(x_{1,eq}, x_{3,eq}) - \frac{\partial f_1}{\partial x_3}(x_{1,eq}, x_{3,eq})\frac{\partial f_2}{\partial x_1}(x_{1,eq}, x_{3,eq})$$

and

$$tr(A) = \frac{\partial f_1}{\partial x_1}(x_{1,eq}, x_{3,eq}) + \frac{\partial f_2}{\partial x_3}(x_{1,eq}, x_{3,eq})$$

we can deduce that $det(A) > 0$ and $tr(A) < 0$. Therefore the eigenvalues of A have a negative real part. The system is locally asymptotically stable around its state of equilibrium.

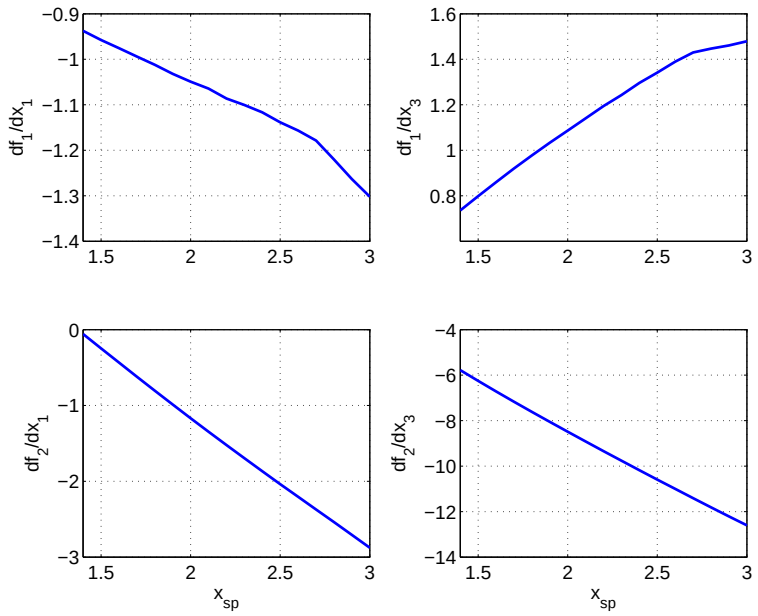

FIGURE 6.5. Coefficients of matrix A at the state of equilibrium

We can also deduce from the figures 6.4 that the trajectories of the system are bounded. Indeed it is possible to define an invariant space by $1 \leq x_1 \leq x_{1,0}$ and $1 \leq x_3 \leq x_{3,0}$. If $x_{1,0}$ and $x_{3,0}$ are sufficiently high it can be checked that $f_1 < 0$ on $x_1 = x_{1,0}$ and $f_2 < 0$ on $x_3 = x_{3,0}$. Since $f_1 > 0$ for $x_1 = 1$ and $f_2 \geq 0$ on $x_3 = 1$, then the space thus defined is invariant because on its boundaries the vector (f_1, f_2) is always directed to the interior of this space.

Finally, we know that the trace of the jacobian matrix $\dfrac{\partial f_1}{\partial x_1} + \dfrac{\partial f_2}{\partial x_3}$ is always strictly negative (proprieties i and ii). Therefore, the system cannot converge to a closed path other than the state of equilibrium (see [**20**]).

We can deduce from the Poincaré Bendixon theory that the system globally converges asymptotically to a unique state of equilibrium.

6.3.5. Application of a proportional feedback control. — Let's apply a feedback control $u = g(x_1, x_3)$ on system (6.7). The function $f_2(x_1, x_3, g(x_1, x_3))$ is called $\tilde{f}_2$. The jacobian matrix A_{cl} of the closed loop system becomes :

$$A_{cl} = \begin{pmatrix} \frac{\partial f_1}{\partial x_1} & \frac{\partial f_1}{\partial x_3} \\ \frac{\partial \tilde{f}_2}{\partial x_1} & \frac{\partial \tilde{f}_2}{\partial x_3} \end{pmatrix} \tag{6.9}$$

where $\frac{\partial \tilde{f}_2}{\partial x_1} = \frac{\partial f_2}{\partial x_1} + \frac{\partial g}{\partial x_1}\frac{\partial f_2}{\partial u}$ and $\frac{\partial \tilde{f}_2}{\partial x_3} = \frac{\partial f_2}{\partial x_3} + \frac{\partial g}{\partial x_3}\frac{\partial f_2}{\partial u}$

So :

$$det(A_{cl}) = det(A) + (\frac{\partial f_1}{\partial x_1}\frac{\partial g}{\partial x_3} - \frac{\partial f_1}{\partial x_3}\frac{\partial g}{\partial x_1})\frac{\partial f_2}{\partial u}$$

and

$$tr(A_{cl}) = tr(A) + \frac{\partial g}{\partial x_3}\frac{\partial f_2}{\partial u}$$

There are conditions on g to ensure that the equilibrium is stable and that the global convergence of the system to a unique state of equilibrium is ensured.

Let's first consider the feedforward $u_{2,ff}$ given by the inversion (6.6). We choose a proportional controller :

$$g(x_1, x_3) = u_{2,ff} - \mu_p(x_{sp} - x_1 x_3) \tag{6.10}$$

We have :

$$det(A_{cl}) = det(A) + (\frac{\partial f_1}{\partial x_1}\mu_p x_1 - \frac{\partial f_1}{\partial x_3}\mu_p x_3)\frac{\partial f_2}{\partial u}$$

and

$$tr(A_{cl}) = tr(A) + \mu_p x_1 \frac{\partial f_2}{\partial u}$$

We know that $\frac{\partial f_2}{\partial u} < 0$, $\frac{\partial f_1}{\partial x_3} > 0$, $\frac{\partial f_1}{\partial x_1} < 0$, that at the equilibrium state $det(A) > 0$ and that $tr(A) < 0$. Therefore $det(A_{cl}) > 0$ at the equilibrium state and $tr(A_{cl}) < 0$. It is obvious that the system's trajectories remain bounded. The stability is guaranteed for any positive value of the proportional gain μ_p and the equilibrium is unique.

The trajectories are represented in the phase plane (x_1, x_3) on figure 6.6 for two different values of μ_p. In the plane (x_1, x_3), the lines corresponding to a given intake manifold pressure define hyperbolas. The system is on its setpoint x_{sp} on the line $\mathcal{H}$ defined by $x_1 x_3 = x_{sp}$ which is represented in red.

We can see that the proportional action is needed to force the system to converge to the hyperbola $\mathcal{H}$. However, this strategy does not take into account the constraints $x_{3,max}$ and $P_{exh,max}$.

We will consider that the HP turbocharger speed limit corresponds to $x_{3,max} = 1.4$. This limit is exceeded for some trajectories on figure 6.6. We must now improve the control strategy in order to ensure that the constraints $x_{3,max}$ and $P_{exh,max}$ are satisfied while forcing the system towards the hyperbola $\mathcal{H}$.

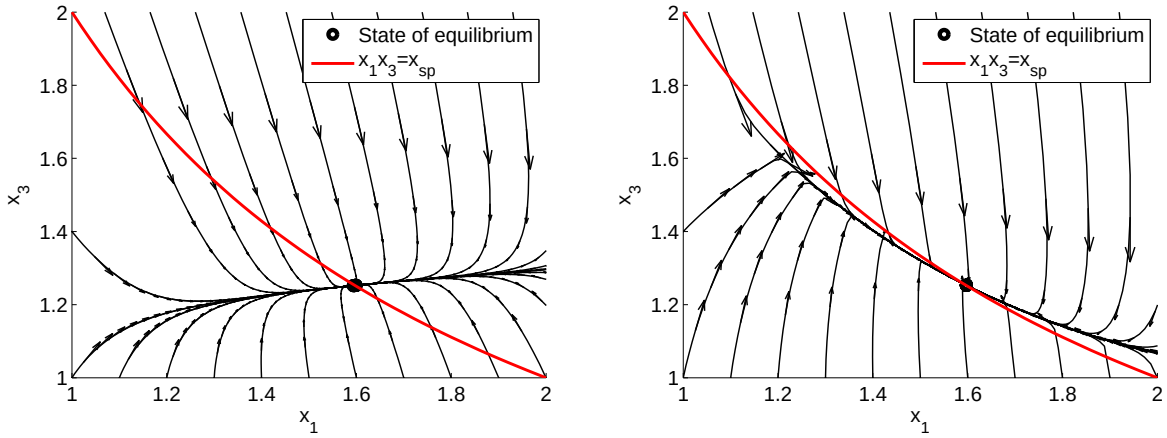

$\mu_p = 0$ $\mu_p = 0.1$

FIGURE 6.6. System trajectories for a constant feedforward and a proportional controller.

6.4. Design of a two stage turbocharger control strategy

6.4.1. LP turbocharger Estimation. —

We first change the control variable. Rather than considering $x_1 x_3$, we design a control on x_3. It is easier to consider the constraint $x_{3,max}$ in this referential. For this purpose it is necessary to estimate x_1.

From the equations (6.5) it is possible to deduce an estimator for the LP turbocharger when the HP turbocharger is controlled. The linear relationship between D_{air} and the intake manifold pressure mentioned in 2.4 can be transformed in this case into a relationship between D_{air} and $x_1 x_3$. It is used in order to remove x_3 from the two first equations and obtain (6.11).

$$\begin{cases} \dot{\hat{x}}_1 &= \alpha_1 \psi_t(\hat{x}_2) - \beta_2 \dfrac{\psi_c(\hat{x}_1)}{\hat{x}_1} \\ \hat{x}_2 &= \phi^{-1}_{turb,1}(\beta_3) \end{cases} \tag{6.11}$$

with β_i given in the appendix in (6.23).

where $P_{uc,1} = P_{atm}$, $T_{uc,1} = T_{amb}$, $P_{dt,1} = P_{atm} + \Delta P_{pf}$. The turbocharger efficiencies can be estimated from $\hat{x_1}$, D_{air} and the characteristics maps. There is an issue with $T_{ut,1}$, which can be chosen as a first order approximation equal to T_{exh}. A better estimation would take into account the expansion ratio of the HP stage, but the results presented further show that this first approximation is sufficient for our needs.

The LP estimator also provides an estimation of $T_{uc,2}$ (or $T_{dc,1}$) from the compression ratio $\hat{x_1}$ and $\eta_{c,1}$.

6.4.2. Control for the HP stage. — We can now design a control on x_3. Thanks to LP estimator (6.11), the last two equations of two stage turbochargers system (6.5) are similar to (6.1) describing single stage turbochargers. A single stage control strategy can therefore be used. Indeed the system is :

$$\left\{ \begin{array}{rcl} \dot{x_3} & = & \alpha_5 \hat{x_2} \psi_t(x_4) - \alpha_6 \hat{x_1} \psi_c(x_3) \\ \hat{x_1} x_3 & = & \alpha_7 \hat{x_2} (\phi_{turb}(x_4) + u_2 \phi_{wg2}(x_4)) - \alpha_4 \end{array} \right. \tag{6.12}$$

We define the following variable : $\hat{x}_3 = \dfrac{P_{man}}{P_{atm}\hat{x}_1}$

We use the setpoint : $x_{3,sp} = \dfrac{x_{sp}}{\hat{x}_1}$

We choose a control strategy corresponding to the sum of two terms. The first one, $u_{2,sp}$ is the steady state of HP turbocharger : $f_2(x_1, x_{3,sp}, u_{2,sp}) = 0$. The second term is a proportional controller. The closed loop strategy becomes :

$$\left\{ \begin{array}{rcl} x_{4,sp} & = & \psi_t^{-1}\big(\dfrac{\alpha_6 \hat{x_1}}{\alpha_5 \hat{x_2}} \psi_c(x_{3,sp})\big) \\ u_{2,sp} & = & \dfrac{x_{3,sp}\hat{x_1} + \alpha_4 - \alpha_7 \hat{x_2} \phi_{turb}(x_{4,sp})}{\alpha_7 \hat{x_2} \phi_{wg}(x_{4,sp})} \\ g(x_1, x_3) & = & u_{2,sp} - \mu_p(x_{3,sp} - \hat{x}_3) \end{array} \right. \tag{6.13}$$

The determinant of matrix A_{cl} is computed as below. We know by construction that :

$$f_2(x_1, \frac{x_{sp}}{x_1}, g(x_1, x_3) + \mu_p(\frac{x_{sp}}{x_1} - \hat{x}_3)) = 0$$

So

$$\frac{\partial f_2}{\partial x_1} - \frac{x_{sp}}{x_1^2}\frac{\partial f_2}{\partial x_3} + (\frac{\partial g}{\partial x_1} - \frac{\mu_p x_{sp}}{x_1^2})\frac{\partial f_2}{\partial u} = 0$$

And

$$\frac{\partial \tilde{f}_2}{\partial x_1} = \frac{\partial f_2}{\partial x_1} + \frac{\partial g}{\partial x_1}\frac{\partial f_2}{\partial u} = \frac{x_{sp}}{x_1^2}\left(\frac{\partial f_2}{\partial x_3} + \mu_p \frac{\partial f_2}{\partial u}\right) < 0$$

Since $\dfrac{\partial g}{\partial x_3} = \mu_p$, we can deduce that if we choose $\mu_p > 0$:

$$det(A_{cl}) = \overbrace{\frac{\partial f_1}{\partial x_1}}^{<0}\overbrace{\left(\frac{\partial f_2}{\partial x_3} + \mu_p \frac{\partial f_2}{\partial u}\right)}^{<0} - \overbrace{\frac{\partial f_1}{\partial x_3}\frac{x_{sp}}{x_1^2}}^{>0}\overbrace{\left(\frac{\partial f_2}{\partial x_3} + \mu_p \frac{\partial f_2}{\partial u}\right)}^{<0} > 0$$

and

$$tr(A_{cl}) = tr(A) + \mu_p \frac{\partial f_2}{\partial u} < 0$$

Therefore if the proportional gain μ_p is positive, then the system converges to a unique stable equilibrium point.

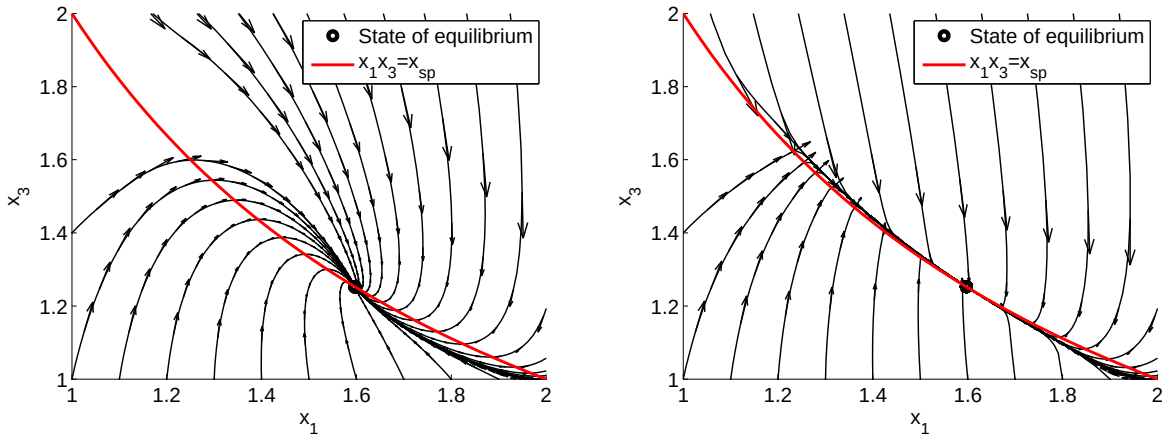

$\mu_p = 0$ $\mu_p = 0.1$

FIGURE 6.7. System trajectories for a feedforward on HP turbocharger and a proportional controller.

The trajectories of the system are shown on figure 6.7. When the feedback gain is set to 0, the strategy (6.13) based on the steady state of the HP turbocharger brings the system closer to the hyperbola $\mathcal{H}$ than strategy (6.10) when the feedforward is constant. The system is stable and converges to a unique state of equilibrium.

The constraint $x_{3,max}$ is still exceeded, but we now have a structure adapted for implementing a limitation on x_3.

6.4.3. Constraints consideration. — The maximum compression ratio $x_{3,max}$ can now be included in the setpoint, and therefore taken into account by the controller.

We must notice that the exhaust pressure constraint can be transformed into an actuator constraint. The two algebraic equations of system (6.5) can be inverted. The first one leads to the estimation $\hat{x}_2$ given above. The second one leads to a monotonic relationship between u_2 and x_4. So, if the maximum exhaust pressure is called $P_{exh,max}$, we note $x_{4,max} = \dfrac{P_{exh,max}}{(P_{atm} + \Delta P_{pf})\hat{x}_2}$ and we can compute a limit on the actuator :

$$u_{2,min} = \frac{x_1 x_3 + \alpha_4 - \alpha_7 \hat{x}_2 \phi_{turb,2}(x_{4,max})}{\phi_{wg,2}(x_{4,max})} \tag{6.14}$$

This limit can be taken into account like an actuator constraint in the strategy.

The closed loop strategy becomes :

$$\begin{cases} x_{3,lim} &= \min\{x_{3,max}, \dfrac{x_{sp}}{\hat{x}_1}\} \\ x_{4,sp} &= \psi_t^{-1}\Big(\dfrac{\alpha_6 \hat{x_1}}{\alpha_5 \hat{x_2}} \psi_c(x_{3,lim})\Big) \\ u_{2,sp} &= \dfrac{x_{3,lim}\hat{x_1} + \alpha_4 - \alpha_7 \hat{x}_2 \phi_{turb}(x_{4,sp})}{\alpha_7 \hat{x}_2 \phi_{wg}(x_{4,sp})} \\ g(x_1, x_3) &= \max\{u_{2,min}, u_{2,sp} - \mu_p(x_{3,lim} - \hat{x}_3)\} \end{cases} \tag{6.15}$$

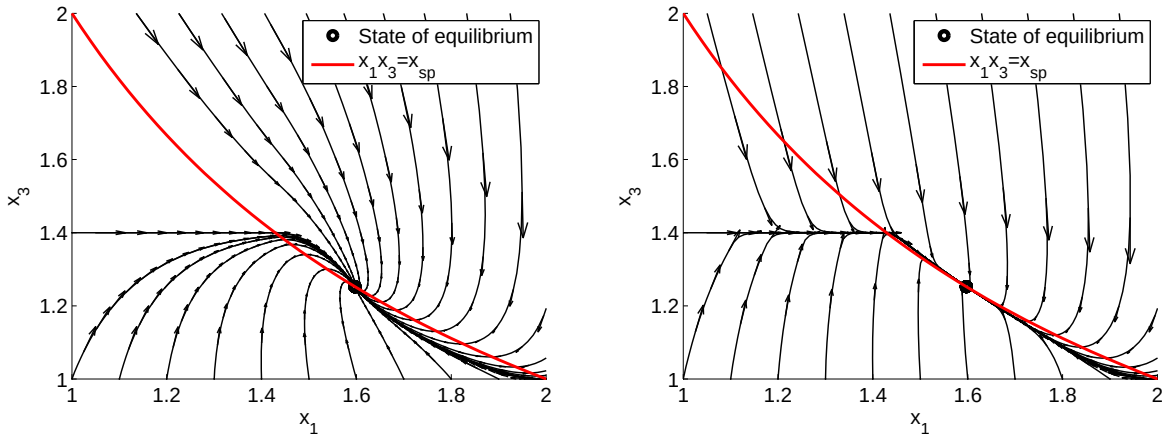

$\mu_p = 0$ $\mu_p = 0.1$

FIGURE 6.8. System trajectories when $x_{3,max}$ is taken into account.

The system trajectories are now shown on figure 6.8. The system is brought to the line $\mathcal{H}_{min}$ corresponding to $x_3 = \min\{x_{3,max}, \frac{x_{sp}}{x_1}\}$.

To prove that the closed loop strategy (6.15) maintains the system within the constraint $x_{3,max}$, we will define an invariant rectangle $\mathcal{R}$ as shown on figure 6.9. We first consider that the constraint $x_{4,max}$ is never active. We know that the unconstrained closed loop system consisting of (6.12) and (6.13) converges globally. We assume that the equilibrium point P_{eq} satisfies the constraint $x_{3,max}$. The strategy (6.15) is designed so that on $\mathcal{H}_{min}$ we have $\frac{dx_3}{dt} = \tilde{f}_2 = 0$. We know from above that $\frac{\partial \tilde{f}_2}{\partial x_3} < 0$ and $\frac{\partial \tilde{f}_2}{\partial x_1} < 0$. So $\tilde{f}_2 < 0$ above $\mathcal{H}_{min}$ and $\tilde{f}_2 > 0$ below $\mathcal{H}_{min}$. We start with a point $P_0(x_{1,0}, x_{3,0})$ so that $x_{1,0}x_{3,0} \leq x_{sp}$ and $x_{3,0} < x_{3,max}$. $\mathcal{R}$ is built in the following way :

- If $f_1(P_0) < 0$, we choose $P_1(x_{1,1}, x_{3,1})$ so that $x_{3,1} = x_{3,0}$ and $f_1(P_1) = 0$. We know that this point exists from figure 6.4. If $f_1(P_0) > 0$, then $x_{1,1} = x_{1,0}$ and $f_1(P_1) = 0$. If this point does not exist, then $x_{3,1} = 1$. We know that $f_2(P_1) > 0$.
- Point $P_2(x_{1,2}, x_{3,2})$ is defined so that $x_{1,2} = x_{1,1}$, and $\tilde{f}_2(P_2) = 0$. We know that this point exists because $\frac{\partial \tilde{f}_2}{\partial x_3} < 0$ and $f_2(x_{1,2}, x_{3,max}) \leq 0$. Since $\frac{\partial f_1}{\partial x_3} > 0$ then $f_1(P_2) > 0$.
- We choose $P_3(x_{1,3}, x_{3,3})$ so that $x_{3,3} = x_{3,2}$, and $f_1(P_3) = 0$. This point exists from figure 6.4. $f_2(P_3) < 0$ because $\frac{\partial \tilde{f}_2}{\partial x_1} < 0$.
- We choose $P_4(x_{1,4}, x_{3,4})$ so that $x_{1,4} = x_{1,3}$, and $\tilde{f}_2(P_4) = 0$. We know that this point exists on $\mathcal{H}$. $f_1(P_4) < 0$ because $\frac{\partial f_1}{\partial x_3} > 0$.

Now we need to close the space $\mathcal{R}$. There are two cases. The first case corresponds to $x_{3,4} < x_{3,1}$, then we choose another point P_1' so that $f_1(P_1') = 0$ and $x_{3,1}' = x_{3,4}$, and the corresponding P_2' on $\mathcal{H}_{min}$. Then the rectangle defined by the points P_1', P_2', P_3, P_4 is invariant because the field of vectors $(f_1, \tilde{f}_2)$ always points to the interior of $\mathcal{R}$ along its borders. Indeed, $f_1 \geq 0$ along $[P_1', P_2']$, $\tilde{f}_2 \leq 0$ along $[P_2', P_3]$, $f_1 \leq 0$ along $[P_3, P_4]$ and $\tilde{f}_2 \geq 0$ along $[P_4, P_1']$.

The second case corresponds to $x_{3,4} > x_{3,1}$. We choose P_1' so that $x_{1,1}' = x_{1,1}$ and $x_{3,1}' = x_{3,4}$. Similarly, the rectangle $\mathcal{R}$ is invariant.

In both cases, the rectangle $\mathcal{R}$ stays below the constraint $x_3 = x_{3,max}$. Therefore, we can conclude that any trajectory that starts from a point satisfying the constraint $x_{3,max}$ will satisfy the constraint at any time.

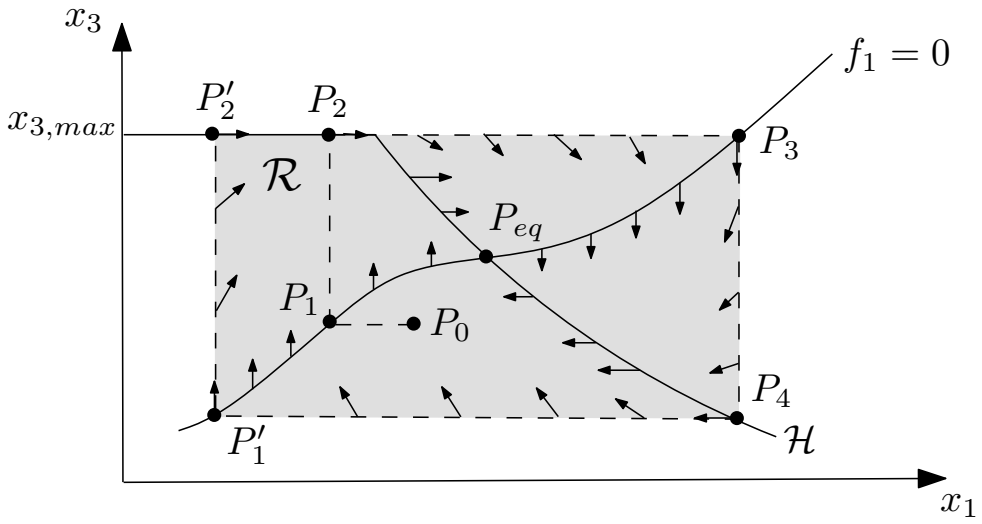

FIGURE 6.9. Invariant space $\mathcal{R}$

Of course this is not the case when the feedback strategy is more complex and contains one state (integral term for example), but this property can be used even when the feedback strategy is a PI controller. It is then sufficient to force the state of the PI to 0 when $x_3 = x_{3,max}$ and $x_1 x_3 < x_{sp}$. This might generate some bumps but ensures to stay below $x_{3,max}$.

Let's now consider the constraint $x_{4,max}$. It forces the command u to a minimum value. Since the function f_2 is decreasing with respect to u, then the proof made above is still valid on $[P_1', P_2']$, $[P_2', P_3]$, and $[P_3, P_4]$. The rectangle $\mathcal{R}$ is still invariant if the constraint $x_{4,max}$ is not valid on $[P_4, P_1']$, which is a reasonable assumption.

Both constraints are easily included into the strategy, showing the relevance of the choice of the control structure variables.

However, the control is not completely satisfying since $\mathcal{H}_{min}$ is a trajectory of the system only on the part where $x_3 = x_{3,max}$. On $\mathcal{H}$ we would prefer to ensure $\dfrac{d(x_1 x_3)}{dt} = 0$ rather than $\dfrac{dx_3}{dt} = 0$.

The feedforward is modified so that on $\mathcal{H}$ we have $\dfrac{dx_3}{dt} = -\dfrac{dx_1}{dt}\dfrac{x_3}{x_1}$. Only a slight modification is needed.

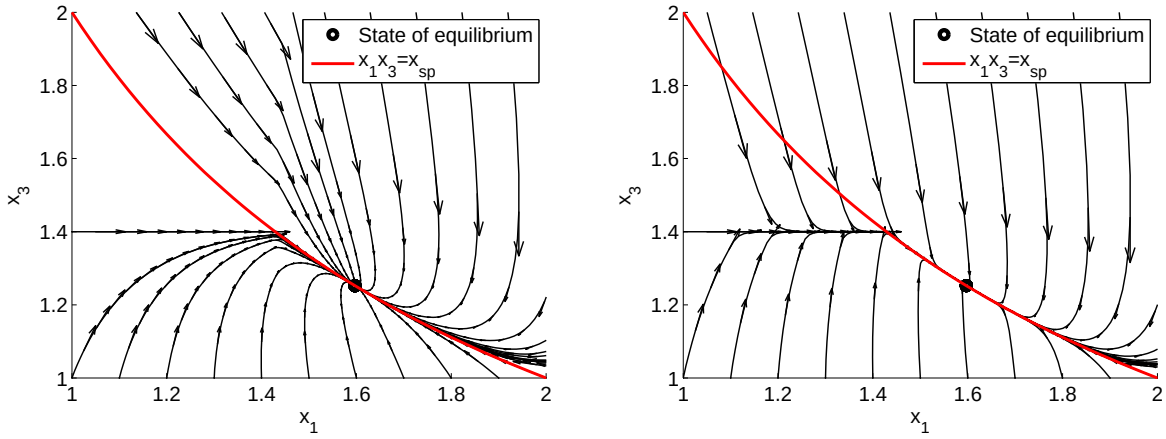

$\mu_p = 0$ $\mu_p = 0.1$

FIGURE 6.10. Trajectories with a control forcing the system on $\mathcal{H}_{min}$.

$$\begin{cases} x_{3,lim} &= \min\{x_{3,max}, \dfrac{x_{sp}}{\hat{x}_1}\} \\ x_{4,sp} &= \psi_t^{-1}\Big(\dfrac{1}{\alpha_5 \hat{x}_2}(\alpha_6 \hat{x}_1 \psi_c(x_{3,lim}) - \dfrac{\hat{x}_3}{\hat{x}_1}\dot{\hat{x}}_1)\Big) \\ u_{2,sp} &= \dfrac{x_{3,lim}\hat{x}_1 + \alpha_4 - \alpha_7 \hat{x}_2 \phi_{turb}(x_{4,sp})}{\alpha_7 \hat{x}_2 \phi_{wg}(x_{4,sp})} \\ g(x_1, x_3) &= \max\{u_{2,min}, u_{2,ff} - \mu_p(x_{3,lim} - \hat{x}_3)\} \end{cases} \tag{6.16}$$

Concerning the stability, we have :

$$\frac{\partial \tilde{f}_2}{\partial x_3} = \frac{\partial f_2}{\partial x_3} + \frac{\partial g}{\partial x_3}\frac{\partial f_2}{\partial u} = \frac{\partial f_2}{\partial x_3} + \mu_p \frac{\partial f_2}{\partial u} - \frac{x_3}{x_1}\frac{\partial f_1}{\partial x_3} - \frac{f_1}{x_1} < 0$$

So the trace of the jacobian matrix A_{cl} is strictly negative. Also :

$$\frac{\partial \tilde{f}_2}{\partial x_1} = \frac{\partial f_2}{\partial x_1} + \frac{\partial g}{\partial x_1}\frac{\partial f_2}{\partial u} = \frac{x_{sp}}{x_1^2}\Big(\frac{\partial f_2}{\partial x_3} + \mu_p \frac{\partial f_2}{\partial u}\Big) + \frac{x_3}{x_1^2}\Big(f_1 - x_1 \frac{\partial f_1}{\partial x_1}\Big)$$

This formulation does not give enough information to conclude. We need to compute the determinant of the jacobian matrix A_{cl} :

$$det(A_{cl}) = \overbrace{\frac{\partial f_1}{\partial x_1}\Big(\frac{\partial f_2}{\partial x_3} - \frac{f_1}{x_1}\Big)}^{\geq 0} - \overbrace{\frac{1}{x_1^2}\frac{\partial f_1}{\partial x_3}}^{\geq 0}(x_{sp}\frac{\partial f_2}{\partial x_3} + x_3 f_1) + \overbrace{\mu_p \frac{\partial f_2}{\partial u}\Big(\frac{\partial f_1}{\partial x_1} - \frac{x_{sp}}{x_1^2}\frac{\partial f_1}{\partial x_3}\Big)}^{\geq 0}$$

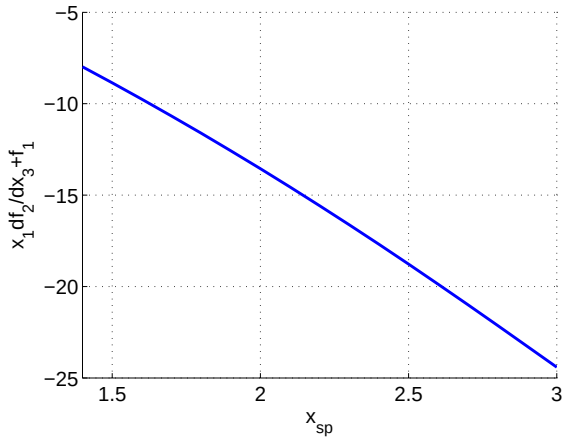

FIGURE 6.11. value of $x_1 \dfrac{\partial f_2}{\partial x_3} + f_1$ as a function of x_{sp}.

There is a condition on the value of μ_p to ensure the stability of the equilibrium state. If $\mu_p = 0$ the stability about the equilibrium state depends on the sign of $x_{sp}\dfrac{\partial f_2}{\partial x_3} + x_3 f_1$. Since the equilibrium corresponds to $x_{sp} = x_1 x_3$, this sign depends on the difference between $\dfrac{\partial f_2}{\partial x_3}$ and $-\dfrac{f_1}{x_1}$. This is consistent with the difference between the dynamics of the open loop system and that brought by the dynamic feedforward on $\dfrac{dx_3}{dt}$. This condition means that the feedforward term should not affect the stability of the HP turbocharger. It can be checked on figure 6.11 that this value is negative at all equilibrium points. Therefore $det(A_{cl}) \geq 0$ at the equilibrium. The system is stable.

The system trajectories illustrate on figure 6.10 the effect of this modification. The line $\mathcal{H}_{min}$ is now a trajectory of the system.

The constraint $x_{3,max}$ is still respected. We can build the same rectangle $\mathcal{R}$ as before. The term $-f_1 \frac{x_3}{x_1}$ has been added on $\tilde{f}_2$. Since $f_1 \geq 0$ along $[P_1', P_2']$ and $[P_2', P_3]$, and $f_1 \leq 0$ along $[P_3, P_4]$ and $[P_4, P_1']$, the proof is trivial.

6.4.4. Conclusion on the control of the system. — We have discussed in this section the properties of the system and the control issues. We have designed a control strategy that tracks the intake manifold pressure to its setpoint while satisfying the constraints on the HP turbocharger speed. This control strategy consists of the dynamic inversion of the

system and a proportional controller. The controlled system is stable and converges to a unique state of equilibrium for any positive proportional gain.

In reality this strategy is not accurate because of modeling errors. We therefore need to add an integral term to the strategy. The constraint on HP turbocharger speed will still be satisfied if the integral term is set to 0 when the constraint is active.

The control structure proposed is different than that used as reference for single stage turbocharger control in section 6.2. Therefore the control strategy is slightly modified in order to reflect the cascade structure. These modifications do not affect the properties of the closed loop system analyzed above.

We now give the control laws that have been implemented. In the next section we will compare in simulation and experimentally two different strategies.

Strategy 1 *: application of the single stage controller to HP stage.* — This strategy is the copy of the single stage turbocharger strategy, but with a feedforward part consistent with the suggestions made for two stage systems.

The closed loop strategy becomes :

$$\left\{\begin{array}{rcl} e_1 &=& x_{3,lim} - \hat{x}_3 \\ \dot{z_1} &=& e_1 \\ x_{4,cl} &=& c_1(e_1, z_1) \\ x_{4,sp} &=& \min\{x_{4,max}, x_{4,cl} + x_{4,ff}\} \\ e_2 &=& x_{4,sp} - x_4 \\ \dot{z_2} &=& e_2 \\ u_{2,cl} &=& c_2(e_2, z_2) \\ u_2 &=& \max\{u_{2,min}, u_{2,cl} + u_{2,ff}\} \end{array}\right. \tag{6.17}$$

With the feedforward strategy corresponding to the steady state of HP turbocharger :

$$\left\{\begin{array}{rcl} x_{4,ff} &=& \psi_t^{-1}\big(\frac{\alpha_6 \hat{x_1}}{\alpha_5 \hat{x_2}} \psi_c(x_{3,sp})\big) \\ u_{2,ff} &=& \dfrac{x_{3,sp}\hat{x_1} + \alpha_4 - \alpha_7 \hat{x_2} \phi_{turb}(x_{4,ff})}{\alpha_7 \hat{x_2} \phi_{wg}(x_{4,sp})} \end{array}\right. \tag{6.18}$$

Strategy 2 *: simplified feedback.* — The cascaded structure of strategy 1 is complex and thus difficult to tune. Also, it requires two specific sensors. The objective of strategy 2 is to evaluate how the exhaust manifold pressure sensor can be removed and the impact on the system performances.

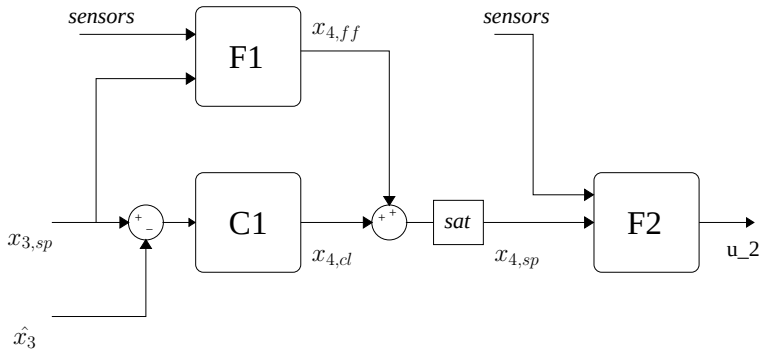

FIGURE 6.12. Strategy 2

It is shown in figure 6.12. We keep the same feed forward structure as for strategy 1 and the linear controller $C1$. The second step of the cascade controller is changed. The feedback $C2$ is removed, but we keep the inversion of the actuator $F2$. Compared to the strategy shown in figure 6.1, this structure is easier to calibrate because there is only one controller. The non linearities of the system are taken into account in the feed forward part $F1$ of the strategy and in the actuator inversion $F2$.

We keep the same feedforward strategy but contrary to (6.17), we have the feedback :

$$\begin{cases} e_1 &= x_{3,lim} - \hat{x}_3 \\ \dot{z_1} &= e_1 \\ x_{4,cl} &= c_1(e_1, z_1) \\ x_{4,sp} &= \min\{x_{4,max}, x_{4,cl} + x_{4,ff}\} \\ u_2 &= u_{2,ff} \end{cases} \tag{6.19}$$

The constraint $P_{exh,max}$ is taken into account in $x_{4,max}$. This strategy is very similar to (6.15), except the output of the controller has changed.

6.5. Simulation and experimental results

In this section, we first check the efficiency of the strategy in simulation. Then we compare the cascaded controller (6.17) (called 1) with the simplified (6.19) (called 2).

6.5.1. Simulation results. — Figure 6.13 shows validation results obtained in simulation. The strategy 1 described above is compared to a strategy which does not take into account the turbocharger speed limitation. The LP estimator is validated by the bottom

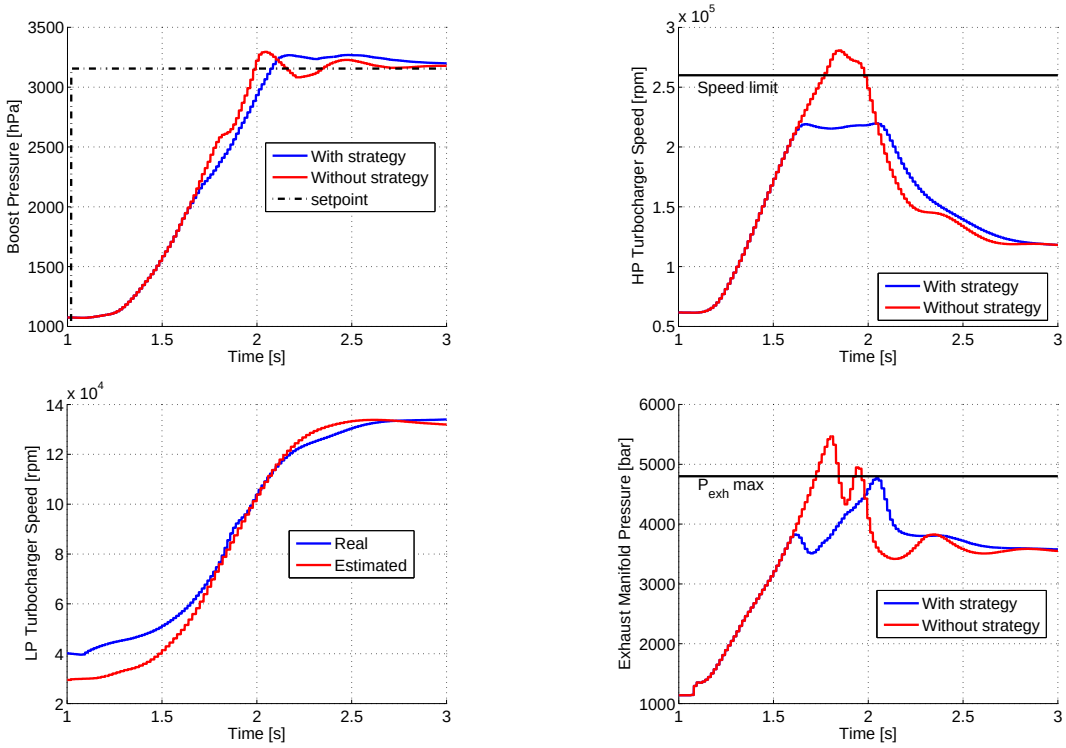

FIGURE 6.13. Comparison between boost pressure with and without the HP speed limitation strategy

left graph which shows real and estimated LP turbocharger speed. The effectiveness of the HP turbocharger speed limitation strategy is illustrated by the other figures. The control manages to maintain the HP turbocharger speed to a high value in order to use the capacity of the system, but below the limit. The impact on the boost pressure dynamics is minor.

6.5.2. Experimental results. —

6.5.2.1. Performances. — Both strategies have been integrated in a rapid prototyping system and tested on a vehicle. Controllers c_1 and c_2 are linear PI controllers, where the integral term is reinitialized if the maximum turbocharger speed constraint is hit and if the error is outside a 0 centered window defined by : $|P_{man,sp} - P_{man}| < P_{max}$. Figure 6.14 shows results obtained with the two strategies during load transients starting from a low

engine speed in third gear. For both of them, an analysis of the maneuver shows several phases :

1. The actuators are commanded to their maximum values in order to reach the maximum dynamics of the system.
2. The HP turbocharger speed and the exhaust manifold pressure are limited. The HP wastegate is open before reaching the boost pressure setpoint in order to maintain the system in safe operating conditions.
3. The boost pressure reaches its setpoint and is controlled to this value. The engine intake manifold is constant, but the HP wastegate command continues to vary because the HP turbocharger is still in transient.
4. When HP compression ratio reaches 1, the transition between HP and BP turbocharger occurs. The boost pressure is then controlled by the LP wastegate and the system behaves as a single stage turbocharger.

No major difference in terms of performance can be seen between the two strategies. The dynamics in boost pressure and turbocharger speeds are very close.

However, the transition between HP and LP operating modes is very different. The boost pressure is well controlled with strategy 2 whereas a big excursion can be observed with strategy 1. This is linked with the initialization of the cascaded structure of strategy 1 and the use of the exhaust pressure measurement. When the transition occurs, the exhaust pressure is high because it corresponds to the two expansion stages, this generates an important error at the input of controller c_2 which impacts the LP wastegate command. The pressure then decreases naturally and stabilizes at values corresponding to a single stage expansion. It is possible to smoothen this transition problem by, for example, filtering the setpoint, but this would increase the calibration effort necessary for structure 1. These problems are not seen for structure 2 because c_1 is not affected during the transition.

6.5.2.2. Robustness. — Since structure 2 inverses an actuator model to take account of the exhaust pressure limitation, it is less robust with respect to actuator dispersions than structure 1 which uses a measurement. If the actuator dispersion is assumed to be an offset on the wastegate command, it is possible to compensate for this effect by tuning safely the controller so that the exhaust pressure constraint is not violated in the worst case. This tuning is called "robust" tuning. Vehicle tests have been performed in order to evaluate the impact of this tuning on the performance of the nominal system. Figure 6.15 presents the results and compares the dynamics of the system with nominal and robust tuning. This difference is representative of the difference between the two strategy structures tested

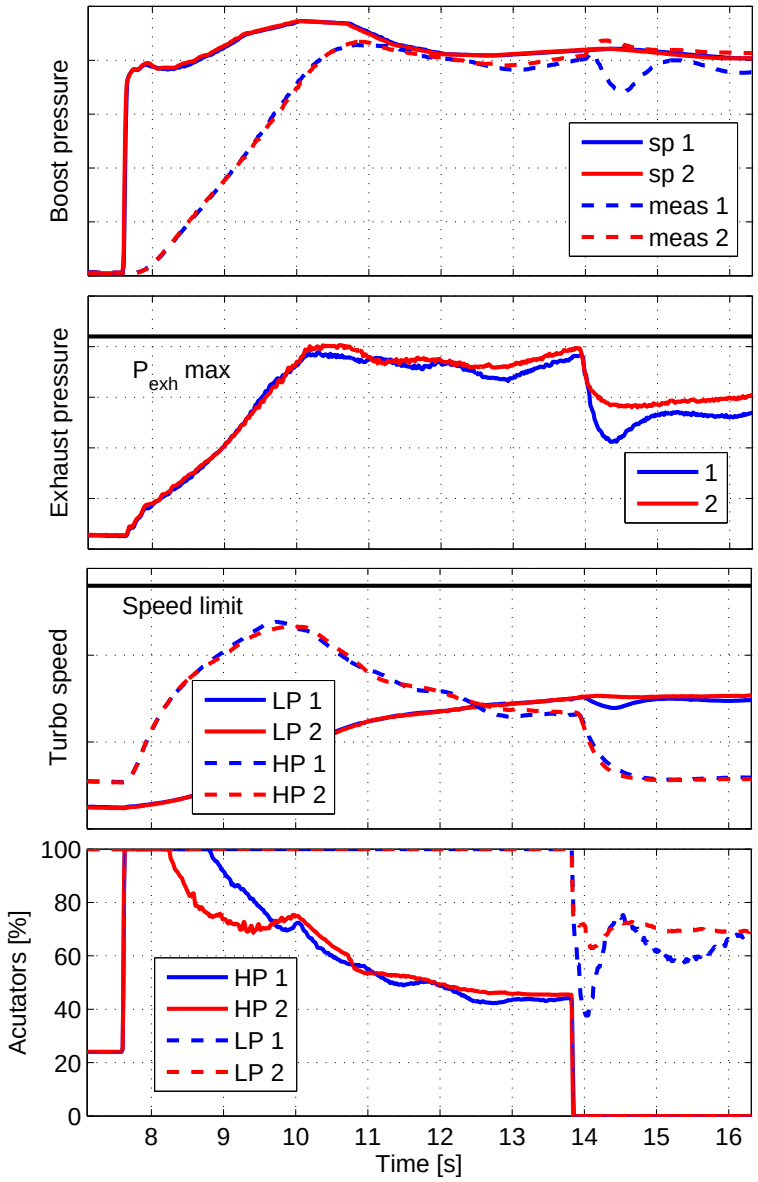

FIGURE 6.14. Comparison between strategies 1 and 2

in this section. The experimental results show that the boost pressure dynamics are not changed by the robust tuning, but that the boost pressure stabilizes at a lower value. In

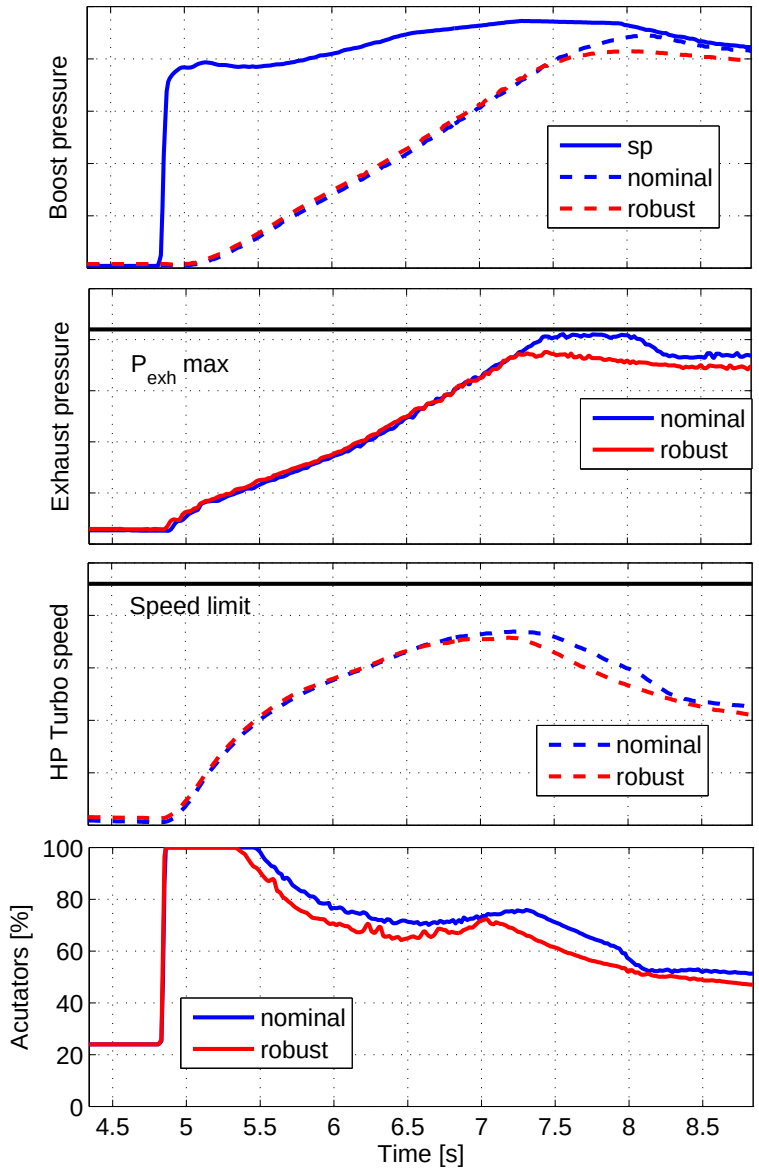

FIGURE 6.15. Comparison between nominal tuning and robust tuning

this case the setpoint cannot be reached because the constraint on the exhaust manifold pressure is active in steady state at the end of the test.

Finally, the following remarks are the main conclusions for this section :

– The nominal dynamic performances of the two strategies are similar.
– Because of robustness issues, the tuning of structure 2 has to take into account a safety margin which results in small steady state errors.
– The calibration effort is lower for structure 2, because the structure is more simple and because the transition between HP and LP mode is better managed.

The experimental tests show good results. However, some problems remain open and existing control techniques could help improve various aspects. In particular the following points could be investigated :

– Controllers c_1 and c_2 could be better adapted to nonlinear systems.
– The transition problem with structure 1
– The inversion of model $F2$ and the static error obtained with structure 2 and the "robust" tuning

6.6. Conclusion

This chapter discusses the specific issues of two stage turbochargers control, proposes different control structures, analyses their differences and shows an experimental comparison. These structures are based on a SISO strategy similar to that used for single stage turbochargers. A LP stage estimator provides the pressures and temperatures between the turbochargers necessary when operating in HP mode, particularly for the HP speed limitation. It is shown that the exhaust pressure sensor is not required to control the system but improves the robustness.

The approach presented in this paper is based on a reduced model of turbochargers which was first proposed in chapter 4 for single stage turbochargers on a gasoline engine. It is extended here for two stage turbochargers on a Diesel engine. The level of representation chosen is well adapted. It offers a useful basis for studying the control issues specific to the system, and it can be included both in the feed forward part of the control strategy and in the estimation of the LP turbocharger. It is therefore believed that the same kind of approach will be relevant for other turbocharging technologies such as electrical or mechanical compressor or variable geometry compressor.

Appendix

The functions used for system (6.1) are :

$$\begin{cases} \phi_{turb}(\Pi) \triangleq S_t \dfrac{\Pi^{\frac{3}{2}}}{\sqrt{R}} \sqrt{\dfrac{2\gamma}{\gamma-1}\left(\Pi^{\frac{-2}{\gamma}} - \Pi^{\frac{-\gamma-1}{\gamma}}\right)} \\ \psi_t(\Pi) \triangleq (1 - \Pi^{\frac{1-\gamma}{\gamma}})\phi_{turb}(\Pi) \\ \psi_c(\Pi) \triangleq \Pi(\Pi^{\frac{\gamma-1}{\gamma}} - 1) \\ \phi_{wg}(\Pi) \triangleq S_{wg} \dfrac{\Pi}{\sqrt{R}} \sqrt{\dfrac{2\gamma}{\gamma-1}\left(\Pi^{\frac{-2}{\gamma}} - \Pi^{\frac{-\gamma-1}{\gamma}}\right)} \end{cases} \tag{6.20}$$

The variables for modeling single stage turbochargers or the LP stage are :

$$\begin{cases} \alpha_1 \triangleq c_p \sqrt{T_{ut}} \eta_t P_{dt} \dfrac{2}{J_t a} \\ \alpha_2 \triangleq \eta_v \dfrac{P_{uc} V_{cyl}}{120 R T_{man}} N_e c_p T_{uc} \dfrac{1}{\eta_c} \dfrac{2}{J_t a} \\ \alpha_3 \triangleq \dfrac{120 R T_{man} P_{dt}}{\sqrt{T_{ut}} N_e V_{cyl} P_{uc} \eta_{vol}} \\ \alpha_4 \triangleq \dfrac{D_f 120 R T_{man}}{N_e V_{cyl} \eta_{vol} P_{uc}} \end{cases} \tag{6.21}$$

The variables for modeling the HP stage are :

$$\begin{cases} \alpha_5 \triangleq c_p \sqrt{T_{ut,2}} \eta_{t,2} P_{dt,1} \dfrac{2}{J_{t,2} a_2} \\ \alpha_6 \triangleq \eta_v \dfrac{P_{uc,1} V_{cyl}}{120 R T_{man}} N_e c_p T_{uc,2} \dfrac{1}{\eta_{c,2}} \dfrac{2}{J_{t,2} a_2} \\ \alpha_7 \triangleq \dfrac{120 R T_{man} P_{dt,1}}{\sqrt{T_{ut,2}} N_e V_{cyl} P_{uc} \eta_{vol}} \end{cases} \tag{6.22}$$

The variables used in the LP estimator are :

$$\begin{cases} \beta_2 \triangleq D_{air} c_p T_{uc,1} \dfrac{1}{\eta_{c,1}} \dfrac{2}{J_{t,1} a_1} \\ \beta_3 \triangleq \dfrac{(D_{air} + D_f)\sqrt{T_{ut,1}}}{P_{dt,1}} \end{cases} \tag{6.23}$$

GENERAL CONCLUSION

This thesis describes the development of turbochargers control strategies based on a reduced physical model of the system. It studies three different architectures :

- Gasoline engines with fixed geometry turbines
- Diesel engines with variable geometry turbocharger and two exhaust gas recirculation loops
- Diesel engines with two stage turbochargers

For each case study we propose similar solutions but the specificities of each case are taken into account. The first case is the most simple, the system is first order and single input single output (SISO) but constraints on the actuator must be taken into account. The control strategy is based on feedback linearization and constrained motion planning. For the second case, the dynamics of the EGR systems are neglected, but the turbocharger trajectory is modified to ensure that the EGR setpoint can be satisfied. The third case is second order, the analysis of the closed loop system trajectories in the phase plan leads to the proposition of a simple control law that ensures a rapid tracking of the setpoint while satisfying a constraint on one of the system states.

The control strategies are thus based on a reduced physical model of turbochargers that is adapted to each case study with simple modifications. This model takes account of the interactions between the considered system and the surrounding components or environment, thus decoupling the dynamics of the different subsystems. We design simple nonlinear control strategies which take advantage both of the steady state and the dynamics part of the model.

This approach offers the possibility to prove properties of the closed loop system with the reduced model, such as convergence, stability and constraints satisfaction. The relevance of the strategy is then demonstrated experimentally on the real system, thus justifying a posteriori the assumptions used to reduce the model.

The application of similar models to three different architectures shows that the chosen representation is generic, and that the level of details is relevant. Therefore, the developments proposed in this document offer a useful basis for the consideration of future complex air systems.

We answer to the main requirements of air systems control issues :
– A generic solution that can be adapted to various systems architectures
– A limited calibration effort
– Good transient performances
– Decoupling of the different subsystems

Perspectives

Future air systems. — Other air systems are investigated in the industry, consisting of complex architectures with turbochargers sometimes associated with other supercharging devices (see a review of dual stage turbocharging systems in [**62**]; pressure wave superchargers are studied in [**84**]). Also, EGR is introduced at high load on gasoline engines. This changes the control problem considered in chapter 5 because in this case the combustion is stoichiometric and therefore the EGR affects directly the torque production. However, the developments presented in this thesis are flexible enough to be adapted easily to these new architectures because they are based on the description of the interactions between the different subsystems and their decoupling.

Electrified powertrains. — The hybridization of powertrains may also lead to the introduction of electric systems in air systems. Power assist turbochargers or turbo compound systems are investigated respectively in [**56**] and [**22**]. These systems will require the development of new control strategies. Since the strategies developed in this thesis allow to take into account the interactions with other components, they can be adapted easily to this new context.

Moreover, the control issues for air systems may change in an hybrid context because the torque request from the internal combustion engine is less important if an electric engine can provide some additional power. In this case, the trajectory computed in the different examples studied in this thesis can also be used for the supervisory control of electric and combustion engines. Indeed, the trajectory computed in chapter 4 is representative of the maximum torque that can be produced by the internal combustion engine. That of chapter 5 is representative of a pollution constraint. In both cases these constraints can be transformed into a torque constraint for the internal combustion engine and therefore into an additional torque request for the electric engine.

Diagnostic. — Diagnostic is also becoming a crucial issue for these complex systems. Model based diagnostic seems appropriate, and the model reductions made for designing control strategies and computing trajectories can be used to diagnose the systems. First results have been published concerning the estimation of leakage at the intake of a Diesel engine with VGT and HP EGR in [**24, 23**]. An extension of the works presented in this thesis to the estimation of turbocharger efficiency for diagnostic purposes will be published in [**25**]. In this paper a turbine efficiency observer is based on the same level of modeling as used in chapter 5. A sensitivity analysis of the observer allows to compute the impact of sensors or system dispersions on this estimation, and to design a threshold representative of the operating range of the system in normal conditions. A fault is detected if the estimated efficiency is lower than this threshold.

APPENDIX A

GAS EXCHANGES MODELING

In the more general case, we consider that the air path of the engine consists in a succession of restrictions and receivers (or volumes) containing different gas species (in our case, we consider generally three species : fresh air, burned gas and fuel). The restriction determine the energy and mass flows between the receivers, and each receiver is described by state variables : temperature and the different gas masses. This modeling structure is widely used for the design of simulation libraries. It is very useful for the description of the interactions between the components, and it can also be adapted for model based control structures as is shown in this thesis.

A.1. Receivers and manifolds

A.1.1. General case. — The mixtures of gas in receivers are modeled using fundamental thermodynamics principles : ideal gas law, mass and energy conservation. If we note M_i the mass of each gas, P the pressure, T the temperature, and if we assume that the volume V of the receiver is constant, the evolution of the thermodynamics conditions in a receiver is described by the following equations :

$$\begin{cases} \dfrac{dM_i}{dt} &= \Sigma_j D_{i,j} \\ PV &= \Sigma_i (M_i R_i) T \\ \dfrac{dE}{dt} &= Q + \Sigma_j D_{i,j} h_i \\ E &= \Sigma_i M_i C_{v,i} T \end{cases} \tag{A.1}$$

The composition of each gas species is given by $F_i = \frac{M_i}{\Sigma M_i}$ These equations are the basis of all the representations used in this document. However, it is difficult to manipulate them in this form. The number of states is equal to the number of gas species considered, plus the energy. The number of inputs depends on the number of ports. These equations must and can be simplified, for two reasons : either the system is less complex than the general case, or some aspects can be neglected because of the specificity of the component considered. The main simplifications are the following :

1. The dependence on temperature of the thermodynamics coefficients $C_{p,i}$, $C_{v,i}$ and R_i is neglected, because the temperature variations of the component considered are small.
2. The coefficients R_i are equal to R, independent of the gas species.
3. Isothermal assumption : the temperature dynamics are neglected because they are considered much slower than other dynamics (concentration or pressure)
4. Adiabatic assumption : the external heat flow Q is neglected
5. Only one gas species is considered, for example fresh air in the intake part (no exhaust gas recirculation), or burned gas in the exhaust part (at stoichiometry in gasoline engines). In this case we consider mean values for the thermodynamics coefficients.

Heat exchangers are considered as the addition of a volume and a pressure drop, represented as described below. In this volume, the energy conservation of system A.1 is valid. The computation of the heat exchange Q with an external medium (usually air or water) depends on the technology used. The most simple representation consists in considering that it is proportional to the difference of temperature between the internal gas temperature and the medium temperature T_{ext}.

$$Q = \lambda(T_{ext} - T) \tag{A.2}$$

where λ is representative of the exchange efficiency.

A.1.2. Basic examples. — In this section we give basic examples of systems that can be considered in the control issues exposed further, and give the corresponding state equations. We present the assumptions that can be used for each specific case. Pressure and temperature are chosen as state variables because it is usually possible to measure these variables. In the case with several gas species, the mass fraction is the state variable because it is more relevant for the combustion than the mass of each species. This referential is therefore adequate for designing observers for the systems.

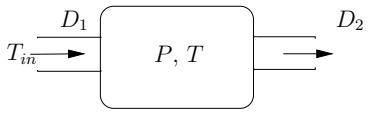

FIGURE A.1. Adiabatic manifold with two ports and one gas species

Manifold with two ports and one gas species - isothermal case. — This is the most simple case. It corresponds, for example, to the intake manifold with fresh air only or to the exhaust manifold with burned gas only. It is particularly valid when the variations of temperature are small, for example when there is a heat exchanger upstream the system. Assumptions 1, 3 and 5 are made. System A.1 can be reformulated in order to express the dynamics in pressure, leading to the following state equation :

$$\left\{ \begin{array}{rcl} \dfrac{dP}{dt} & = & \dfrac{RT}{V}(D_1 - D_2) \end{array} \right. \tag{A.3}$$

Manifold with two ports and one gas species - adiabatic case. — This case is similar to the previous one, but is more detailed. It can be useful when the amplitude of variation of the gas temperature is high. Assumptions 1, 4 and 5 are made. System A.1 can be reformulated in order to express the dynamics in pressure and temperature, leading to the following state equations :

$$\left\{ \begin{array}{rcl} \dfrac{dP}{dt} & = & \dfrac{\gamma R}{V}(D_1 T_1 - D_2 T) \\ \dfrac{dT}{dt} & = & \dfrac{RT}{PV}(D_1 \gamma T_1 - D_2 \gamma T + (D_2 - D_1)T) \end{array} \right. \tag{A.4}$$

Manifold with two ports and two gas species - isothermal case. — In this case we consider two gas species, for example fresh air and burned gas, as is usually the case in presence of exhaust gas recirculation. If heat exchangers filter the temperature variations, we can also assume that the mixture is isothermal. Assumptions 1, 2 and 3 are made. The composition is indeed generally more convenient when considering the combustion process. Eventually, we have :

$$\begin{cases} \dfrac{dP}{dt} &= \dfrac{RT}{V}(D_1 - D_2) \\ \dfrac{dF}{dt} &= \dfrac{RT}{PV}D_1(F_1 - F) \end{cases} \tag{A.5}$$

In this document the isothermal assumption is favored because we focus on turbochargers which are not affected by this assumption. A comparison between these two assumptions in the modeling of engines air systems is made in **[30, 46]**.

A.2. Restrictions and Valves

Most restrictions are represented using the standard equations of compressible gas flow through an orifice. This is usually the case for throttles and valves. We have :

$$D = S\phi(\Pi)\frac{P_u}{\sqrt{T_u}}$$

where S is the cross section of the orifice, Π is the maximum between $\dfrac{P_d}{P_u}$ (normal conditions) and $\Pi_{crit} = (\dfrac{2}{\gamma+1})^{\frac{\gamma}{\gamma-1}}$ (critical or choke conditions), and

$$\phi(\Pi) = \sqrt{\frac{2\gamma}{R(\gamma-1)}\left(\Pi^{\frac{2}{\gamma}} - \Pi^{\frac{\gamma+1}{\gamma}}\right)} \tag{A.6}$$

Function ϕ is shown in figure A.2. From a control point of view, this function is very important because it describes flows through actuators, and thus usually the effect of the control action available on air systems. In particular, the form of function ϕ when the pressure ratio across a valve is close to one has to be noticed. There is a vertical tangent at $\Pi = 1$, meaning that when two volumes are connected with this function the dynamics are very fast. This can lead to numerical instabilities. Also, the pressure ocillations generated in all the air system by the engine breathing means that a model which considers average values over an engine cycle is inaccurate in this zone. The strong non linearity in this function complexifies a lot the air systems control issues.

Other components, like air filters, particulate filters or heat exchangers generate a pressure drop but cannot be represented with this equation. In this case we consider that the gas is incompressible, and the pressure drop is related to the gas mass flow and its

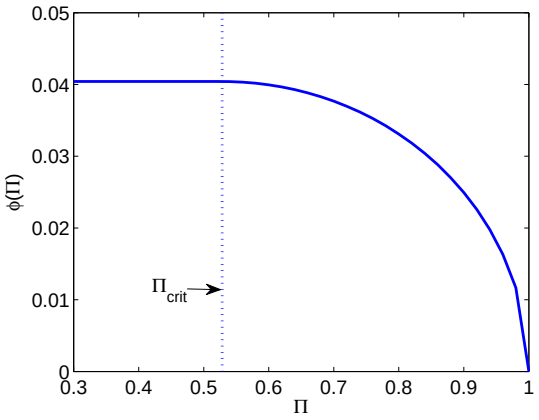

FIGURE A.2. Function ϕ describing the flow through a restriction as a function of pressure ratio

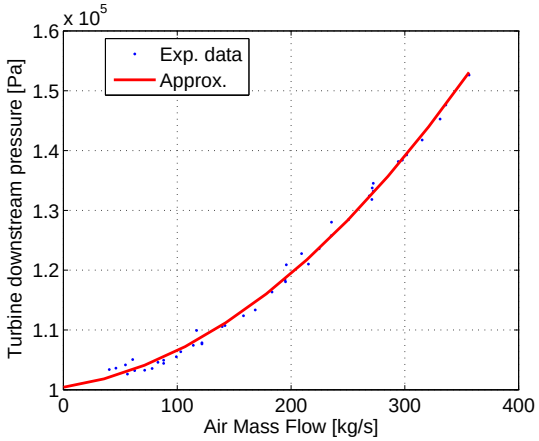

FIGURE A.3. Pressure drop across exhaust line on a gasoline, as a function of air mass flow. Comparison between experimental data and approximation made with a second order polynomial.

temperature. Usually this is represented via a table computed experimentally :

$$P_u - P_d = f(\sqrt{\frac{T_u}{P_u}}D) \tag{A.7}$$

For example, figure A.3 shows the pressure drop across the exhaust line of a gasoline engine, including a catalyst filter. The pressure downstream from turbine can be computed by a second order polynomial as a function of air mass flow.

PERSONAL PUBLICATIONS AND PATENTS

In this appendix we list the communications, articles and patents where most of the results described in the previous chapters have been published.

[1] A. Albrecht, G. Grondin, P. Moulin, and G. Corde, "Hcci diesel engine control design using advanced simulation with real time capabilities," *Oil & Gas Science and Technology - Rev. IFP*, vol. 63, pp. 535–551, 2008.

[2] A. Albrecht, O. Grondin, J. Schmitt, L. Malbec, B. Youssef, G. Font, P. Gautier, and P. Moulin, "Simulation support for control issues in the context of modern diesel air path systems," *Oil & Gas Science and Technology - Rev. IFP*, vol. 64, no. 3, p. 381, 2009.

[3] A. Albrecht, M. Marbaix, P. Moulin, A. Guinois, and L. Fontvieille, "Extensive use of simulation for two-stage turbocharger diesel engine control strategy development," in *Engine Process Simulation and Supercharging*, June 2007, berlin.

[4] A. Albrecht, P. Moulin, O. Grondin, and G. Corde, "Control design for hcci combustion engine based on virtual engine simulator: from control development to real-time calibration," in *Proc. of THIESEL Conference*, 2006.

[5] A. Chasse, P. Moulin, P. Gautier, A. Albrecht, L. Fontvieille, A. Guinois, and L. Doléac, "Double stage turbocharger control strategies development," *SAE Int. J. Engines*, vol. 1, no. 2008-01-0988, pp. 636–646, 2008.

[6] J. Chauvin, O. Grondin, and P. Moulin, "Control oriented model of a variable geometry turbocharger in an engine with two egr loops," in *Proc. of the ECOSM conference*, 2009.

[7] P. Gautier, A. Albrecht, A. Chasse, P. Moulin, A. Pagot, L. Fontvieille, and D. Issartel, "A simulation study of the impact of lp egr on a two-stage turbocharged diesel engine," *Oil & Gas Science and Technology - Rev. IFP*, vol. 64, no. 3, p. 361, 2009.

[8] P. Gautier, A. Albrecht, P. Moulin, A. Chasse, L. Fontvieille, A. Guinois, and L. Doléac, "A new simulation step towards virtual bench through the challenging case of two stage turbocharger diesel engine control design," in *Proc. of the SAE conference*, no. 2008-01-0355, 2008.

[9] O. Grondin, P. Moulin, and J. Chauvin, "Control of a turbocharger diesel engine fitted with high pressure and low pressure exhaust gas recirculation systems," in *Proc. of the CDC conference*, 2009, pp. 6582–6589.

[10] A. Guinois, L. Fontvieille, P. Moulin, and A. Saab, "Système de régulation de la pression de suralimentation pour moteur à combustion interne à deux turbocompresseurs étagés," French Patent FR2 917 128, 2008.

[11] P. Moulin and J. Chauvin, "Analysis and control of the air system of a turbocharged gasoline engine," in *Proc. of the 47th IEEE Conference on Decision and Control*, 2008, pp. 5643–5649.

[12] ——, "Modelling and control of the air system of a turbocharged gasoline engine," *Control Engineering Practice*, 2009, In Press.

[13] P. Moulin, J. Chauvin, and B. Youssef, "Modelling and control of the air system of a turbocharged gasoline engine," in *Proc. of IFAC World Congress*, 2008, pp. 8487–8494.

[14] P. Moulin, O. Grondin, and J. Chauvin, "Impact of egr on turbocharger control on a diesel engine with two egr loops," in *Proc. of the IFAC Symposium Advances in Automotive Control*, 2010, Submitted.

[15] P. Moulin, O. Grondin, and L. Fontvieille, "Control of a two stage tubocharger on a diesel engine," in *Proc. of the CDC conference*, 2009, pp. 5200–5206.

[16] F. Perez and P. Moulin, "Road load simulation on an engine test bench," in *Proc. of SIA Diesel Engine International Conference*, 2008.

[17] B. Youssef and P. Moulin, "Method for controlling a turbocharger with the help of a physical model of the turbocharger's load," French Patent FR2 921 691, 2009.

[18] B. Youssef, P. Moulin, and O. Grondin, "Model based control of turbochargers: Application to a diesel hcci engine," in *Proc. of the IEEE International Conference on Control Applications*, 2007, pp. 1100–1105.

BIBLIOGRAPHY

[19] M. Ammann, N. Fekete, L. Guzzella, and A. Glattfelder, "Model-based control of the vgt and egr in a turbocharged common-rail diesel engine : Theory and passenger car implementation," in *Proc. of the SAE conference*, no. 2003-01-0357, 2003.

[20] A. A. Andronov, A. A. Vitt, and S. E. Khaikin, *Theory of Oscillators*. Dover Publications, 1987.

[21] J. Arnold, N. Langlois, and H. Chafouk, "Fuzzy controller of the air system of a diesel engine : Real-time simulation," *European Journal of Operational Research*, vol. 193, pp. 282–288, 2009.

[22] C. Brockbank, "Application of a variable drive to supercharger & turbo compounder applications," in *Proc. of the SAE conference*, no. 2009-01-1465, 2009.

[23] R. Ceccarelli, C. Canudas-de Wit, P. Moulin, and A. Sciarretta, "Model-based adaptive observers for intake leakage detection in diesel engines," in *Proc. of the American Control Conference*, 2009.

[24] R. Ceccarelli, P. Moulin, and C. Canudas-de Wit, "Robust strategy for intake leakage detection in diesel engines," in *Proc. of the Conference on Control Applications*, 2009.

[25] ——, "Turbine efficiency estimation for fault detection application," in *Proc. of the SAE conference*, 2010 (Submitted).

[26] J. Chauvin, "Estimation et contrôle d'un moteur diesel hcci. estimation des systèmes périodiques," Ph.D. dissertation, Ecole Nationale Supérieure des Mines de Paris, 2006.

[27] J. Chauvin, G. Corde, N. Petit, and P. Rouchon, "Experimental motion planning in airpath control for hcci engine," in *Proc. of the American Control Conference*, 2006, pp. 1874–1879.

[28] ——, "Motion planning for experimental airpath control of a diesel homogeneous charge-compression ignition engine," *Control Engineering Practice*, vol. 16, pp. 1081–1091, 2008.

[29] J. Chauvin, G. Corde, C. Vigild, N. Petit, and P. Rouchon, "Air path estimation on diesel hcci engine," in *Proc. of the SAE conference*, no. 2006-01-1085, 2006.

[30] A. Chevalier, M. Müller, and E. Hendricks, "On the validity of mean value engine models during transient operation," in *Proc. of the SAE conference*, no. 2000-01-1261, 2000.

[31] R. Christmann, H.-P. Schmalzl, F. Schmitt, and A. Schwarz, "Regulated 2-stage turbocharging," *MTZ Worldwide edition*, vol. 66, no. 1, 2005.

[32] G. Colin, Y. Chamaillard, G. Bloch, and A. Charlet, "Exact and linearized neural predictive control: A turbocharged SI engine example," *Journal of Dynamic Systems Measurement and Control*, vol. 129, no. 4, pp. 527–533, 2007.

[33] G. Colin, Y. Chamaillard, G. Bloch, and G. Corde, "Neural control of fast nonlinear systems application to a turbocharger SI engine with VCT," *IEEE Transactions on Neural Networks*, vol. 18, no. 4, pp. 1101–1114, 2007.

[34] L. Daubler, C. Bessai, and O. Predelli, "Tuning strategies for online-adaptive PI controllers," *Oil & Gas Science and Technology - Rev. IFP*, vol. 62, no. 4, pp. 493–500, 2007.

[35] L. Eriksson, "Mean value models for exhaust system temperatures," in *Proc. of the SAE conference*, no. 2002-01-0374, 2002.

[36] L. Eriksson, L. Nielsen, J. Brugard, J. Bergstrom, F. Petterson, and P. Andersson, "Modeling of a turbocharged si engine," *Annual Reviews in Control*, vol. 26, pp. 129–137, 2002.

[37] L. Eriksson, "Modeling and control of turbocharged SI and DI engines," *Oil & Gas Science and Technology - Rev. IFP*, vol. 62, no. 4, pp. 523–538, 2007.

[38] M. Fliess, J. Levine, P. Martin, and P. Rouchon, "Flatness and defect of nonlinear systems : Introductory theory and examples," *International Journal of Control*, vol. 61, no. 6, pp. 1327–1361, 1995.

[39] S. Frei, L. Guzzella, and C. Onder, "Improved dynamic performance of turbocharged si engine vehicles due to clutch actuation," in *Proc. of the IFAC Symposium on Advances in Automotive Control*, 2004.

[40] S. A. Frei, L. Guzzella, C. H. Onder, and C. Nizzola, "Improved dynamic performance of turbocharged si engine power trains using clutch actuation," *Control Engineering Practice*, vol. 14, no. 4, pp. 363 – 373, 2006.

[41] J. Galindo, H. Climent, C. Guardiola, and J. Domenech, "Modeling the vacuum circuit of a pneumatic valve system," *Journal of Dynamic Systems, Measurement, and Control*, vol. 131, no. 031011, 2009.

[42] V. Gheorghiu, D. Ueberschär, V. Müller, and R. Christmann, "Model of a supercharged diesel engine with high and low pressure egr as part of an nmpc for ecu implementation," in *Proc. of the SAE conference*, no. 2007-24-0084, 2007.

[43] L. Guzzella and A. Amstutz, "Control of diesel engines," *Control Systems Magazine, IEEE*, vol. 18, pp. 53–71, 1998.

[44] L. Guzzella and C. Onder, *Introduction To Modelling And Control Of Internal Combustion Engine Systems*. Springer Verlag, 2004.

[45] L. Guzzella, U. Wenger, and R. Martin, "Ic-engine downsizing and pressure-wave supercharging for fuel economy," in *Proc. of the SAE conference*, no. 2000-01-1019, 2000.

[46] E. Hendricks, "Isothermal vs. adiabatic si engine mean value engine models," in *Proc. of the IFAC workshop on Advances in Automotive Control*, 2001.

[47] J. Heywood, *Internal Combustion Engine Fundamentals*. McGraw-Hill, Inc, 1988.

[48] M. Jankovic, M. Jankovic, and I. Kolmanovsky, "Robust nonlinear controller for turbocharged diesel engines," in *Proc. of the American Control Conference*, 1998.

[49] J. Jensen, A. Kristensen, S. Sorensen, N. Houbak, and E. Hendricks, "Mean value modeling of a small turbocharged Diesel engine," in *Proc. of the SAE Conference*, no. 910070, 1991.

[50] M. Jung, "Mean-value modelling and robust control of the airpath of a turbocharged diesel engine," Ph.D. dissertation, University of Cambridge, 2003.

[51] M. Jung, R. Ford, K. Glover, N. Collings, U. Christen, and M. Watts, "Parameterization and transient validation of a variable geometry turbocharger for mean-value modeling at low and medium speed-load points," in *Proc. of the SAE Conference*, no. 2002-01-2729, 2002.

[52] M. Jung, K. Glover, and U. Christen, "Comparison of uncertainty parameterisations for h infinity robust control of turbocharged diesel engines," *Control Engineering Practice*, vol. 13, no. 1, pp. 15–25, 2005.

[53] A. Karnik, J. Buckland, and J. Freundenberg, "Electronic throttle and wastegate control for turbocharged gasoline engines," in *Proc. of the American Control Conference*, 2005, pp. 4434–4439.

[54] H. Khalil, *Nonlinear Systems*. Prentice-Hall, Inc., 1992.

[55] P. Kokotović, O. O'Reilly, and H. Khalil, *Singular Perturbation Methods in Control: Analysis and Design*. Soc. for Industrial & Applied Math, 1999.

[56] I. Kolmanovsky and A. Stefanopoulou, "Evaluation of turbocharger power assist system using optimal control techniques," in *Proc. of the SAE conference*, no. 2000-01-0519, 2000.

[57] I. Kolmanovsky, M. Van Nieuwstadt, and P. Moraal, "Optimal control of variable geometry turbocharged diesel engines with exhaust gas recirculation," in *Proc. of the ASME dynamic systems and control division IMECE conference*, 1999.

[58] T. Lake, J. Stokes, R. Murphy, R. Osborne, and A. Schamel, "Turbocharging concepts for downsized DI gasoline engines," in *Proc. of the SAE Conference*, no. 2004-01-0036, 2004.

[59] F. Le Berr, M. Miche, G. Colin, G. Le Solliec, and F. Lafossas, "Modelling of a turbocharged si engine with variable camshaft timing for engine control purposes," in *Proc. of the SAE conference*, no. 2006-01-3264, 2006.

[60] G. Le Solliec, F. Le Berr, G. Colin, and G. Corde, "Engine control of a downsized spark ignition engine: from simulation to vehicle," in *Proc. of ECOSM conference*, 2006.

[61] P. Leduc, B. Dunbar, A. Ranini, and G. Monnier, "Downsizing of gasoline engine: an efficient way to reduce CO_2 emissions," *Oil & Gas Science and Technology, special issue "Development and Control of Combustion Systems"*, vol. 58, no. 1, pp. 115–127, 2003.

[62] B. Lee, Z. Filipi, D. Assanis, and D. Jung, "Simulation-based assessment of various dual-stage turbocharging systems in terms of performance and fuel economy improvement," in *Proc. of the SAE conference*, no. 2009-01-1471, 2009.

[63] T. Leroy, J. Chauvin, and N. Petit, "Airpath Control of a SI Engine with Variable Valve Timing Actuators," in *Proc. of the American Control Conference*, 2008, pp. 2076–2083.

[64] ——, "Motion planning for experimental air path control of a variable-valve-timing spark ignition engine," *Control Engineering Practice*, vol. 17, pp. 1432–1439, 2009.

[65] T. Leroy, J. Chauvin, N. Petit, and M. Bitauld, "In-cylinder burned gas rate estimation and control on vva diesel engines," in *Proc. of the SAE conference*, no. 2009-01-0366, 2009.

[66] O. Leufven and L. Eriksson, "Time to surge concept and surge control for acceleration performance," in *Proc. of the IFAC World Congress*, 2008.

[67] P. Moraal and I. Kolmanovsky, "Turbocharger modeling for automotive control applications," in *Proc. of the SAE Conference*, no. 1999-01-0908, 1999.

[68] P. Moraal, I. Kolmanovsky, and M. Van Nieuwstadt, "Modeling and identification of a current to vacuum transducer and vnt actuator," in *Proc. of the IEEE/ASME international conference on Advanced Intelligent Mechatronics*, 1999.

[69] V. Mueller, R. Christmann, S. Muenz, and V. Gheorghiu, "System structure and controller concept for an advanced turbocharger / egr system for a turbocharged passenger car diesel engine," in *Proc. of the SAE conference*, no. 2005-01-3888, 2005.

[70] M. Muller, "Estimation and control of turbocharged engines," in *Proc. of the SAE Conference*, no. 2008-01-1013, 2008.

[71] P. Ortner and L. del Re, "Predictive control of a Diesel engine air path," *IEEE Transactions on Control Systems Technology*, vol. 15, no. 3, pp. 449–456, 2007.

[72] D. Petitjean, L. Bernardini, C. Middlemass, and S. Shahed, "Advanced gasoline engine turbocharging technology for fuel economy improvements," in *Proc. of the SAE Conference*, no. 2004-01-0988, 2004.

[73] A. Plianos and R. Stobart, "Modeling and control of diesel engines equipped with a two-stage turbo-system," in *Proc. of the SAE Conference*, no. 2008-01-1018, 2008.

[74] D. Schwarzmann, R. Nitsche, and J. Lunze, "Diesel boost pressure control using flatness-based internal model control," in *Proc. of the SAE Conference*, no. 2006-01-0855, 2006.

[75] ——, "Modelling of the air-system of a two-stage turbocharged passenger car diesel engine," in *Proc. of the 5th MATHMOD*, 2006.

[76] D. Schwarzmann, R. Nitsche, J. Lunze, and A. Schanz, "Pressure control of a two-stage turbocharged diesel engine using a novel nonlinear imc approach," in *Proc. of the IEEE International Conference on Control Applications*, 2006, pp. 1454–1459.

[77] D. Schwarzmann, R. Nitsche, J. Lunze, and M. Schmidt, "Nonlinear multivariable robust internal model control of a two-stage turbocharged diesel engine," in *Proc. of the IFAC Conference Advances in Automotive Control*, 2007.

[78] J. Shamma and M. Athans, "Guaranteed properties of gain scheduled control for linear parameter varying plants," *Automatica*, vol. 27, no. 3, pp. 559–564, 1991.

[79] Y. Shu and M. Van Nieuwstadt, "Two-stage turbocharger modeling for engine control and estimation," in *Proc. of the ASME International Mechanical Engineering Congress and Exposition*, 2007, pp. 243–252.

[80] J. Shutty, "Control strategy optimization for hybrid egr engines," in *Proc. of the SAE conference*, no. 2009-01-1451, 2009.

[81] J. Shutty, H. Benali, L. Daeubler, and M. Traver, "Air system control for advanced diesel engines," in *Proc. of the SAE conference*, no. 2007-01-0970, 2007.

[82] J.-J. Slotine and W. Li, *Applied nonlinear control*, I. Prentice-Hall, Ed., 1991.

[83] S. Sorenson, E. Hendricks, S. Magnusson, and A. Bertelsen, "Compact and accurate turbocharger modelling for engine control," in *Proc. of the SAE Conference*, no. 2005-01-1942, 2005.

[84] P. Spring, C. Onder, and L. Guzzella, "Egr control of pressure-wave supercharged ic engines," *Control Engineering Practice*, vol. 15, pp. 1520–1532, 2007.

[85] A. Stefanopoulou, I. Kolmanowsky, and J. Freudenberg, "Control of variable geometry turbocharged diesel engines for reduced emissions," *IEEE Transactions on Control Systems Technology*, vol. 8, no. 4, pp. 527–533, 2000.

[86] A. Teel and N. Kapoor, "Uniting local and global controllers," in *Proceedings of the European Control Conference*, 1997.

[87] A. Teel, L. Zaccarian, and J. Marcinkowski, "An anti-windup strategy for active vibration isolation systems," *Control Engineering Practice*, vol. 14, pp. 17–27, 2006.

[88] V. Utkin, H. Chang, I. Kolmanovsky, and J. Cook, "Sliding mode control for variable geometry turbocharged diesel engines," in *Proc. of the American Control Conference*, 2000, pp. 584–588.

[89] J. Wahlström, "Control of EGR and VGT for emission control and pumping work minimization in diesel engines," Ph.D. dissertation, Linköpings universitet, 2009.

[90] J. Wang, "Robust nonlinear control with singularity avoidance for diesel engines having multiple combustion modes," in *Proc. of the American Control Conference*, 2007, pp. 435–440.

[91] ——, "Air fraction estimation for multiple combustion mode diesel engines with dual-loop egr systems," *Control Engineering Practice*, vol. 16, pp. 1479–1486, 2008.

[92] X. Wei and L. del Re, "Gain scheduled H^∞ control for air path systems of Diesel engines using LPV techniques," *IEEE Transactions on Control Systems Technology*, vol. 15, no. 3, pp. 406–415, 2007.

[93] N. Winkler and H. Angstrom, "Simulations and measurements of a two-stage turbocharged heavy -duty diesel engine including egr in transient operation," in *Proc. of the SAE conference*, no. 2008-01-0539, 2008.

Modélisation et Commande des Systèmes d'Air des Moteurs Suralimentés

Résumé : Les performances des moteurs à combustion interne sont limitées par la quantité de gaz que leur système d'air peut apporter dans le cylindre. Les turbocompresseurs permettent d'augmenter cette quantité et c'est donc pour cette raison qu'ils sont maintenant couramment utilisés, parfois en combinaison avec d'autres composants. Ces systèmes présentent l'inconvénient d'entraîner une dynamique lente sur le moteur. Les stratégies de commande associées doivent donc exploiter au maximum la dynamique d'un système complexe. Cette thèse examine les problèmes de commande des systèmes d'air suralimentés à travers trois études de cas : un turbocompresseur à géométrie fixe sur un moteur essence, une turbine à géométrie variable sur un moteur Diesel avec deux circuits de recirculation des gaz brûlés, et un turbocompresseur à deux étages sur un moteur Diesel.

La démarche proposée consiste à réduire un modèle physique du système et à synthétiser des stratégies de commande simples basées sur l'analyse de ce modèle. Grâce à la simplicité du modèle réduit et de la loi de commande, on peut prouver des propriétés du système en boucle fermée telles que la convergence, la stabilité et le respect des contraintes. Des résultats expérimentaux sont fournis dans chaque cas pour démontrer la pertinence de la démarche.

La thèse montre donc que différents problèmes de commande de sytèmes d'air peuvent être traités avec des solutions similaires et cohérentes. La démarche globale et le niveau de modélisation retenu sont génériques. Ils pourront ainsi être étendus à de futurs problèmes de commandes de systèmes d'air, mais également à des problèmes de diagnostic pour lesquels ils sont bien adaptés.

Mots clés : Controle Moteur, Commande Turbocompresseur, Commande Non Linéaire, Planification de Trajectoire, Linéarisation par Retour d'Etat

Air Systems Modeling and Control for Turbocharged Engines

Abstract: The performances of internal combustion engines are limited by the quantity of fresh air and burned gas that can be brought into the cylinder by their air system. Turbochagers enable to increase this quantity and this is the reason why they are now used commonly, often combined with other complex components. These systems generate a slow dynamics on the engine. The associated control strategies are therefore complex because they must utilize the full dynamics of a complex system. This thesis investigates the control problems of turbocharged air systems through three case studies : a fixed geometry turbocharger on a gasoline engine, a variable geometry turbine on a Diesel engine fitted with two exhaust gas recirculation circuits, and a two stage turbocharger on a Diesel engine.

The proposed approach consists in the reduction of a physical model of the system and in the design of simple control strategies based on the analysis this model. Thanks to the simplicity of both the reduced model and the control law, it is possible to prove properties of the closed loop system such as the convergence, the stability and the satisfaction of constraints. Experimental results are provided for each case study in order to demonstrate the relevance of the approach.

The thesis thus shows that different air systems control problems can be addressed with similar coherent solutions. The global approach and the chosen modeling level are generic. They can therefore be extended to future air systems control problems, but also to diagnostic problems for which they are well adapted.

Keywords: Engine Control, Turbocharger Control, Nonlinear Control, Motion Planning, Feedback Linearization

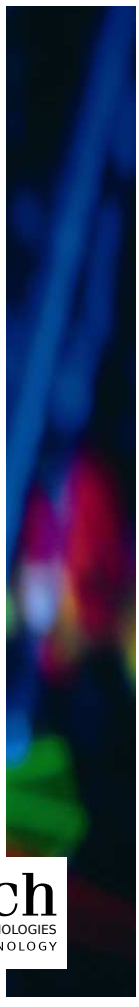

MINES ParisTech

ParisTech
INSTITUT DES SCIENCES ET TECHNOLOGIES
PARIS INSTITUTE OF TECHNOLOGY